USGS
science for a changing world

In cooperation with the University of Connecticut

Borehole-Geophysical and Hydraulic Investigation of the Fractured-Rock Aquifer near the University of Connecticut Landfill, Storrs, Connecticut, 2000 to 2001

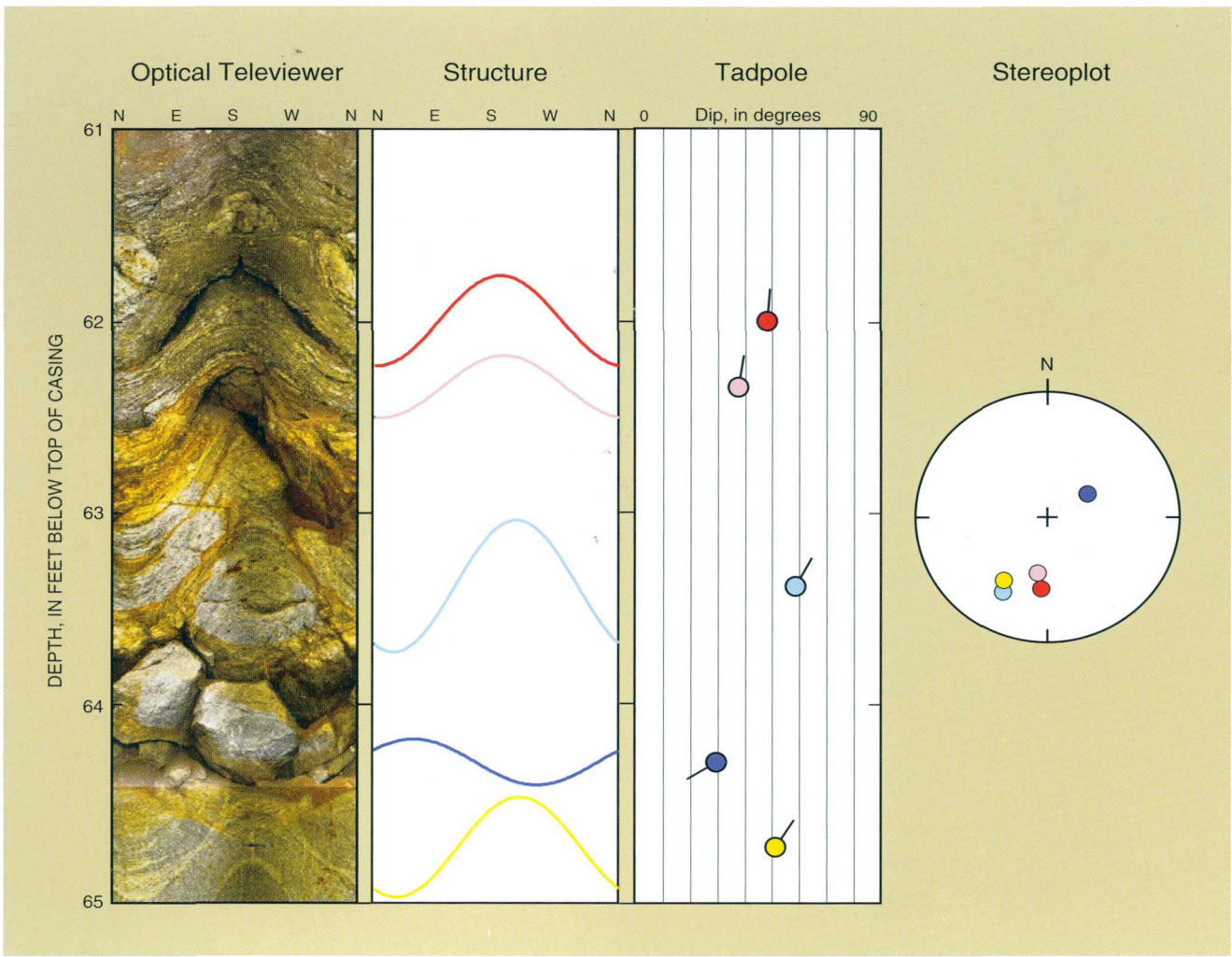

Water-Resources Investigations Report 03-4125

U.S. Department of the Interior
U.S. Geological Survey

BOREHOLE-GEOPHYSICAL AND HYDRAULIC INVESTIGATION OF THE FRACTURED-ROCK AQUIFER NEAR THE UNIVERSITY OF CONNECTICUT LANDFILL, STORRS, CONNECTICUT, 2000-2001--USGS WRIR 03-4125--Johnson, Joesten, and Mondazzi

Cover.—Optical-televiewer image and the corresponding interpretation and display of planar data in structural, tadpole, and stereographic-projection plots.

Borehole-Geophysical and Hydraulic Investigation of the Fractured-Rock Aquifer near the University of Connecticut Landfill, Storrs, Connecticut, 2000 to 2001

By Carole D. Johnson, Peter K. Joesten, and Remo A. Mondazzi

In cooperation with the University of Connecticut

Water-Resources Investigations Report 03-4125

U.S. Department of the Interior
U.S. Geological Survey

U.S. Department of the Interior
Gale A. Norton, Secretary

U.S. Geological Survey
Charles G. Groat, Director

U.S. Geological Survey, Reston, Virginia: 2005
For sale by U.S. Geological Survey, Information Services
Box 25286, Denver Federal Center
Denver, CO 80225

For more information about the USGS and its products:
Telephone: 1-888-ASK-USGS
World Wide Web: http://www.usgs.gov/

Contents

Figures

Tables

Conversion Factors, Vertical Datum, and Abbreviations

Multiply	By	To obtain
inch (in)	25.4	millimeter
foot (ft)	0.3048	meter
foot squared (ft^2)	0.09290	meter squared
gallon (gal)	0.003785	cubic meter

Electrical conductivity in millisiemens per meter (mS/m) may be converted to millimhos per meter (mmho/m) as follows: 1 mmho/m = 1 mS/m.

Temperature in degrees Fahrenheit (° F) can be converted to degrees Celsius (° C) as follows:

° C = 5/9 (° F - 32).

Transmissivity: Transmissivity is a measure of the ability of the aquifer to transmit water. The units of measurement are $[(ft^3/d)/ft^2]ft$, which represents a volumetric flow rate over a given area for a known thickness of aquifer. These terms simplify to units of ft^2/d, which will be used in this report.

Vertical datum: Vertical coordinate information is referenced to the North American Vertical Datum of 1988 (NAVD 88). For the UConn landfill study area, the change from NGVD29 to NGVD88 is 0.830 ± 0.003 foot.

Other abbreviations used in this report:

°, degree

ft/µs, feet per microsecond

ft^2/d, foot (feet) squared per day

ft^2/s, feet squared per second

gal/min, gallons per minute

gal/min/ft, gallons per minute per foot

h, hour

MHz, megahertz

min, minute

mS/m, millisiemens per meter

psi, pounds of force per square inch

s, second

µs, microsecond

µS/cm, microsiemens per centimeter

Borehole-Geophysical and Hydraulic Investigation of the Fractured-Rock Aquifer near the University of Connecticut Landfill, Storrs, Connecticut, 2000 to 2001

By Carole D. Johnson, Peter K. Joesten, *and* Remo A. Mondazzi

ABSTRACT

An integrated borehole-geophysical and hydraulic investigation was conducted at the former landfill area near the University of Connecticut in Storrs, Connecticut, where solvents and landfill leachate have contaminated a fractured-bedrock aquifer. Borehole-geophysical techniques and hydraulic methods were used to characterize the site bedrock lithology and structure, fractures, and hydraulic properties. The geophysical and hydraulic methods included conventional logs, borehole imaging, borehole radar, flowmeter under ambient- and stressed-hydraulic conditions, and discrete-zone hydraulic testing, sampling, and monitoring.

The conventional geophysical-logging methods included caliper, deviation, electromagnetic induction, gamma, specific conductance, and fluid temperature. The advanced methods included optical and acoustic imaging of the borehole wall, heat-pulse flowmeter, and directional radar reflection.

Borehole-geophysical methods were used to further define conductive features identified with surface-geophysical methods in the first phase of the investigation. The results of the surface- and borehole-geophysical logging were evaluated in an iterative and integrated manner to develop a conceptual model of ground-water flow at the site.

The rock type, foliation, and fractures at the site were characterized from high-resolution optical televiewer (OTV) images of rocks penetrated by the boreholes and were compared to drilling logs and conventional geophysical logs. The rocks are interpreted as fine- to medium-grained quartz-feldspar-biotite-garnet gneiss and schist with local intrusions of quartz diorite and pegmatite and minor concentrations of sulfide mineralization similar to rocks described as the Bigelow Brook Formation on regional geologic maps. Layers containing high concentrations of sulfide minerals appear as high electrical conductivity zones on electromagnetic-induction and borehole-radar logs. Foliation in the rocks generally strikes to the southwest and northeast, and dips to the northwest and southeast consistent with previous investigations in this area. The orientation of foliation, however, varies locally and with depth in some of the boreholes. These results are consistent with geologic mapping that has identified small-scale folding.

The orientations of the transmissive fractures identified in the six boreholes logged for this investigation are similar to the fracture orientations mapped in a previous investigation. Many of these fractures are oriented with a north-northwest strike and have a shallow dip to the west. Other transmissive fractures have a southwest strike and dip at shallow angles to the northwest, and some strike roughly east-west and dip to the north and south.

Flowmeter logging was used to identify transmissive fractures and to estimate the hydraulic properties in the boreholes. Ambient down flow was measured in one borehole, and ambient up flow and down flow were measured in another borehole. The other four bedrock boreholes did not have measurable vertical flow. Under low-rate pumping conditions (0.25 to 0.5 gallons

per minute), one to three inflow zones were identified in each well. Commonly, fractures that are active under ambient conditions contribute to the well under pumping conditions. The ambient conditions were incorporated into the determination of the relative proportions of transmissivity.

Specific capacity and transmissivity were determined for these open-hole low-rate pumping tests. Quasi-steady-state water levels were reached in four of the boreholes, including MW201R, MW204R, MW302R, and W202-NE. When pumped at low-rate conditions for 0.5 to 4 hours, the specific capacity ranged from 0.03 to 0.18 gallons per minute per foot. The open-hole transmissivity estimates ranged from 4.9 to 30 feet squared per day (ft^2/d).

Open-hole transmissivity was determined for boreholes that did not reach quasi-steady-state conditions under low-rate pumping conditions. Transmissivity was estimated for MW201R, MW202R, and MW203R using non-equilibrium methods, pumping rate, and the transient drawdown data to estimate the open-hole transmissivity. Transmissivity in these boreholes ranged from 0.98 to 3.2 ft^2/d.

The transmissivity and head of individual fractures or zones of fractures were estimated from heat-pulse flowmeter data acquired under ambient and stressed conditions. In the absence of ambient flow, data from two profiles of heat-pulse flowmeter data under two different stressed conditions were used to estimate the transmissivity and head of individual fracture zones. Only two boreholes, MW302R and W202-NE, had sufficient data for these analyses. The estimated transmissivity of individual transmissive zones ranged from 1.2 to 9.2 ft^2/d. The transmissivity values determined by this numerical simulation method were less than the open-hole estimations, which were 15 and 30 ft^2/d.

Transmissivity also was measured directly over discrete intervals of the borehole using a straddle-packer apparatus and constant-rate pumping tests. Pumping rates were less than or equal to 0.25 gallons per minute. These discrete-zone single-hole pumping tests were conducted over a short period of time, usually about 30 minutes to 1 hour in duration. Pumping continued until the test zone reached a steady-state water level or until it was determined that the zone could not yield water at the pumped rate. The estimated transmissivity of individual transmissive zones ranged from about 0.21 to 11 ft^2/d. The zone at a depth of 197 feet in W202-NE was the only zone that had discrete-interval testing with a straddle packer and sufficient heat-pulse flowmeter data for modeling the flow and estimating transmissivity and head. The two methods produced similar results. The straddle-packer method estimated a transmissivity of 4.7 ft^2/d, and the heat-pulse flowmeter modeling results estimated a transmissivity of 6.9 ft^2/d.

A comparison of the transmissivity estimates indicate estimates typically are within an order of magnitude. The heat-pulse flowmeter methods used in this investigation to determine transmissivity of the boreholes and the individual fractures measure only the upper two or three orders of magnitude of transmissivity. Hence, other fractures in these boreholes permit the movement of water; their transmissivities, however, are lower than the detection limits of the methods that were used for this investigation and very small compared to the transmissive fractures that were studied.

The data collected in this investigation were used to design discrete-zone monitoring systems for four of the boreholes used for monitoring. The results of the investigation are useful for refining the conceptual site model of ground-water flow, and for providing critical information for interpreting the results of water-quality sampling.

INTRODUCTION

A borehole-geophysical investigation was conducted to help characterize the hydrogeology of the fractured-rock aquifer near the former landfill and chemical-waste disposal pits at the University of Connecticut in Storrs, Connecticut. Five bedrock boreholes near the landfill and one abandoned domestic well about 1,700 ft from the landfill were logged from August 2000 to October 2001 using conventional and advanced borehole-geophysical methods.

Geophysical data collected as part of an initial investigation of the University of Connecticut landfill were used to characterize the hydrogeology of the fractured-bedrock aquifer, identify contamination or potential pathways for contaminant migration (primarily landfill leachate), and form a site conceptual model of ground-water flow (Powers and others, 1999; Johnson and others, 2002a, 2002b). Previous investigations have shown the complexity of fractured-rock aquifers and have highlighted the importance of using multiple methods of investigation to characterize bedrock hydrogeologic properties and the interaction of fractured rock and surficial aquifers. In 2000, the U.S. Geological Survey (USGS) in cooperation with the University of Connecticut, began a supplemental hydrogeologic investigation of the former landfill and vicinity to (1) further characterize the hydrogeology of the fractured-bedrock aquifer near the landfill and former chemical-waste disposal pits; (2) test new equipment for a discrete-zone monitoring (DZM) system and design a DZM system and sampling network that could be used to characterize flow potentials and to monitor remediation measures; and (3) refine the conceptual site model of ground-water flow and solute transport.

Background

The University of Connecticut (UConn) in Storrs, Connecticut, operated a landfill and chemical-waste disposal pits from about 1966 to 1989. In the early 1970's, the landfill was estimated to receive 18,000 cubic yards of waste annually, including the sand and gravel for waste-cell construction and cover. The contents of the landfill were estimated to be 85 percent paper (Izraeli, 1985). The chemical-waste disposal pits, which were located approximately 130 to 180 ft west of the landfill, were operated from 1966 to 1978. No official documentation of the wastes that were deposited in the chemical-waste disposal pits is available; however, Bienko and others (1980) indicated that pesticides, chlorinated hydrocarbons, solvents, and ammonium hydroxide may have been deposited. A detailed review by Haley and Aldrich, Inc. and others (2000) indicates acids, ethers, peroxides, heavy metals, cyanide, arsenic, toluene, acetone, benzene, pesticides, and herbicides also were disposed of in the chemical-waste disposal pits. In 1987, the soils in and surrounding two of the pits were removed (Connecticut Department of Environmental Protection, 1993). In August 2000, eight trenches were excavated in the area of the former chemical-waste disposal pits to assess whether the chemical pits were completely removed, and to further assess the materials in the area of the former chemical-waste disposal pits (Haley and Aldrich Inc. and others, 2002). Based on the results of these excavations, approximately 165 tons of material were removed.

In 1998, the Connecticut Department of Environmental Protection issued a consent order to UConn requiring an investigation of the potential effect of the UConn landfill on human health and the environment. An initial hydrogeologic investigation included a preliminary assessment of the amount of soil, surface-water, and ground-water contamination near the landfill (Haley and Aldrich, Inc., 1999). The methods of investigation used at this site included surface geophysics, exploratory drilling and monitoring-well installation, borehole geophysics, and surface-water, ground-water, sediment, leachate, soil, and soil-gas sampling.

Purpose and Scope

This report describes the borehole-geophysical logging methods used in the UConn landfill study; presents the interpretation of the geophysical measurements; and compares the data with previously collected borehole-geophysical data (Johnson and others, 2002a) and surface-geophysical data (Powers and others, 1999; Johnson and others 2002b) and with the local fracture patterns mapped in nearby outcrops (Fahey and Pease, 1977). An integrated suite of borehole-geophysical methods was used to determine the location, extent, and nature of fractures in the bedrock aquifer near the landfill. Geophysical logs were collected from six boreholes completed in bedrock (fig. 1). The borehole methods used in this investigation include conventional and advanced geophysical logs and hydraulic testing. Conventional geophysical logs were used to delineate fractures and provide information on lithology and borehole construction. Advanced geophysical logs were used in the bedrock boreholes to obtain information on the locations, orientations, and lateral continuity of fractures identified in the boreholes and to quantify the hydraulic properties of the transmissive fractures. The results were used for developing a conceptual model of ground-water flow at the site.

Fractures that were identified as transmissive were targeted for water-quality sampling and hydraulic testing using a straddle-packer apparatus and constant-rate pumping. The purpose of the hydraulic test was to measure the hydraulic response to pumping and to quantify the ability of a fracture (or closely spaced fractures) to transmit water and solutes.

Description of the Study Area

The UConn campus is in Storrs, Connecticut, in the northeastern part of the State. The study area occupies a north-northwest trending valley with highlands to the northeast and southwest. The UConn landfill is in the northwestern corner of the campus and covers about 15 acres (fig. 1). The landfill is located over a minor ground-water divide that drains to the north and south along the axis of the valley (Haley and Aldrich, Inc., 1999). The surface runoff flows north through a wetland towards Cedar Swamp Brook and south towards Eagleville Brook through seasonal drainage. The study area is bounded on the east by a steep hill and on the west by local minor topographic relief and Hunting Lodge Road. Regional ground-water flow is inferred to follow the topography; however, the local flow and transport in bedrock follows fractures that may be oriented differently than the regional gradient. In this report, the term "UConn landfill study area" is used to describe the area shown in figure 1 that includes the landfill, the former chemical-waste disposal pits, and the area southwest of the landfill near the intersection of Hunting Lodge Road and North Eagleville Road.

The bedrock underlying the UConn landfill study area is a medium-grained sillimanite gneiss that is folded, faulted, and fractured metasedimentary rocks mapped as Bigelow Brook Formation (Fahey and Pease, 1977). Regional bedrock maps show that bedrock foliation and fractures strike approximately north-south and dip 30 to 40° west (Fahey and Pease, 1977). Foliation in the area surrounding the landfill strikes from 15° west of north to 15° east of north and dips 20 to 60° to the west. The fabric of the bedrock in the area around the landfill generally strikes south-southeast and dips to the west (Fahey and Pease, 1977). Joints and faults are reported to trend north-northeast and dip 30 to 40° to the west. The bedrock aquifer is overlain by glacial till and other unconsolidated deposits, which range in thickness from 0 to about 20 ft and locally up to 50 ft.

Previous Geophysical Investigations

In 1998 and 1999, the USGS, in cooperation with UConn, used a suite of surface- and borehole-geophysical methods as part of the preliminary hydrogeologic investigation (Haley and Aldrich, Inc. and others, 2000) to characterize the fractured-bedrock aquifer near the UConn landfill. (Powers and others, 1999; Johnson and others, 2001, 2002a, 2002b). Collectively, surface- and borehole-geophysical methods and hydraulic techniques were used to (1) identify landfill structure, including the extent and location of trash disposal trenches that received trash and were surrounded by sand and gravel deposits; identify subsurface structures in the area of the former chemical-waste disposal pits; and verify excavation of the former chemical-waste disposal pits; (2) identify anisotropy caused by fractures and fabric in the rock; (3) identify electrically conductive features, such as transmissive fractures, conductive sulfide-rich layers in bedrock, and landfill leachates; (4) identify contamination or potential pathways for contaminant migration from the landfill and former chemical-waste disposal pits; (5) design a DZM program in the boreholes completed in bedrock; (6) identify and characterize transmissive fractures in the boreholes; and (7) develop and refine a conceptual ground-water flow model for the site.

Surface-geophysical methods including azimuthal square-array dc-resistivity surveys, two-dimensional dc-resistivity profiles, inductive-terrain conductivity surveys, and ground-penetrating radar surveys were used as screening tools to identify potential contamination pathways and to locate potential leachate plumes (Powers and others, 1999). The surface-geophysical methods were used to identify electrically conductive anomalies that were targeted for further evaluation by surface geophysics, exploratory drilling, and borehole-geophysical methods.

As part of the preliminary assessment, a total of 11 boreholes were logged with borehole-geophysical methods to characterize the hydrogeology of the bedrock underlying the landfill and vicinity and to further evaluate the anomalies identified in the surface-geophysical surveys (Johnson and others, 2002b). Two of the boreholes that were drilled for the UConn landfill investigation (Johnson and others, 2001) were sited to further explore the two sheet-like surface-geophysical anomalies identified by Powers and others (1999). Results of water-quality analyses were reported by

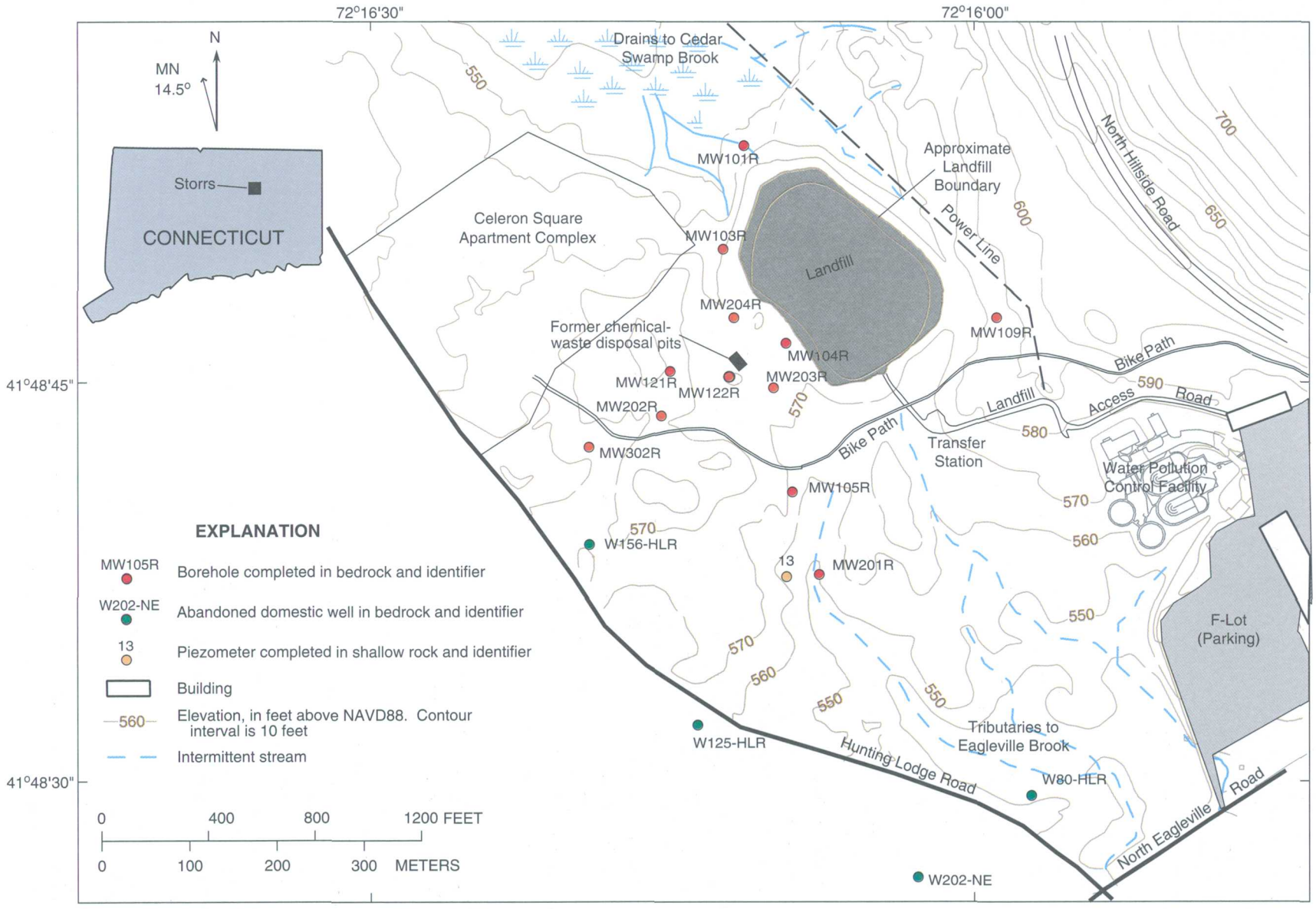

Base from Haley and Aldrich, Inc. and others, 2000, 1:2,400 scale

Figure 1. Location of boreholes in the UConn landfill study area, Storrs, Connecticut.

Haley and Aldrich, Inc., and others (2002). Discrete-interval sampling indicates that one of the conductive anomalies identified with surface-geophysical methods was in part caused by increased conductivity associated with landfill leachate.

DZM systems (Johnson and others, 2001) were installed in boreholes MW201R, MW202R, MW203R, and MW204R during the spring of 2001. The DZM completions used in each borehole and the results of the long-term monitoring are described in Johnson and others (2005). Hydrographs were constructed for the DZM systems. In addition, the discrete-interval water levels are compared to the water levels in adjacent zones, to seasonal fluctuations, precipitation, and cross-hole connections during pumping.

Acknowledgments

The authors gratefully acknowledge the homeowner who permitted access to his private well for geophysical logging, hydraulic testing, and water-quality sampling. The authors appreciate the guidance of Dr. Allen Shapiro, John H. Williams, and F. Peter Haeni of the USGS. Special thanks are extended to Dr. Susan Soloyanis of Mitretek Systems, and John Kastrinos, Elida Danaher, and Steve Russo of Haley and Aldrich, Inc., who provided supporting information and technical assistance. We appreciate and acknowledge the many USGS personnel who provided assistance with geophysical logging and analysis: Alton Anderson, Marcel Belaval, C.B. Dawson, Ellen Douglas, and Christopher Kochiss.

BOREHOLE-GEOPHYSICAL AND HYDRAULIC METHODS

Multiple logs that measure a range of earth properties at different scales of resolution were collected in each of the bedrock boreholes. The geophysical data from each borehole were analyzed together to provide an integrated interpretation, thereby reducing the ambiguity that can occur by interpreting each geophysical log individually. Descriptions of the borehole-geophysical methods used for this investigation are provided in this section.

Conventional and advanced borehole-geophysical methods were used in this study to provide information about the physical, electrical, and chemical properties of the bedrock and fluids in the subsurface and to provide important information on subsurface structures including the lithology, bedrock fabric, and location, orientation, and hydraulic properties of fractures. The conventional methods include caliper, deviation, electromagnetic induction, gamma, specific conductance, and fluid temperature. The advanced methods include optical- and acoustic-televiewer imaging, flowmeter (under ambient and pumping conditions), and single-hole directional radar reflection. Optical- and acoustic-borehole-imaging methods provide high-resolution images of lithology, structure, and fractures of the borehole walls, whereas single-hole directional radar reflection logs image electromagnetic reflectors in the bedrock that surrounds the boreholes.

Hydraulic characterization included fluid temperature and resistivity (whose inverse is specific conductance), heat-pulse flowmeter along with discrete-interval testing with the multifunction bedrock-aquifer transportable testing tool (BAT^3), and DZM with a semi-permanent packer system. The hydrogeologic interpretation included determination of the magnitude and direction of vertical flow within boreholes and the specific capacity and transmissivity of the open holes and selected fractures or fracture zones in the boreholes. Borehole liners were used to isolate transmissive zones and prevent vertical flow and the potential for cross contamination in five boreholes.

Conventional Borehole-Geophysical Methods

Conventional geophysical logging methods are used to provide preliminary information on borehole construction and conditions, lithology, fracture locations, and infer locations where water enters or exits boreholes (Keys, 1990). Conventional logs collected in all six boreholes include caliper, deviation, electromagnetic induction, natural gamma, specific conductance, and fluid temperature.

Caliper Logging

Caliper logging generates a continuous profile of the borehole diameter with depth. The caliper tool is pulled up the borehole allowing three spring-loaded arms to open as they pass borehole enlargements (Keys, 1990). Changes in the borehole diameter generally are related to fractures, but also can be caused by changes in the lithology or borehole construction.

Deviation Logging

The borehole deviation log is important to determine the true location and orientation of planar features intersected by the borehole. Deviation logging records the three-dimensional location of the borehole (Keys, 1990). The deviation log records the azimuthal direction (0 to 360°) and the inclination (0 to 90°) of the borehole over the depth of the borehole. Borehole deviation tools generally indicate direction to within ±2° and inclination to within ±0.5°. The results of this log are used to correct the orientation of planar features determined from the optical- and acoustic-imaging tools.

Electromagnetic-Induction Logging

Electromagnetic (EM)-induction logging records the electrical conductivity of the rocks and the fluids contained in the rocks surrounding the borehole (Williams and others, 1993). Changes in electrical conductivity are caused by variations in porosity, borehole diameter, concentration of total dissolved solids in the water in the rocks, and metallic minerals. The EM-induction probe is designed to maximize vertical resolution and radial penetration, and to minimize the effects of the borehole fluid. The peak tool response to the bedrock and pore water is approximately 1 ft away from the probe, and the tool has a vertical resolution of approximately 2 ft. In boreholes with diameters of 6 in. or less, the conductance of the borehole fluids has a negligible effect on the induction log response (Keys, 1990). The EM-induction log is used to delineate changes in rock type or in electrical properties of water contained in the rock formation.

Natural-Gamma Logging

Gamma logging measures the natural gamma radioactivity of the formation surrounding the borehole (Keys, 1990). The most common naturally occurring sources of gamma radiation are potassium-40 and daughter products of uranium- and thorium-decay series. Gamma emissions can commonly be correlated with rock type or with fracture infilling. Potassium-40 is abundant in some feldspar and mica, and uranium and thorium can be concentrated by geochemical processes. Gamma logs are recorded in counts per second.

Deviations in the gamma log indicate changes in lithology or the presence of altered zones or mineralized fractures. The vertical resolution of the gamma probe is 1 to 2 ft, and the probe is able to detect gamma radiation through plastic and steel casings. Because the gamma log does not have a unique lithologic response, interpretation must be correlated with other information such as drilling logs and other geophysical logs.

Specific-Conductance (Fluid-Resistivity) Logging

The electrical resistivity of the borehole fluid is measured, and its inverse, the specific conductance, is calculated. Changes in the specific conductance indicate differences in the concentration of the total dissolved solids in the fluid within the borehole (Williams and Conger, 1990). These differences typically indicate sources of water that have contrasting chemistries and are from different transmissive zones.

Fluid resistivity and temperature usually are measured simultaneously with a single borehole tool. These logs are typically run first in order to measure an undisturbed water column that represents ambient conditions. The logs can be collected after pumping has stopped, and a comparison between ambient and pumping conditions can help identify the location of the contributing inflow zones.

Fluid-Temperature Logging

Fluid temperature is one of several logs used to identify where water enters or exits the borehole (Williams and Conger, 1990). In the absence of fluid flow in the borehole, the temperature gradually increases with the geothermal gradient, about 1° Fahrenheit per 100 ft of depth (Keys, 1990). Deviations from the expected geothermal gradient indicate transmissive zones in the borehole. Changes in the fluid temperature may indicate water-producing and (or) water-receiving zones. Intervals of vertical flow are characterized by little or no temperature gradient. Temperature logs are used with specific conductance and flowmeter logs to identify flow under ambient and stressed conditions.

Advanced Borehole-Geophysical Methods

Advanced borehole-geophysical logs are used to aid in identifying the lithology of the boreholes and in determining the location and orientation of foliation and laminations in the bedrock and the fractures intersected by the boreholes.

Optical-Televiewer Logging

Optical-televiewer (OTV) logging records a high-resolution, continuous, magnetically oriented (to the earth's magnetic field) and digitized 360° color image of the borehole wall (Williams and Johnson, 2000). The images permit direct inspection of the borehole, which can be examined for fractures, changes in lithology, water level, bottom of casing, and borehole enlargements. The high-resolution images can be used to characterize fracture orientation, relative aperture, and presence of infilling, alteration and oxidation.

Optical images can be collected above or below the water surface, provided the water is sufficiently clear for viewing the borehole wall. The vertical resolution of the OTV is 0.01 ft. Because the resolution of this tool is higher than the resolution of the acoustic and electromagnetic imaging tools, OTV is able to view features that the other tools cannot resolve.

The digital image of a borehole can be viewed as an unrolled, flattened image that is split vertically along the north side of the borehole image. This is called the projected image, because it is projected onto a flattened plane. The image shows the depth in feet along the vertical axis (y) and the magnetic direction along the horizontal (x) axis. The x-axis represents a 360° scan of the borehole wall from north through east, south, west and north again. The sinusoidal curves on the flattened image represent planar surfaces. Thus, planar features such as fractures, foliation, lithologic contacts, and the water level can be identified directly on the images. Because the image is oriented to magnetic north, the strike and dip can be determined.

Because the OTV is an optical system, low contrast features, such as small fractures in dark rocks, can be difficult to delineate. Also, sediment, oxidation products, and biological activity that obscure the borehole wall can degrade the quality of the OTV image. The OTV logs were analyzed to identify lithology and to determine the physical characteristics and orientation of foliation and fractures.

Acoustic-Televiewer Logging

The acoustic televiewer (ATV) produces a high-resolution, magnetically oriented, digital image that is used to map the location and orientation of fractures that intersect the borehole (Williams and Johnson, 2000). The ATV tool emits a narrow acoustic beam that rotates 360° and is focused at the borehole wall. The acoustic wave moves through the fluid in the borehole, is reflected off of the borehole wall, and is received by the tool. The log records the amplitude and traveltime of the reflected signal, which can be displayed as a flattened 360° view of the borehole wall. The vertical sampling interval of the ATV tool is 0.02 ft.

A fracture that intersects the borehole causes scattering of the acoustic wave and appears as a high contrast, low amplitude line (dark feature) on the acoustic amplitude log. On the acoustic travel-time log, a fracture is indicated by an increase in the one-way traveltime of the wave, due to an increase in borehole diameter. The "acoustic caliper" log is used to confirm whether a feature observed in any of the other logs corresponds to an enlarged borehole diameter.

Because the OTV and ATV tools measure different properties, not all features are seen by both imaging tools. Characteristics such as oxidation, chemical or mineral precipitation, or fracture infilling, may be seen only by the OTV, helping to identify a fracture. The ATV image may show an increase in borehole diameter where a fracture cannot visually be confirmed in the OTV image. A side-by-side comparison of the images provides for an integrated interpretation of the results. The relative sizes of the fracture apertures observed in the OTV and ATV images were described in terms of "fracture" or "minor fracture." The term "possible fracture" was used to describe a planar feature where the interpretation was unclear from the image and from the integrated interpretation with other logs. In general, both the OTV and ATV detected the transmissive fractures.

Borehole-Radar Reflection Logging

Borehole-radar reflection logging records the transmitted and reflected wave amplitude and transit time of high-frequency EM waves using a pair of downhole transmitting and receiving antennas. The EM waves emitted by the borehole-radar tool penetrate into the formation surrounding the borehole. The waves are reflected by water-filled fractures, faults, bedding, and changes in rock type or water quality, and are detected by the receiving antenna. EM waves cannot penetrate through steel casing, but can penetrate PVC- cased boreholes, such as in MW302R. The total radial penetration of EM waves into the formation depends on the electrical and magnetic properties of the rock and water surrounding the borehole, and on antenna frequency, power, and separation. In previous surveys at this site,

radar reflections have been detected up to 80 ft into the rock (from the borehole) (Johnson and others, 2002b). In electrically conductive rocks, such as sulfide layers, the EM waves are rapidly attenuated, severely reducing or eliminating penetration. Borehole-radar reflection data are interpreted to determine the location and orientation of reflections from fracture zones, voids, and lithologic changes, and to estimate the radial extent of planar reflectors.

Based on methods described in Lane and others (1994), single-hole directional-radar reflection surveys were conducted in the six bedrock boreholes. A directional antenna was used to determine the orientation and location of discrete fractures or fracture zones surrounding the borehole. For this investigation, the radar tool was configured with a broadband electric-dipole transmitting antenna and a magnetically oriented, perpendicular electric-loop directional-receiving antenna with center frequencies in air of 60 MHz. The center points of the antennas were separated by a distance of 20.7 ft. Radar measurements were made every 0.65 ft along the open portion of each logged borehole. A total of 64 complete scans were stacked (averaged) at each measurement location to enhance the signal quality.

Data processing of directional-radar reflection surveys included removal of direct-current offsets, application of linear and exponential gains, and band-pass filtering to remove random and coherent noise. Interpretation included the determination of the strike, dip, and projected borehole intersection depth of planar reflectors as well as determination of the distance and azimuthal direction to point-like reflectors. Methods of interpretation are described by Olsson and others (1992). An estimate of radar-wave velocity is needed for the interpretation of the dip of radar reflectors and estimates of the lengths of reflectors. For this investigation, a uniform radar-wave velocity of 372.4 ft/μs was used for the processing and interpretation of the radar reflection surveys. This velocity was determined from a vertical-radar-profile analysis conducted in a borehole near the landfill (Johnson and others, 2002b).

The length of individual radar reflectors was estimated using measurements of the maximum radial extent over which a given reflector could be observed in the radar record and applying a correction factor that accounts for the dip of the reflector. Because this estimate is affected by the maximum radial radar penetration distance, the actual length of a reflector may be greater than that estimated from the radar images.

Hydraulic Methods

Flow in fractured rock is a function of the hydraulic head gradient and the physical properties of the bedrock such as location, orientation, openness, and connectivity of fractures. Water flows from higher hydraulic head to lower hydraulic head through a series of interconnected fractures in the bedrock. Although a small amount of water moves through the primary pores that constitute the matrix of the bedrock, most of the water is channeled through interconnected fractures and is driven by the hydraulic gradient. Thus, to characterize the flow and transport of solutes through fractured crystalline rock, the physical and hydraulic properties of the rock have to be defined and understood. It is necessary to identify the fractures in the network, determine which fractures in the network are transmissive, and estimate the transmissivity and connectivity of these fractures. Heat-pulse flowmeter logs were used in conjunction with fluid-resistivity and temperature logs to identify the transmissive fractures and their relative heads and flow contributions.

Temporary Borehole Liners

Open boreholes can connect fractures with different hydraulic heads and permit vertical flow through the borehole. The vertical flow within an open borehole may cause cross contamination and dilution by providing a conduit between fractures containing different chemical constituents and concentrations. Vertical flow in open boreholes in the bedrock was minimized with the use of removable borehole liners designed by Flexible Liner Technology, Inc. A borehole liner is a long flexible plastic sleeve that is attached to the top of the borehole casing, inverted, and filled with water until it is lowered to the bottom of the borehole. In low transmissivity boreholes, the water can be pumped from the bottom of a tube that extends to the bottom of the borehole outside the liner. The installation of the liner is facilitated by removing water from below the liner, while simultaneously adding water to the inside of the liner. The temporary liners provided a means for minimizing flow prior to geophysical logging and before the DZM systems were designed, built, and installed. Borehole liners were installed in MW201R, MW202R, MW203R, and MW204R following the completion of the borehole,

and were removed for geophysical logging. If vertical flow had been measured with the heat-pulse flowmeter, the liners would have been reinstalled. Because vertical flow was not measured in any of these boreholes, the liners were not reinstalled.

This process was reversed to remove the liners for geophysical and hydraulic logging. In order to facilitate the removal of liners, water was injected into the bottom of the borehole while simultaneously pumping water from inside the liner and hoisting the liner out of the borehole. The lower the transmissivity of the borehole, the more water that had to be added to the bottom of the borehole to remove the liner.

Heat-Pulse Flowmeter Logging

Heat-pulse flowmeter logging measures the direction and rate of vertical flow in a borehole. Used in conjunction with other geophysical logs, individual fractures or fracture zones where water enters or exits the borehole can be identified. Under ambient conditions, differences in hydraulic head between two sufficiently transmissive fractures produce vertical flow in the borehole. Water enters the borehole at the fracture zone with the higher head and flows towards and out of the borehole at the fracture with the lower head. In the presence of a differential head, the rate of flow will be limited by the fracture with the lower transmissivity. If the heads in transmissive zones are the same, then no vertical flow will occur in the borehole. Therefore, flowmeter logging was conducted under low-rate (0.25 to 0.5 gal/min) pumping conditions to identify transmissive zones with similar ambient heads that would not be identified without stressing the aquifer. The flow under pumped conditions was proportioned and attributed to specific fracture zones in the borehole. The ambient flow regimes were incorporated into the determination of proportions using methods described by F.L. Paillet and P.A. Stamile (U.S. Geological Survey, written commun., 1999).

The flowmeter used in this investigation uses a heat-pulse tracer that moves upward or downward in the presence of vertical flow. The flowmeter was outfitted with a diverter that is designed to channel all of the vertical flow within the borehole through a measurement channel where the movement of the heat pulse is measured. Flowmeter measurements were collected at discrete locations in the borehole, usually above and below fractures identified in the other geophysical logs. The heat-pulse flowmeter can measure flows as small as 0.01 ± 0.005 gal/min (Hess and Paillet, 1990), which corresponds to a transmissivity of about 10^{-5} ft^2/s (Paillet, 1999). Flowmeter logging conducted at the USGS Mirror Lake Fractured-Rock Research Site, Grafton County, New Hampshire, by Paillet (1998) consistently identified only those zones with transmissivities within 1.5 to 2.0 orders of magnitude of the most transmissive zone of each borehole. Therefore, the flowmeter technique used in this investigation is sufficient to identify the most transmissive fracture in the borehole and other fractures with transmissivities within an order or two of magnitude. In general, the flow rates measured within these boreholes were low, and there were no problems with low transmissivity fractures being masked by high transmissivity fractures.

Estimates of Transmissivity

Flowmeter profiles were collected under ambient and pumped conditions. In the absence of measurable ambient flow, two steady-state heat-pulse flowmeter profiles were collected under two different pumping conditions. Some of the boreholes were unable to achieve steady state under low-rate pumping conditions and the water levels continued to decline gradually. In these boreholes, heat-pulse flowmeter data were collected only under ambient conditions and under one pumping rate. The open-hole water levels were recorded during pumping and heat-pulse flowmeter measurements were made after the borehole reached a quasi-steady state in which the amount of water coming out of storage was less than the measurement resolution of the tool. In this study, a second pumping rate was used to confirm the results of the first test.

Transmissivity is a measure of the ability of the aquifer to transmit water. The units of measurement are cubic foot per day per square foot times foot of aquifer thickness "$[(ft^3/d)/ft^2]ft$," which represents a volumetric flow rate over a given area for a known thickness of aquifer. These terms simplify to units of foot squared per day "ft^2/d," which will be used in this report.

Transmissivity was determined using three methods. (1) The transmissivity of the entire borehole was calculated using open-hole hydraulic data collected during pumping associated with heat-pulse flowmeter logging. The transmissivity results for the open-hole measurements were proportioned using the results of heat-pulse flowmeter testing to estimate the

transmissivity of individual fractures or fracture zones in the borehole. (2) Estimates of transmissivity and head were made for individual hydraulically active fracture zones using a numerical modeling technique that uses ambient open-hole water levels, the water level under pumping conditions, and heat-pulse flowmeter results under two different flow conditions – under ambient flow and a pumping condition, or, in the absence of ambient flow, under two different pumping conditions. (3) Transmissivity also was measured directly in discrete intervals of the borehole using a straddle-packer apparatus and single-hole hydraulic discharge tests. All transmissivity values in this report should be considered estimates that are within an order of magnitude of the true borehole transmissivity. The transmissivity tests that were conducted in each borehole are shown in table 1.

Analysis of Hydraulic Data

For the boreholes that reached a steady water level under pumping conditions, the transmissivity of the entire borehole was calculated using specific capacity, which was determined using open-hole hydraulic data collected during pumping associated with heat-pulse flowmeter logging. For the boreholes that did not reach steady state conditions while pumping, the Cooper-Jacob time-drawdown straight-line solution was used to estimate the transmissivity.

Table 1. Transmissivity testing of boreholes in the UConn landfill study area, Storrs, Connecticut

[DZM, discrete-zone monitoring system for long-term monitoring of head and water quality. T_{ss}, transmissivity determined with an analytical model for drawdown that reached steady-state conditions. T_t, transmissivity determined with a Cooper-Jacob non-equilibrium method using drawdown data under transient conditions. HPFM, heat-pulse flowmeter. X indicates test was conducted. – indicates test was not conducted. ND, No data indicates that although water was produced from the pumping zone, the transducer was beyond its operating range. NW, no water indicates that the zone was unable to produce water for sampling even at rates less than 0.25 gallons per minute]

Borehole	Open-hole testing				Discrete interval testing using a straddle-packer apparatus					Date of DZM installation
	Specific capacity	Transmissivity		Transmissivity modeled with HPFM data	Depth of fracture, in feet	Test interval, in feet	Differential head	Withdrawal test	Sample collected	
		T_{ss}	T_t							
MW201R	X	X	X	-	-	-	-	-	-	3/29/01
	-	-	-	-	39	37.1-43.5	X	ND	X	-
	-	-	-	-	60	56.1-62.5	X	X	X	-
	-	-	-	-	76	74.6-81.0	X	-	-	-
	-	-	-	-	97	95.6-102.0	X	-	-	-
MW202R	-	-	X	-	-	-	-	-	-	3/29/01
	-	-	-	-	31	27.3-33.7	X	ND	X	-
	-	-	-	-	107	104-110.7	X	X	X	-
MW203R	-	-	X	-	-	-	-	-	-	3/20/01
	-	-	-	-	32	28.3-35.7	X	X	X	-
	-	-	-	-	65	61.8-69.3	X	-	-	-
MW204R	X	X	-	-	-	-	-	-	-	3/23/01
	-	-	-	-	21-22	13.1-29.7	X	X	X	-
	-	-	-	-	45	41.3-47.7	X	NW	-	-
	-	-	-	-	76	74.3-80.7	X	-	-	-
MW302R	X	X	-	X	-	-	-	-	-	-
W202-NE	X	X	-	X	-	-	-	-	-	-
	-	-	-	-	105	104.4-115.2	X	-	-	-
	-	-	-	-	197	195.4-206.2	X	X	X	-

Estimation of Specific Capacity and Transmissivity of Open Boreholes

The transmissivity was estimated in open boreholes from specific-capacity data collected concurrently with the heat-pulse flowmeter logging under pumped conditions. The water-level drawdown and elapsed time of pumping was recorded in response to low-rate pumping. The duration of the single-hole pumping test was typically 1 h, but ranged from 0.6 to 1.2 h. The pumping rates for these tests were 0.25 to 1 gal/min. Specific capacity, which is the yield of the borehole per unit length of drawdown, was calculated and recorded in gallons per minute per foot. In addition, an open-hole transmissivity was calculated using a program described by Bradbury and Rothschild (1985) with an assumed storage coefficient of 0.0005 (Freeze and Cherry, 1979). Well-loss coefficient is a parameter that quantifies the effects of turbulent flow, which causes drawdown in the borehole relative to the formation. The well-loss coefficient was not determined explicitly for these boreholes; thus, the value was set equal to 1.0 (Bradbury and Rothschild, 1985).

For selected boreholes that did not reach steady state, the Cooper-Jacob straight-line solution was used to estimate the transmissivity of the open borehole (Lohman, 1979). By this method, the drawdown was plotted against logarithmic time, and a straight line was fitted through late-time data. The change in water level over 1 log cycle was used in the formula below to estimate transmissivity:

$$T_k = (2.3Q)/(4\pi\Delta S_l) \qquad (1)$$

where T_k is the transmissivity of zone k, in length squared per time,

Q is the constant pumping rate, in length cubed per time, and

ΔS_l is the drawdown over 1 log cycle, in length.

For this method to be valid, the dimensionless parameter, u, should be less than or equal to about 0.01, where $u = (r^2 S)/(4 Tt)$; r is the borehole radius, S is the storativity, T is the transmissivity, and t is the elapsed time of pumping. This method works best under confined conditions and when distance is small. When this method is used in a single-hole test, distance is set equal to 1. For comparative purposes, the pumping tests with the straight-line approximation also were analyzed with a Theis curve-matching solution (Lohman, 1979).

Estimation of Transmissivity and Hydraulic Head of Fractures with Heat-Pulse Flowmeter Data

In boreholes with no measurable ambient flow, the open-hole transmissivity was apportioned according to heat-pulse flowmeter results under pumping conditions. The total transmissivity determined for the entire open borehole was distributed among the hydraulically active zones in proportion to the relative contribution of each transmissive zone as measured by the heat-pulse flowmeter. Proportioning the transmissivity to the individual fracture zones was used to estimate fracture-zone transmissivity; however, the transmissivity values determined by this method should be viewed qualitatively.

In boreholes with measurable ambient flow (MW302R and W202-NE), numerical flow modeling was used to estimate transmissivity and the hydraulic head of each transmissive zone using methods described by Paillet (1998). The difference between steady flows for each transmissive zone in a borehole under ambient and pumping conditions is related to the transmissivity and water levels by

$$Q^s_k - Q^p_k = 2\pi T_k (w_p - w_s) \ln(r_0/r), \qquad (2)$$

where Q^s_k is the flow into borehole from zone k under ambient conditions, in length cubed per time,

Q^p_k is the flow into borehole from zone k under pumping conditions, in length cubed per time,

T_k is the transmissivity of zone k, in length squared per time.

w_p is the water level in the borehole under pumping conditions, in length,

w_s is the water level in the borehole under ambient conditions, in length,

r_0 is the zone radius, distance to the recharge boundary of the producing zone, in length, and

r is the borehole radius, in length.

The difference in flow between two fractures is directly proportional to zone transmissivity, because the ratio between the zone and borehole radius can be treated as a constant. Because the open-hole head is a transmissivity-weighted average of all the heads in the

borehole, the solution is further constrained by the open-hole heads under pumping and ambient conditions.

Using the computer program of Paillet (1998, 2000), the transmissivity and hydraulic-head were determined for each hydraulically active zone. The method requires two flow regimes including either flow data for ambient and for one pumping condition or flow data for two different pumping conditions and the difference in water level between the two regimes. The program simulates two flow regimes as a function of transmissivity and hydraulic head from all hydraulically active zones intersecting the borehole. Model input requires information on the location of the transmissive fractures, ambient open-hole water level, quasi-steady state water level under pumping conditions, heat-pulse flowmeter data under two flow regimes, and estimates of transmissivity and head for each zone. The simulated regimes were compared to measured flow profiles, and the head and transmissivity parameters were iteratively varied until a unique solution was obtained for the transmissivity and head of each fracture. The model produces ambient and pumped profiles that are qualitatively matched to the observed flow profiles. The model also provides the sum of squared (SS) errors to assess the fit of the predicted flow profile to the measured profile, and hence the validity of the solution.

Estimation of Transmissivity and Differential Hydraulic Head of Isolated Zones in the Borehole with BAT^3

Transmissivity also was measured directly using constant-rate pumping tests conducted in discretely isolated zones (Shapiro and Hsieh, 1998). Not all zones could be tested with this method because a sufficiently transmissive fracture is required to sustain discharge at a minimal pumping rate, which was about 0.1 gal/min. Using injection-test methods at the USGS Fractured-Rock Research Site in central New Hampshire, Shapiro and Hsieh (1998) measured transmissivities as low as 10^{-9} ft^2/s; which is orders of magnitude lower than the transmissivity that can be measured by the constant-rate pumping methods used in this investigation.

A total of eight constant-rate pumping tests were attempted. One of the tests was aborted because the zone could not produce enough water to sustain the test. Two other tests produced enough water to obtain samples, but the water level declined below the height of the transducer, and transmissivity values could not be determined. Table 1 shows the locations of the withdrawal tests.

Hydraulic tests were conducted and water-quality samples were collected concurrently from discretely isolated zones in five bedrock monitoring wells—MW201R, MW202R, MW203R, MW204R, and abandoned domestic well W202-NE. The purpose of the hydraulic test is to measure the hydraulic response to pumping and to quantify the ability of a fracture (or closely spaced fractures) to transmit water and solutes. A straddle-packer apparatus, called the BAT^3 (Bedrock-Aquifer Transportable Testing Tool), was used to obtain the samples and monitor the heads during pumping (Shapiro, 2001). The BAT^3 is shown in figure 2. Two inflatable packers separated by 6.5 ft were used to isolate the test zone from the zones above and below the test interval. A submersible, variable-rate pump located between the two packers was used to directly sample the fractures in the test zone. Pumping rates ranged from 0.1 to 0.3 gal/min. An inline flowmeter, which was capable of measuring flows between 0.00088 and 2.0 gal/min, measured the discharge rate while sampling, and the results were recorded on a data logger. Data acquisition was linked to a computer for real-time monitoring and data storage. Manual discharge and water-level measurements were made to verify the rate of pumping and the water level in the upper zone.

In boreholes MW201R-MW204R, pressure transducers were used to continuously monitor the water levels in, above, and below the test zone to (1) ensure the hydraulic isolation of the test zone, (2) identify possible cross connections between the zones, and (3) determine the transmissivity of the test zone. The pressure transducers were vented to the atmosphere. The upper zone was monitored with a 10-psi transducer that had a resolution of ±0.06 percent of the full scale of the transducer, which is equivalent to ±0.014 ft. The middle zone was monitored with a 100-psi transducer, with a resolution of ±0.139 ft, and the lower zone used a 200-psi transducer, with a resolution of ±0.277 ft. The transducers used to monitor the middle and lower zones were designed to accommodate and measure deep water. The upper transducer was lowered into the water to a depth approximately 10 ft below the water surface. Small differences in differential head cannot accurately be measured with the BAT^3 equipment because of the resolution of the transducer. Differences in head less than the combined resolution of the two

transducers are within the measurement error of the transducers.

A different type of transducer was used in the abandoned domestic well, W202-NE. The transducers used for those tests were absolute pressure transducers that were sealed relative to a vacuum. Unlike the other vented transducers used in this investigation, the sealed transducers measure the total pressure including the atmospheric pressure. The upper-most monitoring zone was outfitted with a 50-psi transducer that had a resolution of ±0.069 ft. The middle and lower zones were monitored with 200-psi transducers that had a resolution of ±0.277 ft. An additional 15-psi transducer, which had a resolution of ±0.021 ft, was used to monitor the atmospheric pressure during the test, and to remove the atmospheric pressure component from the other transducer measurements.

Test zones were selected based on the interpretation of the geophysical logs (table 1). Fractures and fracture zones that were identified as hydraulically active by use of heat-pulse flowmeter, fluid resistivity, and temperature logs were targeted for sampling. Packers were placed in smooth, unfractured sections of the borehole straddling the hydraulically active fractures. The general procedure at each test zone was as follows:

1. Packers were lowered to the test zones and the transducers were calibrated during installation.
2. At the targeted zone, the packers were inflated with compressed gas to about 80 psi over ambient pressure.
3. Water levels were allowed to reach an equilibrium.

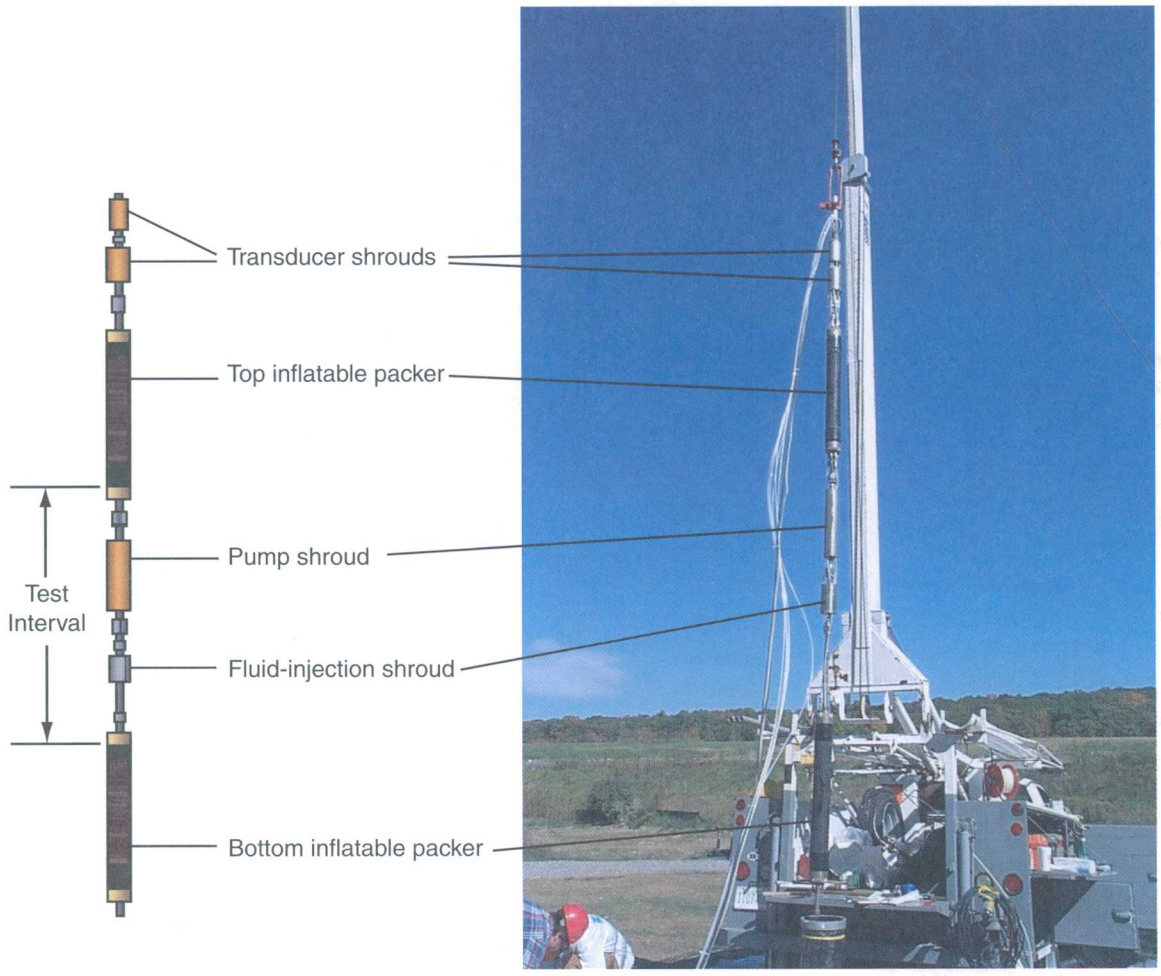

Figure 2. The multifunction bedrock-aquifer transportable testing tool (BAT^3).

4. Pumping was initiated, and a steady pumping rate was achieved. Fluid properties (temperature, specific conductance, pH, dissolved oxygen, turbidity, salinity, and oxidation-reduction potential) were monitored, and water-quality samples were collected when field properties reached steady-state conditions.
5. Pumping continued until the water levels in the test zone reached steady state or until it was determined that the zone could not sustain the low-rate pumping stress.
6. After the water-quality samples were collected and steady-state conditions were achieved, the pump was turned off, and water-level recovery was monitored.
7. Water levels were monitored until the test zone reached the pre-test water level.
8. The results were analyzed using the methods described by Shapiro and Hsieh (1998).

Transmissivity of the test zone was determined using the Thiem equation:

$$T = Q/2\pi(h_a - h_s)\ln(R/r), \quad (3)$$

where Q is the measured discharge rate, in length cubed per time,
h_a is the head under ambient conditions, in length,
h_s is the head under steady-state pumping conditions, in length,
R is the radius of influence beyond which there is no drawdown caused by pumping, which was assumed to be a fixed length of 10 ft, and
r is the radius of the borehole, in length.

This method assumes steady-state conditions, radial flow, in an isotropic homogeneous confined formation. Although these conditions are rarely met and difficult to prove, the method provides a reasonable approximation for the transmissivity (Shapiro and Hsieh, 1998).

Discrete-Zone Head Monitoring

The hydraulic head in fractures can be determined by isolating the individual fracture zones. Several methods were used to determine the hydraulic head of individual fractures and the vertical hydraulic potentials between fractures. As borehole conditions permitted, two sets of flowmeter data were collected to identify transmissive fractures or fracture zones and to solve for individual heads and transmissivities of each zone.

Integrated analysis of borehole-geophysical data collected under ambient and pumped conditions provided information on locations of individual transmissive fracture zones. This information was used to design DZM systems to isolate transmissive zones and develop sampling strategies. By isolating these zones for long-term monitoring and measuring the hydraulic head in these zones, meaningful vertical and horizontal hydraulic gradients were obtained. A separate report summarizes the DZM system design and the monitoring results (Johnson and others, 2005).

Differential-Head Tests with BAT^3

The BAT^3 system also was used to determine the ambient head differential between the isolated zone and the zones above and below the test interval prior to pumping. The equipment was installed in the well and the packers were inflated. The water levels were allowed to equilibrate, which required several minutes to several hours. In the other zones, which were not sufficiently transmissive to produce a water sample, the fractures were isolated and either left for hours or overnight to equilibrate for a differential head test. Differential head tests were collected at a total of 13 zones in 5 boreholes.

Installation of Discrete-Zone Monitoring Systems

Using the information from the hydraulic tests and geophysical logging, DZM systems were designed and installed in the boreholes. Semi-permanent DZM systems were constructed using a continuous multichannel tubing and inflatable packer system commercially available from Solinst Canada, Ltd. The DZM system consists of a 1.7-in.-diameter plastic tube, which is divided into seven discrete channels, and one or more packers that slide over the tubing are placed at predetermined locations to isolate specific zones in the borehole. The tube extends from the top of the borehole to the lowermost zone isolated by packers. Individual channels are punctured at a specific depth to provide a sample port that is open to the isolated zone. Once the tubing and packers are lowered into the borehole, the packers are inflated with water to about 20 psi above ambient pressure. The inflated packers create a seal with the borehole wall, thereby isolating the packed-off zones. With this design, the water level in each channel

equilibrates to the hydraulic head in the isolated zone, and water levels and water-quality samples can be obtained from the top of the borehole.

Detailed information on the DZM designs and data collected from the long-term monitoring in the DZM systems are reported in supplementary reports (Johnson and others, 2001; Johnson and others, 2005). Water-quality data are reported by Haley and Aldrich, Inc. and others (2002).

BOREHOLE-GEOPHYSICAL AND HYDRAULIC DATA COLLECTED AT THE UCONN LANDFILL STUDY AREA: 2000 TO 2001

For this investigation, borehole-geophysical logging was conducted in six bedrock boreholes from July 2000 to October 2001. Five of the bedrock boreholes were drilled as part of a hydrogeologic investigation of the area surrounding the UConn landfill (Haley and Aldrich, Inc. and others, 2000). Four of the boreholes (MW201R, MW202R, MW203R, and MW204R) are approximately 6-in. in diameter and completed to depths of about 125 ft below land surface (fig. 1). Borehole MW302R was completed to a depth of about 301 ft below land surface and was cased to a depth of 125 ft below land surface. Additionally, an abandoned domestic-supply well (W202NE) on private property southwest of the landfill was logged. Information on borehole construction and location is provided in table 2.

Conventional Borehole-Geophysical Logs

The complete suite of conventional borehole-geophysical logs was collected and examined for the six bedrock boreholes. The logs for each individual borehole are presented in appendixes 1 through 6. Displaying the data side-by-side facilitates direct interpretation. The following section describes each type of log, the method of interpretation, and the general results. The results of the conventional logs are not discussed in detail; however, results that support or conflict with the results of advanced logs are noted in the discussion below.

The borehole deviation is shown in a radial plot for each well. The center of the plot represents the borehole location at the top of casing. The borehole location is plotted as a function of depth with respect to true north. Plots of the deviation for each borehole are provided in appendixes 1A-6A. The boreholes installed as part of the hydrogeologic investigation are nearly vertical, with less than 4 ft of offset even for the entire 302.7-ft length of borehole MW302R. Although the magnitude of the deviation for the boreholes was generally small, the data were used to correct the orientations of the features observed in the boreholes to account for the borehole inclination. The boreholes typically deviate normal to the fabric of the rock. For example, abandoned domestic well W202-NE deviates about 14 ft towards the south-southeast (N153°E), whereas the foliation dips gently towards the northwest (appendix 6A).

Advanced Borehole-Geophysical Logs

The advanced logs provide information on the location, orientation, and hydraulic properties of fractures that intersect a borehole. The logs of all boreholes are presented in the appendixes. Not all fractures are observed by each of the optical- and acoustic-imaging methods and borehole-radar methods. The individual interpretations have been provided and the integrated interpretations are discussed in the results section of this report.

Table 2. Construction of boreholes at the UConn landfill study area, Storrs, Connecticut

[Height is in feet; all depths are in feet below the top of casing; pvc, polyvinyl chloride]

Well name	Date drilled	Elevation of top of casing	Height of casing above land surface	Casing material	Depth of casing	Total depth below top of casing
MW201R	06/22/2000	554.22	1.6	steel	15.2	125.7
MW202R	06/20/2000	582.33	2.1	steel	13.5	126.6
MW203R	06/21/2000	576.90	1.9	steel	14.5	127.9
MW204R	06/21/2000	575.34	2.0	steel	13.1	127.8
MW302R	12/20/2000	577.2	1.5	pvc	127	302.7
W202-NE	05/05/1995	549.2	2.1	steel	81	325

The orientations of planar features interpreted from the OTV, ATV, and borehole-radar data have been plotted in two forms—stereoplots and tadpole plots, which provide graphical methods for assessing the pattern of planar features. By convention, the strikes of planar features are reported in tables in the right-hand rule, which specifies that the dip is always in a direction 90° to the right of the strike, and the strike is 0 to 360° east of true north.

In this report, a consistent set of symbols were used to identify the type of planar features identified in the boreholes (fig. 3). The same color codes were used to show the trace of the feature on the projected, tadpole, and stereoplots. For example, a transmissive fracture is shown as a dark blue trace on the projection plot and as blue points on the stereoplots and tadpole plots.

Oriented, planar data interpreted from the borehole imaging logs can be shown in three forms: (a) projected plot, (b) stereoplot, and (c) tadpole plot. The example in figure 4 shows the original projected image and interpretations of five planar features. The type of feature is indicated by the color of the symbol (fig. 3). In the representation in figure 4, the borehole depth is on the y-axis and the oriented image is split vertically along the north and projected onto a flat surface (fig. 4A). The upper two features at midpoint depths of 62.0 and 62.5 ft below top of casing dip to the north (shown as red and pink in fig. 4B to 4D). The feature at a midpoint depth of 63.5 ft below the top of casing is steeply dipping to the north-northeast. A feature at a depth of 64.3 ft dips to the west at an angle of about 30° from horizontal. The deepest fracture at 64.7 ft (shown as yellow in fig. 4B to 4D) has a moderate to steep dip towards the northeast.

The structural projection plot shows the trace of the planar feature superimposed on the projected image of the borehole (fig. 4B). One advantage of representing the data in this form is that it overlays directly on or next to the original borehole images. In this projection, the interpretation of the feature can be compared directly to the borehole image. In addition, the trace of projected features can be determined and plotted for one type of image data (such as for the OTV image), and then can be overlain on the ATV image for direct comparison.

Tadpole plots (fig. 4C) show the orientation of planar features with respect to depth within a borehole. The tadpole plot in figure 4C shows the depth of each feature along the y-axis; the magnitude of dip from 0 to 90° along the x-axis; and the direction of dip (dip azimuth), which is represented by the direction of the tadpole's tail. The tail of the tadpole points in a direction of dip azimuth relative to an imaginary compass with north at the top of the plot. The steeply dipping minor fracture at a depth of 63.5 ft plots toward the right hand side of the plot indicating a steep dip, and the tail points toward the northeast. Conversely, the shallow dipping feature at 64.5 ft plots toward the left side of the plot at about 30° dip and points to the southwest. The tadpole plot can be used to help identify discontinuities, folds, or distinct changes in orientation over the depth of the borehole.

A stereoplot, also called a stereogram, reduces each planar feature to a point that represents the intersection of a pole that is perpendicular to the plane with a lower hemisphere; the point is projected onto the equatorial plane of the hemisphere (fig. 4D). Hence, the points on the circle (which represents the equatorial plane of the hemisphere) are called "poles to planes." In this type of a plot, a nearly horizontal fracture would have a pole that projects to the center of the stereoplot. The pole of a steeply dipping fracture would project to the outside of the stereoplot and would be located on the side of the circle opposite from the direction of dip.

The stereoplots provide a graphical method for assessing the clustering or variability of the poles to planes. Figure 4D shows the features in figure 4A in an equal-area, lower hemisphere stereoplot. In the stereoplot, the steeply dipping feature at 63.5 ft (light blue point) plots towards the outer rim of the projection, and shallow feature at 64.5 ft (dark blue point) plots towards the middle of the circle. In this example, the poles to the planes form a cluster that indicates a northwest strike and a moderate dip to the northeast. The feature at 64.5 ft (dark blue point), which strikes in the opposite direction, plots on the opposite side of the stereoplot.

Depth is not represented in the stereoplot; however, this plot is helpful in assessing the degree to which planar features are clustered or scattered and may help identify sets of planar features. A stereoplot can be constructed for the entire length of a borehole, for selected depths of a single borehole, or for multiple boreholes. Oriented data presented in this form provides the opportunity to effectively compare the results from a number of boreholes.

Figure 3. Symbols used in this report to represent the planar features identified in image logs.

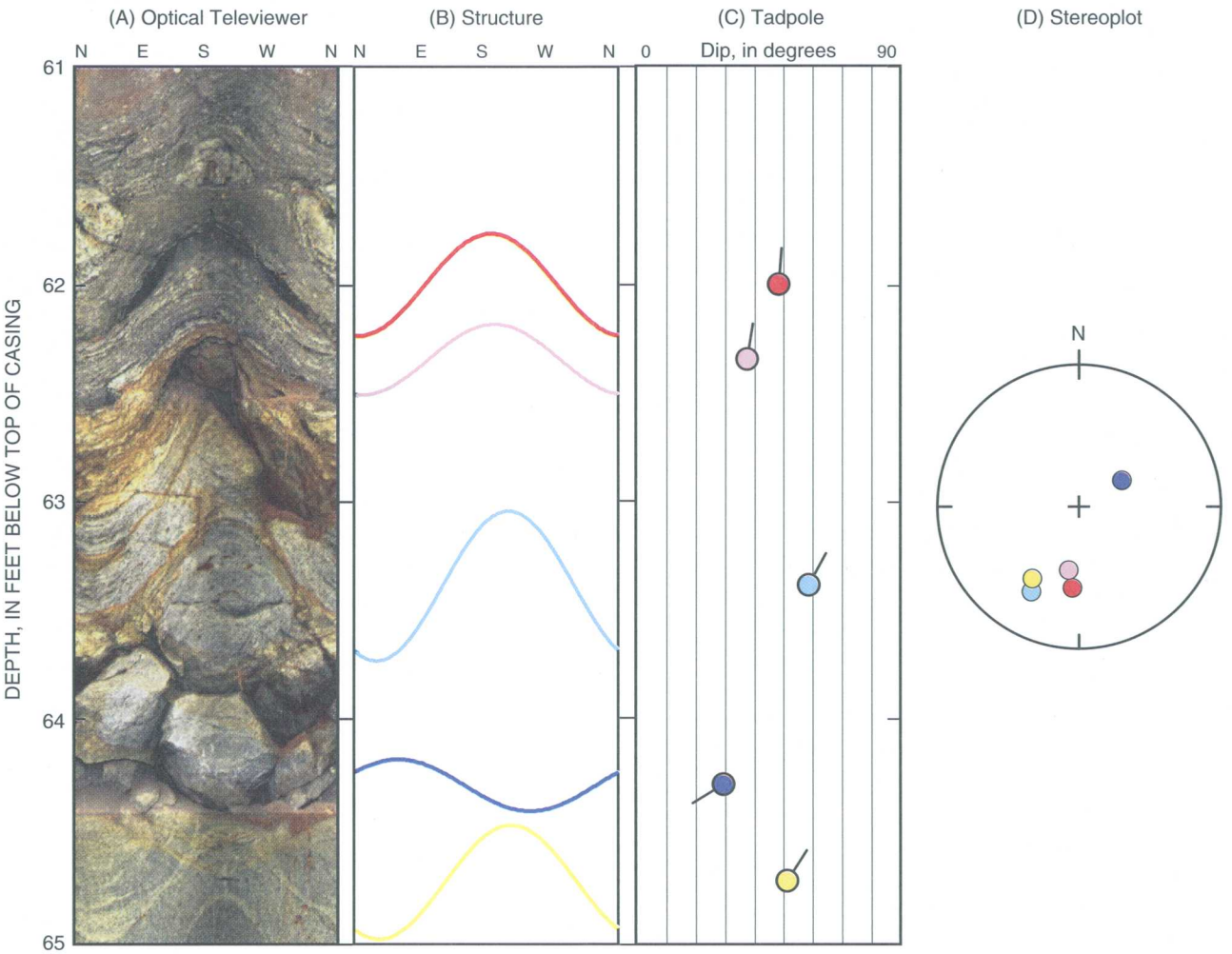

Figure 4. (A) Optical-televiewer image and the corresponding interpretation of planar data in (B) structural, (C) tadpole, and (D) stereographic-projection plots. The trace of the features on the structural projection (B) directly overlays on the image (A). In the tadpole plot (C), depth is plotted along the y-axis and the magnitude of dip is plotted on the x-axis. The tail of the tadpole points in the direction of dip relative to true north, which is at the top of the page. The poles to the planar features are shown in a lower-hemisphere equal-area stereonet (D), which reduces the plane to a point.

Because it is difficult to determine the direction of strike and dip on shallow features (with dips less than 30°), there is more uncertainty and variability in the strike of the poles that plot in the center of the stereoplots. In addition, a nearly vertical borehole is more likely to intersect the shallow dipping fractures and less likely to intersect a steeply dipping feature.

Optical-Televiewer Logs

In general, the quality of the OTV images is good. The water in the boreholes was fairly clear permitting the fracture location and rock type to be determined. The OTV images are provided in appendixes 1C-6C. The midpoint depths of interpreted features and their orientations are listed in tables in appendixes 1E-6E. The interpretations of fractures and foliation are provided in stereoplots and tadpole plots for each borehole in appendixes 1I-6I.

Acoustic-Televiewer Logs

ATV data are provided in appendixes 1C-6C in amplitude and acoustic caliper plots. The amplitude plots represent a continuous 360° view of the borehole wall. The image is shown as a projected image, split along north. A planar feature that intersects the borehole is seen as a sinusoid on the projected image. The acoustic caliper displays the traveltime converted to distance across the borehole in two directions, north-south and east-west. The scale of the north-south caliper has been reversed and decreases from 20 to 0 in., whereas the scale of the east-west caliper extends from 0 to 20 in. (for example, appendix 1C, left side). Plotted this way, the two adjacent traces give the appearance of a cross section of the borehole diameter.

Interpretation of features in the ATV data is presented in tables and in stereoplots and tadpole plots in appendixes 1F-6F and 1J-6J, respectively. The ATV data were used to determine the location and orientation of fractures and to determine the roughness of the borehole wall. Although foliation can sometimes be easily imaged with the ATV data, the foliation was not easy to detect in these boreholes. Thus, the interpretation of oriented features of the rock and foliation was based exclusively on the OTV data.

Heat-Pulse Flowmeter Logs

The heat-pulse flowmeter data are shown in plots and tables in appendixes 1B-6B and 1H-6H, respectively. The rate of flow that was measured in each borehole is reported in gallons per minute. By convention, upflow in a borehole is designated with a positive value and downflow with a negative value. A change in the measured rate of vertical flow in the borehole indicates an addition or removal of water between the two measurement locations. The flowmeter measurements were made from August through November 2001. Because vertical flow in a borehole is controlled by the hydraulic heads of the fractures that intersect the borehole, and those heads vary with time, the magnitude and direction of ambient flow may vary temporally. The date of data collection is noted on each flowmeter profile provided in the appendixes.

The plots of heat-pulse flowmeter data show the measured vertical flow rates on the x-axis and the depth on the y-axis (appendixes 1B-6B). Blue points indicate flow conditions measured under ambient conditions, and red points indicate measurements under pumping conditions. Solid lines indicate the interpretation of ambient flow and flow under pumping conditions. In some cases where only a fraction of the total vertical flow was measured under pumping conditions, the flow profiles were normalized to the pumping rate. This was only done after several attempts were made to obtain better results and only when the drawdown was under steady-state conditions.

For borehole MW302R and domestic well W202-NE, the ambient and pumping profiles were simulated using Paillet's numerical analysis (1998 and 2000) along with measured flow rates and fitted values of transmissivity and head. The modeled profiles are shown in figures 5 and 6 with hatched lines, next to the observed flowmeter profiles.

Borehole-Radar Reflection Logs

The processed borehole-radar data are shown in appendixes 1D-6D for each borehole. The radar plots show radar direct-wave and reflection amplitudes plotted as a function of depth. The horizontal axis represents the two-way traveltime, in microseconds, as well as the radial distance from the borehole, in feet. The location, orientation, and estimated length of reflectors are presented in tables in appendixes 1G-6G.

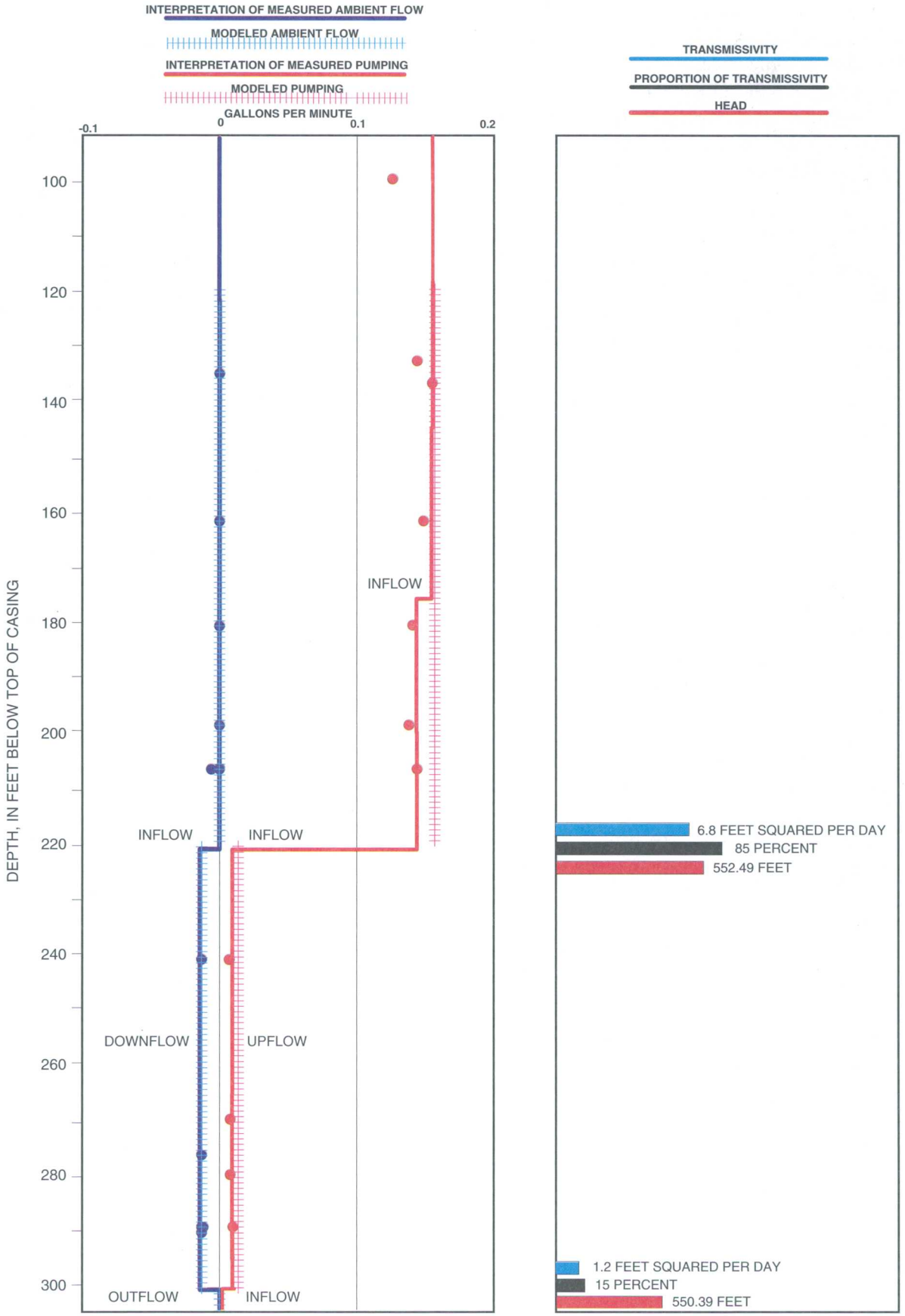

Figure 5. Heat-pulse flowmeter data, interpretation, and predicted flow models for borehole MW302R, UConn landfill study area, Storrs, Connecticut. Actual measurement locations are shown as filled circles on the plots.

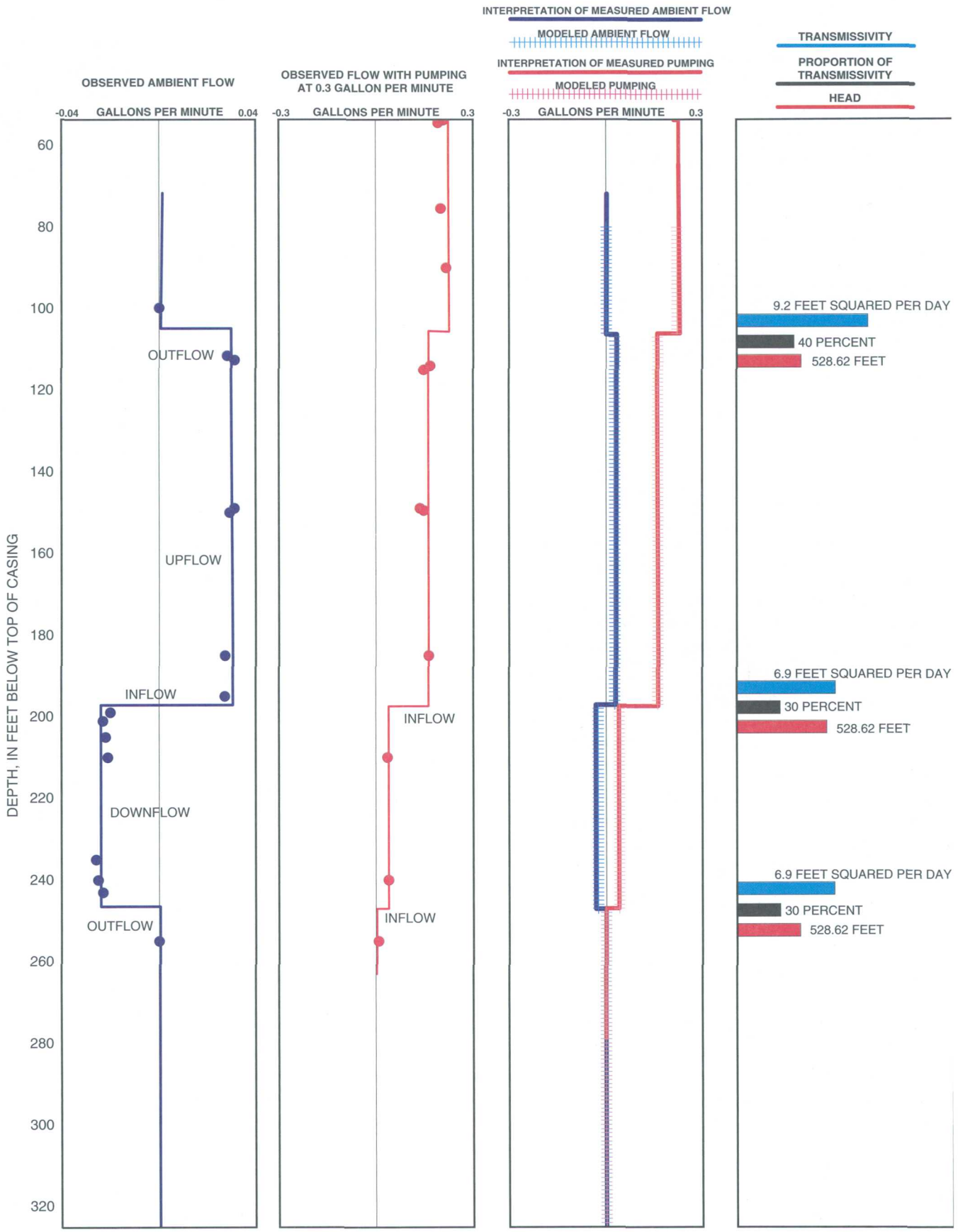

Figure 6. Heat-pulse flowmeter data, interpretation, and predicted flow models for domestic well W202-NE, UConn landfill study area, Storrs, Connecticut. Actual measurement locations are shown as filled circles on the plots.

Hydraulic Test Data

Open-hole hydraulic test data, including the specific capacity, pumping rate, and duration of test, are provided in appendix 7. Open-hole transmissivity estimates are reported in foot squared per day (ft^2/d). Results of all transmissivity testing are discussed and reported in the text. A comparison of the transmissivity values determined with the various methods is provided in the text.

RESULTS OF THE BOREHOLE-GEOPHYSICAL AND HYDRAULIC INVESTIGATION AT THE UCONN LANDFILL STUDY AREA

A detailed explanation of data and interpretation is provided for each of the boreholes, including a summary of the location and construction; lithologic, fracture, and hydraulic characterization; features observed in borehole-radar images; and means used to prevent cross contamination. The data for all boreholes are provided in appendixes 1-7.

In this report, the term "fracture" refers to planar discontinuities in the rock. No attempt was made to determine the genesis or mode of fracturing. The term "transmissive fracture" indicates a single fracture that was identified with the heat-pulse flowmeter as transmitting water to or from the borehole under ambient or low-rate pumping conditions. The term "transmissive zone" refers to a zone of the borehole where two or more closely spaced fractures were identified with the ATV and (or) OTV and where water flowed in or out of the borehole under ambient or pumping conditions. Because the heat-pulse flowmeter could not be placed between the fractures, the measured inflow was attributed to all fractures in the zone.

Borehole MW201R

Location and construction. Borehole MW201R was drilled on June 22, 2000, south of the landfill, adjacent to the intermittent tributary to Eagleville Brook, and near piezometer 13, which is completed about 10 ft into the shallow bedrock (fig. 1). MW201R was drilled using air-hammer rotary methods (Haley and Aldrich, Inc. and others, 2000). The steel casing was grouted to prevent flow between the unconsolidated sediments and the bedrock. MW201R is a 6-in.-diameter borehole, cased to 15.2 ft and open to a total depth of 126 ft below the top of the casing. The borehole location was selected to evaluate subsurface structures and (or) the possible southern migration of contaminants from the landfill and or the former chemical-waste disposal pits.

MW201R deviates about 2 ft towards the east (appendix 1A). The open-hole ambient water level was 0.8 ft below the top of casing on June 24, 2000, which was 0.7 ft above the land surface. All measurements are referenced to the top of casing, which was 1.6 ft above land surface.

On June 26, 2000, a temporary borehole liner was installed over the entire length of the borehole to prevent any vertical flow in the borehole and to minimize the potential for cross contamination. During the liner installation, a total of 220 gal of water was removed from the borehole. On August 7, 2000, the borehole liner was removed from MW201R so that geophysical logging could be conducted and the borehole could be developed. During the removal process, approximately 70 gal of water from a nearby fire hydrant was injected into the bottom of the borehole. Because no ambient flow was measured with the heat-pulse flowmeter in MW201R, the borehole liner was not reinstalled in the borehole.

On August 21, 2000, a total of 485 gal of water was removed from MW201R in an effort to clear cuttings and drilling debris from the borehole. The well reportedly was pumped dry (John Kastrinos, Haley and Aldrich, Inc., written commun., 2000).

Lithologic characterization. MW201R intersects laminated biotite-garnet schist and gneiss with felsic augens and quartzo-felspathic layers. The EM conductivity log showed a conductive spike centered at a depth of 38 ft below the top of casing. The OTV showed no apparent change in the lithology, but drilling records may indicate this conductive zone corresponds to a change in rock type (John Kastrinos, Haley and Aldrich, Inc., written commun., 2000). A fracture at a depth of 39 ft may be associated with this conductivity spike in the EM log (appendix 1B).

The gamma, caliper, electromagnetic, and OTV logs indicate a change in bedrock at a depth of about 82 ft below the top of casing. The logs showed a reduction in natural gamma emissions and a small increase in conductivity below a depth of 82 ft. In the top of the borehole, the caliper log indicated a slightly enlarged and rough borehole wall relative to the smooth and slightly smaller borehole diameter below a depth of

82 ft. Collectively, these logs indicate a possible change in rock type. This interpretation is consistent with the observations of the OTV images, which show a yellowish-greenish color of the gneiss above 82 ft and a darker gneiss below a depth of 82 ft.

Stereoplots (appendixes 1I and 1J) indicate the foliation in MW201R shows some clustering of the poles. The foliation generally strikes southwest and dips from 10 to 50° to the northwest. The tadpole plot (appendixes 1I and 1J) indicates minor variations in the foliation with depth. From a depth of 15 to 45 ft, the foliation strikes east-southeast (N103-152°E) and dips 14 to 21° to the south-southwest and also strikes south-southwest (N165-219°E) and dips 17 to 45° to the west-northwest. From a depth of 45 to 70 ft, the foliation strikes southwest to northwest (N200-330°E) and dips 21 to 54° to the northwest, north, and northeast. Below depths of about 70 ft, the foliation strikes southwest and dips at 15 to 50° to the northwest.

Fracture characterization. The orientation of all fractures observed on the OTV and ATV logs are provided in appendixes 1E and 1F, respectively. The fractures in MW201R have a wide variation in strike and dip at shallow to steep angles. Most of the fractures in MW201R cross cut the foliation.

The most transmissive fracture at a depth of about 60 ft is nearly parallel to foliation. Another fracture extends on the southwest side of the borehole from 57 to 60 ft, but it cannot be traced across the borehole. The other transmissive fracture, at about 39 ft, was identified in the ATV log but is difficult to identify in the OTV log. The strike of fractures identified near 39 ft was different for the OTV and ATV logs. Because the fractures were better imaged in the ATV log, their orientations were used in table 3. The orientations for the other fractures compare fairly well. The orientations of all the transmissive fractures in MW201R are listed in table 3.

Hydraulic characterization. Heat-pulse flowmeter logs were collected on August 29, 2000. No ambient flow was measured in MW201R with the heat-pulse flowmeter; however, the specific conductance logs indicated some potential inflow zones (appendix 1B). On August 16, 2000, a specific-conductance log was collected under ambient conditions. The log showed minor variations in the specific conductance in the open borehole, with minor variations at depths of 28 and 70 ft below the top of casing. Below a depth of 70 ft, the specific conductance decreased from 300 µS/cm to 200 µS/cm. This decrease in specific conductance is attributed to the 70 gal of water injected into the bottom of the well as the borehole liner was removed on August 7, 2000.

An additional specific conductance log, collected after the borehole was developed by pumping on August 29, 2000, showed a fairly uniform specific conductance of 335 µS/cm. This specific conductance log indicates the water that recharged the borehole after well development was likely from a single source or from sources with similar specific conductance.

On September 5, 2000, under pumping rates of 0.25 gal/min, the heat-pulse flowmeter indicated that the majority of water came from the fractures at a depth of about 39 ft below the top of casing (table 3). The remainder of the water was produced from a fracture at a depth of 60.3 ft and possibly a minor amount from the fracture at 76 ft below the top of casing.

Table 3. Transmissive fractures in borehole MW201R in the UConn landfill study area, Storrs, Connecticut

[Strike is reported in right-hand-rule in degrees east of true north. The dip is degrees from horizontal. The compass descriptor (N-E-S-W) of the direction of dip is provided for convenience and clarity]

Depth, in feet below top of casing	Transmissive fracture zone	Strike	Dip, in degrees	Direction of dip	Proportion of transmissivity, in percent
39.2	1	N48°E	43	SE	56
39.3	1	N76°E	14	S	
60.3	2	N261°E	14	N	32
76.0	3	N65°E	76	SE	12

At a pumping rate of 0.25 gal/min on August 29, 2000, the specific capacity was 0.06 gal/min/ft after 2 h. The open-hole transmissivity, estimated by the methods of Bradbury and Rothschild (1985), was 9.7 ft^2/d (appendix 7A). Heat-pulse flowmeter logs were collected under a second flow rate of 0.5 gal/min on September 7, 2000. After 2.25 h of pumping, the water level never reached a quasi-steady state. At a pumping rate of 0.5 gal/min, the open-hole transmissivity was 3.2 ft^2/d (appendix 7B). Flowmeter logs and measurements are provided in appendix 1B and 1H, respectively.

Discrete-interval hydraulic testing was conducted with the BAT^3 equipment on September 28 and 29, 2000. Differential head tests were conducted in four zones that isolate the fractures at depths of 39, 60, 76, and 97 ft below the top of casing.

The fracture at a depth of 39 ft was straddled with packers isolating the zone from 37.1 to 43.5 ft below the top of casing. Prior to pumping, the transducers indicated a downward potential from the upper most zone above 34.8 ft towards the test interval, and an upward potential from below the bottom of the lower packer towards the test interval (table 4). The fracture at a depth of 39 ft was pumped to obtain a water-quality sample and to determine the transmissivity. A constant pumping rate of 0.15 gal/min was used to collect the sample while simultaneously stressing the aquifer for the transmissivity test. Although there was sufficient water flow to produce a sample, the water level dropped below the operating range of the transducer, preventing the determination of transmissivity.

The fracture at 60 ft below the top of casing was straddled with packers isolating the zone from 56.1 to 62.5 ft below the top of casing. The test zone was pumped to obtain a water-quality sample and to determine the transmissivity. Prior to pumping, the transducers indicated similar head in the test zone and the upper zone, and an upward head potential from below 64.8 ft towards the test interval (table 4). A constant pumping rate of 0.25 gal/min was used to collect the sample while simultaneously stressing the aquifer for the transmissivity test. The transmissivity for this zone, determined with the Thiem equation, was 0.57 ft^2/d (or 6.5×10^{-6} ft^2/s) (appendix 7C).

A differential head test was conducted for the fracture at a depth of 76 ft below the top of casing. Because this zone was not thought to be transmissive, it was not sampled for water quality or pumped to estimate transmissivity. The packers were placed at center depths of 73.4 and 81.0 ft, so that the fracture at 76 ft was hydraulically isolated from the zones above and below the test zone. The packers were left overnight to allow the water levels to equilibrate. Results could not be obtained from the test zone because of a data logger error; however, the heads were measured in the upper and lower zones. Results indicate the head in the upper zone was higher than the head in the lower zone.

A differential head test was conducted for the fracture at 97 ft below the top of casing. Because this zone was not thought to be transmissive, it was not sampled for water quality or pumped to estimate transmissivity; however, the packers were placed to isolate the zone at 95.6 to 102.0 ft. The packers were left overnight to allow the water levels to equilibrate. Results indicate the water levels were similar in the test zone and the zone above, and there was downward head potential from 97 ft to the bottom zone (table 4).

Borehole-radar reflectors. Eleven reflectors were interpreted from the borehole-radar reflection

Table 4. Differential heads from BAT^3 testing in borehole MW201R in the UConn landfill study area, Storrs, Connecticut

[TOC, top of casing, in feet above NAVD88. *, no data. -- no value could be computed]

Well	Date of test	Depth of fracture, in feet	TOC	Hydraulic head, in feet above NAVD88			Head differential[1], in feet		
				Upper	Middle	Lower	Upper-Mid	Mid-Lower	Upper-Lower
MW201R	9/28/2000	39	554.22	551.34	550.97	551.59	0.37	-0.62	-0.25
	9/29/2000	60		551.87	551.64	552.12	0.23	-0.48	-0.25
	9/28/2000	76		551.59	*	546.23	--	--	5.36
	9/29/2000	97		551.57	551.55	549.24	0.02	2.31	2.33

[1]Head differential—positive number denotes downward potential; negative number denotes upward potential.

data collected in MW201R (appendix 1G). Seven of these reflectors correlate to interpreted features from the OTV logs, at depths of 39.7, 76.4, 79.7, 84.3, 112.9, 116.1, and 117.8 ft below the top of casing. Four of the reflectors imaged by the OTV are also imaged by the ATV. The other four reflectors that do not correlate with the OTV or ATV are projected to intercept below the bottom of the borehole at depths of 130.9, 156.2, 207.0, and 228.4 ft. The reflector that is projected to intercept the borehole at a depth of 130.9 ft, which is 5 ft below the bottom of the borehole, is significantly stronger than the other radar reflectors, and may indicate a major fracture or conductive lithologic layer. None of the interpreted radar reflectors correlate with the transmissive zones at depths of 39.2 and 60.3 ft.

A high-attenuation zone at the top of the log extends to a depth of about 49 ft below the top of casing (appendix 1D). Below a depth of about 90 ft below top of casing, the signal penetration increased substantially from about 25 to 60 ft radially away from the borehole. This zone also coincides with the change in rock type identified in the gamma, caliper, and OTV logs.

Discrete-interval packer system. A discrete-interval packer system was installed on March 24, 2001 (table 5). Three packers were installed at center depths of about 50, 70, and 90 ft below the top of casing, creating four discrete monitoring zones in the borehole. In general, the hydrographs for MW201R indicate an upward gradient between the upper three zones (Johnson and others, 2005). During the springs of 2001 and 2002, the upward gradient caused water to flow from the top of the borehole.

Table 5. Discrete-zone monitoring system installed in borehole MW201R in the UConn landfill study area, Storrs, Connecticut

[MP, measuring point on steel casing. BOC, bottom of casing. BOH, bottom of borehole. -- indicates no data. P, packer. DZM, discrete-zone monitoring. Height of measuring point relative to land surface. Altitude is based on NAVD88. All depth and elevation measurements are in feet]

Borehole	Elevation of MP on steel casing	Depth to BOC and BOH	Zone number	Depth to top of packer	Depth to bottom of packer	Elevation of top of zone and packer	Elevation of bottom of zone and packer	DZM channels	Water-quality sampling channels[1]
MW201R	554.22	15.2							
			1			539.02	505.22	0, 1	0 or 1
			P	49	51	505.22	503.22		
			2			503.22	485.22	2, 3	3
			P	69	71	485.22	483.22		
			3			483.22	465.22	4, 5	--
			P	89	91	465.22	463.22		
			4			463.22	428.56	6,7	--
		125.7							

[1]The channel number indicates which of the seven channels in the multi-channel tubing was sampled. Channel 0 indicates the sample was collected outside the multi-channel tubing.

Borehole MW202R

Location and construction. Borehole MW202R was installed on June 20, 2000, approximately 400 ft southwest of the former chemical-waste disposal pits and is approximately 200 ft east of MW302R (fig. 1). The borehole location was sited to assess hydraulic conditions and water quality west of the landfill and former chemical-waste disposal pits. MW202R was drilled to a depth of 126.6 ft below the top of casing, using air-hammer rotary methods (Haley and Aldrich, Inc. and others, 2000). A total of 13.5 ft of 6-in.-diameter steel casing was set and grouted to prevent flow between the unconsolidated sediments and the bedrock. MW202R deviates less than 1 ft over the entire length of the borehole. All measurements provided in appendix 2 were referenced to the top of casing, which is 2.1 ft above the land surface.

A borehole liner was installed on June 28, 2000. During installation, 120 gal of water were removed from the well. The borehole liner was removed on August 2, 2000, so that geophysical logging could be conducted and the borehole could be developed. The open-hole water level on August 4, 2000, was 14.29 ft below the top of casing. During the removal of the borehole liner, 53 gal of water were injected into the bottom of the borehole. On August 22, 2000, borehole MW202R was developed by pumping. A total of 187 gal of water was removed from the borehole (John Kastrinos, Haley and Aldrich, Inc., written commun., 2000).

A specific-conductance log collected on August 3, 2000, was fairly uniform at about 150 µS/cm, but showed some minor changes at depths of 32 and 44 ft (appendix 2B). A specific-conductance log collected on August 31, 2000, after the borehole was developed by overpumping, showed a uniform response of about 340 µS/cm over the entire length of the borehole, indicating the borehole was recharged by a single source of water that was more conductive than the water remaining in the borehole after drilling.

Lithologic characterization. MW202R intersects laminated biotite-garnet schist and gneiss with some augen-gneiss zones. Narrow igneous intrusions or quartzo-felspathic layers are parallel to foliation. The stereoplots show the poles to lithologic features in yellow (appendix 2I). These felsic layers cluster in two sets—one set is parallel to foliation and strikes southwest and dips northwest. The other set occurs below a depth of 70 ft and strikes northwest and dips northeast. Both sets of felsic layers have shallow to moderate dips. A felsic zone at depths of 19 to 22 ft below the top of casing is visible on the OTV, ATV, and gamma logs. The upper and lower contacts are parallel to the foliation and layering in the bedrock.

The orientation of the foliation is similar to the felsic layering. In general, the foliation in MW202R strikes southwest and dips to the northwest. The foliation changes abruptly at a depth of 30 ft from southwest dipping to northwest dipping and changes at a depth of about 106 ft from northwest dipping to northeast dipping. The tadpole plot for MW202R shows foliation from depths of 98 to 110 ft below top of casing strikes northwest and dips northeast.

A conductivity spike at a center depth of 31.5 ft in the EM log peaks at 1,265 mS/m. A fracture also was identified at 31 ft below the top of casing. The OTV log indicated a small amount of iron-oxide staining at about 31 ft below the top of casing, which suggests it is a hydraulically active fracture. Another conductivity spike at 40.8 ft below the top of casing peaks at 10,000 mS/m, and does not appear to be related to a fracture.

Fracture characterization. The orientations of all fractures observed on the OTV and ATV logs are provided in appendixes 2E and 2F, respectively. Initially the ATV log was poorly oriented to magnetic north and drifted over the depth of the borehole. The depth and the magnitude of dip of the planar features were not affected by the problem. Duplicate OTV logs collected on August 3 and August 28, 2000, showed reproducible results, and these logs were used to reorient the ATV logs collected in MW202R relative to true north. The images and the interpreted data have been rotated to correct for the problem.

The stereoplots and tadpole plots indicate the fractures observed in the ATV and OTV logs (appendixes 2I and 2J, respectively) are southwest striking and northwest dipping, and northeast striking and southeast dipping. Possible transmissive fractures were identified at depths of 31.0, 105.6, and 107.2 ft (table 6). The fractures at depths of about 31 and 107.2 ft are nearly parallel to foliation.

Hydraulic characterization. Flowmeter logs collected under ambient conditions on August 4 and September 9, 2000, indicated no measurable ambient flow. Flowmeter logs under pumped conditions were collected on August 11, August 16, and September 6, 2000. A pumping rate of 0.25 gal/min was used to

Table 6. Transmissive fractures in borehole MW202R in the UConn landfill study area, Storrs, Connecticut

[Strike is reported in right-hand-rule in degrees east of true north. The dip is degrees from horizontal. The compass descriptor (N-E-S-W) of the direction of dip is provided, for convenience and clarity]

Depth, in feet below top of casing	Transmissive fracture zone	Strike	Dip, in degrees	Direction of dip	Proportion of transmissivity, in percent
30.9	1	N193°E	44	W	5
105.6	2	N245°E	47	NW	95
107.2	2	N290°E	35	NE	

stress the borehole each time. On September 6, 2000, after 4 h of pumping in MW202R, the water level continued to decline at a rate of 0.05 ft/min and did not reach a steady state. After 2.5 h of pumping the borehole at 0.25 gal/min, flowmeter logs were collected despite the fact the borehole did not reach a quasi-steady state. Hence, a small amount (approximately 0.07 gal/min) of water that was going to the pump was derived from well-bore storage rather than from the formation. All three heat-pulse flowmeter profiles indicate that the majority of the inflow comes from the fractures at 105 to 107 feet below top of casing. The log collected on August 11, 2000, along with the specific- conductance logs, shows a possible inflow zone at 30 ft below top of casing (appendix 2B).

The water levels were monitored during open-hole pumping tests. After pumping the borehole at a rate of 0.25 gal/min, the water level in MW202R did not reach a steady state. The water level in the borehole continued to decline at a rate of 0.05 ft/min. Because the water level could not achieve steady state, the open-hole transmissivity was estimated using a non-equilibrium method. The transmissivity was estimated at 1 ft^2/d (appendix 7B).

Discrete-zone hydraulic tests were conducted on fractures at 30.9 ft and from 105 to 107 ft with the BAT^3 equipment. The BAT^3 indicated a downward potential with heads of 567.2 to 558.6 ft in the fracture at 30.9 ft and the fracture zone from 105 to 107 ft, respectively (table 7).

Hydraulic tests were conducted in the test zone from 27.3 to 33.7 ft below the top of casing. The zone was pumped at 0.15 gal/min, and a sample was collected; however, the water level declined below the operating range of the transducer. Consequently, the head and the transmissivity could not be determined. A hydraulic test was conducted from the deeper zone at a depth of 104.3 to 110.7 ft below the top of casing, and a sample was collected. The zone was pumped at 0.15 gal/min for 1.1 h and the transmissivity estimated from this zone was 0.2 ft^2/d (appendix 7C).

Borehole-radar reflectors. The borehole-radar log showed a high-attenuation zone from a depth of about 25 to 50 ft below the top of casing (appendix 2D). The high-attenuation zone coincides with the location of the high conductivity spikes in the EM induction logs. Low-velocity zones were identified at depths of 48 and 85 ft below the top of casing. The low-velocity zone at 49 ft coincides with a feature observed in the OTV logs.

Eight reflectors were interpreted from the borehole-radar reflection data collected in MW202R. Three of the reflectors, at depths of 30.8, 49.9, and 98.8 ft, correspond to features interpreted from the OTV log. The reflector at a depth of 30.8 ft also correlates the results of the ATV interpretation with a known transmissive zone. None of the reflectors correlate with the transmissive zones at 105.6 or 107.2 ft. Two of the reflectors are projected outside of the interval of the borehole, at 38.1 ft above the top of casing and at 143.7 ft below the top of casing.

A high-attenuation zone extends from the top of the log to a depth of about 54 ft below the top of casing (appendix 2D). Below the high-attenuation zone, the radar signal penetrates about 70 ft radially from the borehole. A low-velocity zone centered at about 85 ft does not correlate with any of the interpreted radar reflectors, but does correlate with fractures identified by the OTV. A table of results is provided in appendix 2G.

Discrete-interval packer system. A discrete-interval packer system was installed on March 20, 2001 (table 8). Two packers were installed at center depths of about 38 and 100 ft below the top of casing, creating three discrete monitoring zones in the borehole. In general, the hydrographs for MW202R indicate a downward hydraulic potential between the three zones (Johnson and others, 2005).

Table 7. Differential heads from BAT[3] testing in borehole MW202R in the UConn landfill study area, Storrs, Connecticut

[TOC, top of casing, in feet above NAVD88]

Well	Date of test	Depth of fracture, in feet	TOC	Hydraulic head, in feet above NAVD88			Head differential[1], in feet		
				Upper	Middle	Lower	Upper-Mid	Mid-Lower	Upper-Lower
MW202R	10/4/2000	30.9	582.33	566.43	567.21	564.56	-0.78	2.65	1.87
	10/5/2000	105-107		567.21	558.57	564.17	8.64	-5.60	3.04

[1]Head differential—positive number denotes downward potential; negative number denotes upward potential.

Table 8. Discrete-zone monitoring system installed in borehole MW202R in the UConn landfill study area, Storrs, Connecticut

[MP, measuring point on steel casing. BOC, bottom of casing. BOH, bottom of borehole. -- indicates no data. P, packer. DZM, discrete-zone monitoring. Height of measuring point relative to land surface. Altitude is based on NAVD88. All depth and elevation measurements are in feet]

Borehole	Elevation of MP on steel casing	Depth to BOC and BOH	Zone number	Depth to top of packer	Depth to bottom of packer	Elevation of top of zone and packer	Elevation of bottom of zone and packer	DZM channels	Water-quality sampling channels[1]
MW202R	582.33	13.5							
			1			568.83	545.33	0, 1, 2	0 or 1
			P	37	39	545.33	543.33		
			2			543.33	483.33	3, 4	--
			P	99	101	483.33	481.33		
			3			481.33	455.36	5, 6, 7	5 or 6
		127.0							

[1]The channel number indicates which of the seven channels in the multi-channel tubing was sampled. Channel 0 indicates the sample was collected outside the multi-channel tubing.

Borehole MW203R

Location and construction. Borehole MW203R was drilled on June 21, 2000, in the area of the former chemical-waste disposal pits, west of the landfill (fig. 1). MW203R was drilled using air-hammer rotary methods (Haley and Aldrich, Inc. and others, 2000). The steel casing was set approximately 5 ft into bedrock and grouted to prevent flow between the unconsolidated sediments and the bedrock. MW203R is a 6-in.-diameter borehole cased to 14.5 ft and completed to a depth of 127.9 ft below the top of casing. The borehole location was selected to assess the geohydrology in the area of the former chemical-waste disposal pits. MW203R deviates less than 1 ft from vertical over the length of the borehole (appendix 3A).

The ambient water level in the open borehole was 10.56 ft below the top of casing on June 22, 2000. All measurements are referenced to the top of casing, which was 1.9 ft above land surface.

A borehole liner was installed on June 22, 2000. During installation, 165 gal of water were removed from the borehole. The liner was extracted from the borehole on August 14, 2000, during which 60 gal of water were injected below the borehole liner for removal. On August 23, 2000, borehole MW203R was developed by overpumping (Haley and Aldrich, Inc., and others, 2002). A total of 350 gal of water was removed, and MW203R was reportedly pumped dry. Water-level records obtained during the development indicate a recharge rate of approximately 0.5 gal/min (John Kastrinos, Haley and Aldrich, Inc., written commun., 2000).

The specific-conductance log collected on August 16, 2000, shows two zones of interest—one at the top of the borehole and the other at the bottom (appendix 3B). This specific-conductance log indicates a possible source of inflow at 32 ft below the top of casing. The low specific conductance of the water at the

bottom of the log is attributed to the 60 gal of water injected into the bottom of the borehole during the removal of the borehole liner.

The specific-conductance log collected on September 12, 2000 indicates a change in specific conductance at a depth of approximately 32 to 34 ft and at about 50 ft below the top of casing. Below 50 ft, the specific-conductance log is fairly uniform at about 330 µS/cm and is more conductive than the water that was in the borehole on August 16, 2000, which was about 130 µS/cm. These results suggest that after borehole development on August 23, 2000, the borehole was recharged with water from a single source and the water was more conductive than the water that remained in the borehole after drilling.

Lithologic characterization. Borehole MW203R intersects biotite-garnet schist and gneiss with quartzo-felspathic layers. The texture of the bedrock varies from laminated schist to banded gneiss with fairly uniform orientation in foliation and layering (appendix 3C).

The stereoplot of foliation indicates the foliation strikes in a uniform direction to the southwest and dips to northwest over various dip magnitudes (from 4 to 59°) (appendixes 3I and 3J). The tadpole plot for MW203R shows that the magnitude of dip changes gradually over the depth of the borehole and may indicate the presence of large-scale folding (appendixes 3I and 3J).

Fracture characterization. The orientation of all fractures observed on the OTV and ATV logs are provided in appendixes 3E and 3F, respectively. Most of the fractures observed in MW203R are southwest striking and northwest dipping. The only transmissive fracture in the borehole is at a depth of 32.2 ft below the top of casing and is nearly parallel to foliation (table 9). A tightly clustered set of very steeply dipping, sealed fractures was observed in the OTV logs of MW203R. The tadpole plots (appendixes 3I and 3J) indicate these fractures were observed from depths of 60 to 127 ft below the top of casing. The stereoplot indicates the sealed fractures cross cut the foliation of the schist. The poles to the planes of the sealed fractures cluster, indicating this fracture set strikes northeast and dips steeply to the southeast.

Hydraulic characterization. No ambient flow was measured with the heat-pulse flowmeter on September 12, 2000. Heat-pulse flowmeter logs collected under pumping conditions of 0.25 gal/min on September 12, 2000, indicate possible inflow into the borehole at 32 ft below the top of casing. This was the only transmissive zone identified in the borehole. At this pumping rate, steady-state conditions were not achieved, which indicates some of the water that was going to the pump was derived from well-bore storage. Although quasi-steady state was not reached, the heat-pulse flowmeter data were collected after about 2 h of pumping. The water level continued to decline at a rate of 0.06 ft/min, which is equivalent to 0.08 gal/min. During the heat-pulse flowmeter logging, the water level declined below the productive fracture at a depth of 32 ft below the top of casing. Hence, the inflow from the fracture could not be measured with the heat-pulse flowmeter. By injecting water into the top of the borehole, the outflow could have been measured with the heat-pulse flowmeter; however this may have affected the water chemistry of the zone. The water levels were monitored during the open-hole pumping test. After pumping the borehole at a rate of 0.25 gal/min, MW203R did not reach a steady water level. The open-hole transmissivity was estimated using a non-equilibrium method. The transmissivity was estimated at 1.0 ft^2/d (appendix 7B).

On October 13, 2000, BAT^3 equipment was used to sample and hydraulically test the fracture at a depth of 32 ft and the interval above. The zone was pumped for 0.7 h at 0.22 gal/min. The estimate of transmissivity from the constant-rate pumping test was 3.2 ft^2/d (appendix 7C), which is similar to the open-hole transmissivity results. The differential-head tests indicated downward head potentials from the upper zone toward the test zone and from the test zone to the lower zone.

Table 9. Transmissive fractures in borehole MW203R in the UConn landfill study area, Storrs, Connecticut

[Strike is reported in right-hand-rule in degrees east of true north. The dip is degrees from horizontal. The compass descriptor (N-E-S-W) of the direction of dip is provided, for convenience and clarity]

Depth, in feet below top of casing	Transmissive fracture zone	Strike	Dip, in degrees	Direction of dip	Proportion of transmissivity, in percent
32.2	1	N185°E	15	W	100

Another constant-rate pumping test was attempted in the interval from 61.8 to 69.3 ft below the top of casing, which isolated the most prominent fracture below 32 ft. The fracture at a depth of 63 ft did not produce water. A differential-head test conducted for the same zone produced a downward potential from the upper zone towards the test zone and a downward potential from the test zone to the lower portion of the borehole. Results are summarized in table 10.

Borehole-radar reflectors. Eleven reflectors were interpreted from the borehole-radar reflection data collected in MW203R (appendix 3G). Five of the reflectors, at depths of 16.7, 17.7, 34.5, 83.3, and 111.2 ft, correlate with the features identified in the OTV logs, and a sixth, a near-horizontal feature at a depth of 69.9 ft, is interpreted to have an azimuth of 180° from the OTV feature. Determining the strike of a near-horizontal feature is difficult and subject to error for both methods. The reflector at a depth of 83.3 ft is the only feature that correlates with the ATV logs. None of the reflectors correlate with the transmissive zone at a depth of 32.3 ft. Three of the reflectors project below the bottom of the casing, at depths of 128.9, 149.3, and 181.8 ft below the top of casing.

The radar penetration increases gradually with depth, from about 30 ft radially at the top of the borehole to about 60 ft near the bottom (appendix 3D). The bedrock surrounding MW203R has a generally uniform velocity.

Discrete-interval packer system. A discrete-interval packer system was installed on March 29, 2001 (table 11). Two packers were installed at center depths of about 44 and 89 ft below the top of casing, creating three discrete monitoring zones in the borehole. The hydrographs for MW203R consistently indicate downward potentials between the zones over most of the period of record (Johnson and others, 2005).

Table 10. Differential heads from BAT[3] testing in borehole MW203R in the UConn landfill study area, Storrs, Connecticut

[TOC, top of casing in feet]

Well	Date of test	Depth of fracture, in feet	TOC	Hydraulic head, in feet above NAVD88			Head differential[1], in feet		
				Upper	Middle	Lower	Upper-Mid	Mid-Lower	Upper-Lower
MW203R	10/13/2000	32	576.9	564.71	561.04	561.06	3.67	-0.02[2]	3.65
		63		562.16	560.50	554.50	1.66	6.00	7.66

[1]Head differential—positive number denotes downward potential; negative number denotes upward potential.
[2]Indicates the differential head is less than the resolution of the transducers.

Table 11. Discrete-zone monitoring system installed in borehole MW203R in the UConn landfill study area, Storrs, Connecticut

[MP, measuring point on steel casing. BOC, bottom of casing. BOH, bottom of borehole. -- indicates no data. P, packer. DZM, discrete-zone monitoring. Height of measuring point relative to land surface. Altitude is based on NAVD88. All depth and elevation measurements are in feet]

Borehole	Elevation of MP on steel casing	Depth to BOC and BOH	Zone number	Depth to top of packer	Depth to bottom of packer	Elevation of top of zone and packer	Elevation of bottom of zone and packer	DZM channels	Water-quality sampling channels[1]
MW203R	576.90	14.4							
			1			562.50	533.90	0, 1, 2	0 or 1
			P	43	45	533.90	531.90		
			2			531.90	488.90	3, 4, 5	--
			P	88	90	488.90	486.90		
			3			486.90	451.90	6, 7	--
		125.0							

[1]The channel number indicates which of the seven channels in the multi-channel tubing was sampled. Channel 0 indicates the sample was collected outside the multi-channel tubing.

Borehole MW204R

Location and construction. Borehole MW204R was drilled on June 21, 2000. The borehole is located west of the landfill, north of the former chemical-waste disposal pits, and north of the ground-water divide. The borehole location was selected to assess the ground-water levels near the ground-water divide and possible contaminant migration from the landfill and former chemical-waste disposal pits. MW204R was drilled using air-hammer rotary methods (Haley and Aldrich, Inc. and others, 2000). A total of 13 ft of 6-in.-diameter steel casing was set in the borehole. The steel casing was grouted to prevent flow between the unconsolidated sediments and the bedrock. The borehole is open below the casing to a depth of 127.8 ft below the top of casing. MW204R deviates a total of 2.5 ft to the east (appendix 4A). The ambient water level was 6.96 ft below the top of casing on August 9, 2000. All measurements were referenced to the top of casing, which was 2.0 ft above the land surface.

A borehole liner was installed on June 23, 2000. During the installation, a total of 158 gal of water was removed from the borehole. On August 8, 2000, the borehole liner was removed. During the liner extraction, a total of 147 gal was injected into the bottom of the borehole. On August 18, 2000, MW204R was developed by over pumping. A total of 209 gal was removed and the borehole was reportedly pumped dry (John Kastrinos, Haley and Aldrich, Inc., written commun., 2002).

Specific-conductance logs collected on August 9, 2000, showed an abrupt change at 45 ft (appendix 4B). The specific conductance at the top of the borehole ranged from 230 to 240 µS/cm and gradually declined to about 140 µS/cm below a depth of 45 ft. The decreased specific conductance of water in the lower 80 ft of the borehole is interpreted as water injected into the bottom of the borehole while the borehole liner was being removed. The 147 gal of injected water is equivalent to 95 ft of water in the borehole. These results suggest the bottom of the borehole is not transmissive.

The specific-conductance logs collected on August 22, 2000, have a uniform specific conductance of 240 to 260 µS/cm. The log indicates water that recharged the borehole after well development was likely from a single source of water or sources having the same specific conductance.

The temperature logs collected on August 22, 2000, after pumping for the heat-pulse flowmeter indicate an abrupt change of 2°F at 30 to 32 ft. The profile indicates all of the water entering the borehole occurred at 30 to 32 ft below top of casing.

Lithologic characterization. Images from the OTV logs indicate MW204R intersects laminated biotite-garnet schist that has a fairly uniform texture over the length of the borehole. From the bottom of the casing to a depth of about 25 ft, the schist appears to be lighter in color and possibly altered. Below 25 ft, the schist is biotite-rich with some quartzo-felspathic layers. The foliation generally dips towards the northwest and towards the east at fairly shallow to moderate dip angles. The tadpole and stereoplots (appendixes 4I and 4J) indicate that above a depth of 54 ft, the foliation dips west-northwest at 20 to 40°, which relates to a south-southwest strike. From a depth of 54 to 90 ft below the top of casing, the foliation strikes north and dips from less than 10° to about 50° to the east. Below a depth of 90 ft, most of the foliation strikes south-southwest and dips less than 40° towards the west-northwest.

Stereoplots were constructed for three depth zones in the borehole (appendixes 4I and 4J). Above a depth of 52 ft, the poles to the foliation cluster tightly in the southeast quadrant of the stereoplot, indicating the foliation strikes southwest and dips from 10 to 40° to the northwest. From a depth of 52 to 90 ft below the top of casing, the foliation is fairly uniform and strikes north and dips east. The foliation below a depth of 90 ft is similar to the foliation observed at the top of the borehole, where it strikes southwest and dips northwest.

Fracture characterization. The orientation of all fractures observed on the OTV and ATV logs are provided in appendixes 4E and 4F, respectively. The fractures observed on the OTV and ATV logs from this borehole are oriented over a variety of strikes. Many strike northeast and dip steeply to south-southeast while another group strikes south and dips at a shallower to moderate angle to the west-northwest. The poles to planes of sealed fractures cluster tightly in the northwest quadrant of the stereoplot (appendixes 4I and 4J). These sealed fractures generally strike northeast and dip very steeply to the south and southeast. The orientations of transmissive fractures are listed in table 12. These transmissive fractures were identified near the top of the borehole at 21.3 and 22.4 ft. The fracture at 22.4 ft is nearly parallel to foliation.

Table 12. Transmissive fractures in borehole MW204R in the UConn landfill study area, Storrs, Connecticut

[Strike is reported in right-hand-rule in degrees east of true north. The dip is degrees from horizontal. The compass descriptor (N-E-S-W) of the direction of dip is provided, for convenience and clarity]

Depth, in feet below top of casing	Transmissive fracture zone	Strike	Dip, in degrees	Direction of dip	Proportion of transmissivity, in percent
21.3	1	N68°E	55	S	50
22.4	1	N192°E	30	W	50

Hydraulic characterization. Heat-pulse flowmeter measurements were collected under ambient conditions on August 10, 2000. No ambient flow was measured with the heat-pulse flowmeter in MW204R. Flowmeter measurements under pumping conditions were collected on August 21, August 30, and September 11, 2000. All measurements were taken with pumping rates of about 0.25 gal/min. Flow profiles for each of these testing events identified inflow between depths of about 18 and 25 ft below the top of casing. The flow profile on August 21, 2002, further determined that inflow entered the borehole between depths of 21.0 and 25.4 ft below the top of casing. The flow was attributed to the fractures at depths of 21.3 and 22.4 ft below the top of casing, although the inflow may come from either one or both of the fractures. No other transmissive fractures were identified in MW204R with the heat-pulse flowmeter.

Good periods of quasi-steady-state conditions were achieved in the open-hole pumping tests collected on August 22, August 30, and September 11, 2000. Based on these pumping events, the specific capacity for this borehole ranged from 0.03 to 0.06 gal/min/ft. The open-hole transmissivity, which was attributed to the fractures at depths of 21.3 and 22.4 ft below the top of casing, ranged from 4.9 to 10 ft^2/d (appendix 7A).

Although the heat-pulse flowmeter only identified hydraulically active fractures near 21 ft, the BAT^3 equipment also was used to test the fractures at 45 and 75 ft. The fracture at 75 ft, which is prominent on the OTV and ATV logs, was isolated for a differential head test. Packers were set on October 10, 2000, at center depths of 74.3 and 80.7 ft and were left overnight to allow the heads to equilibrate. The differential heads indicated downward potentials between the upper zone and the test zone, and between the lower zone and the test zone (table 13).

The BAT^3 equipment also was used to isolate the zone from 41.3 to 47.7 ft to test the hydraulic properties and head of the fracture at 45 ft relative to the zones above and below the test interval. The test zone at 45 ft was pumped at 0.15 gal/min; however, the zone was unable to produce water. Hydraulic heads collected at these zones indicate an upward potential between the middle and upper zone and a downward potential between the lower zone and the test zone. The heads of the isolated zones for fractures at 76, 45, and above 29 ft had heads of 563.9, 566.0, and 565.6, respectively (table 13). The tests indicate the heads in the upper two fractures are nearly equal, but there was an upward potential between the fracture at 45 ft and the fractures at the top of the borehole. There was a downward potential between the upper fractures (in the zone from 13 to 29 ft and near 45 ft) and the lowermost fracture at 76 ft below the top of casing (table 13).

The uppermost fractures at 21.3 and 22.4 ft below the top of casing were isolated using the BAT^3 equipment. The top of the lower packer was set at a depth of 29.7 ft and the upper packer was not inflated. Hence, the test zone extended from the base of casing at a depth of 13.1 ft to 29.7 ft below the top of casing. Two pumping tests were conducted at rates of 0.2 and 0.5 gal/min, which yielded transmissivity values of 8.2 and 11 ft^2/d, respectively (appendix 7C).

Borehole-radar reflectors. Ten reflectors were interpreted from the borehole-radar reflection survey conducted in MW204R (appendix 4G). Five of the reflectors, at depths of 22.3, 50.9, 56.1, 61.4, and 63.7 ft, correlate with features interpreted in the OTV logs, and only the reflector at 22.3 ft correlates with the results of the ATV. This reflector correlates with the known transmissive zone at 22.3 ft, but none of the reflectors correlate with the fracture at 21.3 ft. Three of the interpreted reflectors project outside of the borehole interval, and are projected to the line of the borehole at 54.1 ft above the top of casing, 143.7 ft below the top of casing, and at 266.7 ft below the top of casing.

Radar signal penetration in this reflection profile is generally poorer than the other profiles collected at this site (appendix 4D). The maximum radial penetration is about 30 ft. There are two high-attenuation, low-velocity zones in the field data. The first extends from about 52 to 75 ft, and the second from 90 to 105 ft. These zones coincide with sections of the borehole where northeast-southwest striking, southeast-northwest steeply dipping, sealed fractures were identified.

Discrete-interval packer system. Two packers were installed at center depths of about 31 and 69 ft below top of casing (table 14). A downward potential was recorded for most of the period of the water-level record. The potentials were greater during hydraulic periods of recharge in winter and spring than in summer and fall.

Table 13. Differential heads from BAT[3] testing in borehole MW204R in the UConn landfill study area, Storrs, Connecticut

[TOC, top of casing, in feet above NAVD88]

Well	Date of test	Depth of fracture, in feet	TOC	Hydraulic head, in feet above NAVD88			Head differential[1], in feet		
				Upper	Middle	Lower	Upper-Mid	Mid-Lower	Upper-Lower
MW204R	10/11/2000	13-30[2]	575.34	565.63[2]	565.63	563.98	0.00[2]	1.65	1.65
	10/11/2000	45		565.75	566.03	563.87	-0.28	2.16	1.88
	10/10/2000	76		565.62	563.91	556.10	1.71	7.81	9.52

[1]Head differential—positive number denotes downward potential; negative number denotes upward potential.
[2]Upper and middle zone were the same in this test as the upper packer was not inflated

Table 14. Discrete-zone monitoring system installed in borehole MW204R in the UConn landfill study area, Storrs, Connecticut

[MP, measuring point on steel casing. BOC, bottom of casing. BOH, bottom of borehole. -- indicates no data. P, packer. DZM, discrete-zone monitoring. Height of measuring point relative to land surface. Altitude is based on NAVD88. All depth and elevation measurements are in feet]

Borehole	Elevation of MP on steel casing	Depth to BOC and BOH	Zone number	Depth to top of packer	Depth to bottom of packer	Elevation of top of zone and packer	Elevation of bottom of zone and packer	DZM channels	Water-quality sampling channels[1]
MW204R	575.34	13.1							
			1			562.24	545.34	0, 1, 2	0 or 1
			P	30	32	545.34	543.34		
			2			543.34	507.34	3, 4, 5	--
			P	68	70	507.34	505.34		
			3			505.34	447.57	6, 7	--
		127.8							

[1]The channel number indicates which of the seven channels in the multi-channel tubing was sampled. Channel 0 indicates the sample was collected outside the multi-channel tubing.

Borehole MW302R

Location and construction. Borehole MW302R is located about 1,000 ft west of the landfill and about 200 ft west of MW202R (fig. 1). It was drilled during December 2000 to a depth of about 300 ft below land surface using dual-rotary methods that advanced 10-in.-diameter spin casing through the overburden simultaneously with the advancement of an air-rotary hammer. A 10-in.-diameter steel casing was set through the overburden into about 5 ft of bedrock. Below the steel casing, a 10-in.-diameter hole was drilled to 125 ft below land surface, and an 8-in.-diameter polyvinyl chloride (PVC) casing was installed in the hole. PVC casing was used because radar waves can penetrate PVC. The annular space around the PVC casing was grouted with a low bentonite-to-cement ratio grout, in an effort to minimize the attenuation of the EM waves used in borehole-radar imaging. In addition, a 6-in.-diameter temporary steel casing was set to a depth of about 127 ft to protect the PVC casing during drilling. Below the PVC casing, a 6-in.-diameter borehole was drilled with air-hammer rotary methods to a depth of 303 ft below the top of the PVC casing. All measurements are referenced to 1.5 ft above land surface.

Lithologic characterization. Results of borehole-imaging logs and conventional logs indicate the rock type is coarse-grained biotite-garnet schist to gneiss with quartzo-felspathic layers and augens. Below a depth of 225 ft, the bedrock is a banded gneiss. The poles to planes of foliation and felsic veins in MW302R cluster in two sets (appendix 5I). One set strikes southwest and dips northwest, and the other set strikes northwest and dips northeast. From the bottom of the casing at 127 ft to a depth of 180 ft, the foliation dips northwest; from 180 to 225 ft, the foliation dips northeast; and below 225 ft, the foliation dips northwest. Also, most of the felsic veins are present in the middle zone from 180 to 225 ft below the top of casing (appendix 5C). The EM induction log produced a large double-peak spike (of 800 mS/m) from about a depth of 38 to 45.2 ft in the same area where oxidized rock cuttings were observed at the time of drilling (appendix 5B).

Fracture characterization. The orientation of all fractures observed on the OTV and ATV logs are provided in appendixes 5E and 5F, respectively. The orientation of fractures in the borehole strike and dip in many directions and most are parallel to foliation, but many cross cut the foliation of the schist. The stereoplots do not show a clustering of fractures, which indicates wide variation in strike and dip. The characteristics of the transmissive factures are shown in table 15.

Hydraulic characterization. Specific-conductance logs collected on February 15, 2001, indicated the possibility of hydraulically active fractures at depths of 175, 220, and 301 ft, and leakage at the base of the casing.

On February 26, 2001, heat-pulse flowmeter logging indicated minor ambient inflow of 0.012 gal/min, coming from the base of the casing and flowing downward in the borehole. Additional water entered the borehole under ambient conditions at a depth of 220 ft and flowed downward to a depth of 301 ft, where it exited the borehole. Under pumping conditions of 0.25 gal/min, water entered the borehole at 127 ft (at the base of casing) and at the fracture at 221 ft below the top of casing. The majority of water entered the borehole at a depth of 221 ft below the top of the casing. The open-hole specific capacity was 0.08 gal/min/ft with a transmissivity of 15 ft^2/d (appendix 7A).

Table 15. Transmissive fractures in borehole MW302R in the UConn landfill study area, Storrs, Connecticut

[Strike is reported in right-hand-rule in degrees east of true north. The dip is degrees from horizontal. The compass descriptor (N-E-S-W) of the direction of dip is provided, for convenience and clarity]

Depth, in feet below top of casing	Transmissive fracture zone	Strike	Dip, in degrees	Direction of dip	Proportion of transmissivity, in percent
221	1	N340°E	41	S	85
301.5	2	N358°E	76	W	15

On March 15, 2001, a single packer was placed at 132 to 134 ft below the top of casing to stop the vertical flow coming from the base of casing. Water levels were measured on March 20, 2001, after the placement of the packer matched the heads that were predicted with the modeled flowmeter data. The head in the upper zone was 18.73 ft below the top of casing and the head below the packer was 19.36 ft below the top of casing.

On April 5, 2001, when the zone above the packer was pumped, the water level dropped from about 18 ft to 88.6 ft and did not recover, indicating the leakage from the base of the casing had diminished or ended. The water level below the packer remained at about a depth of 18 ft below the top of casing. On April 6, 2001, the water level above the packer was still at about 80 ft below the top of casing. On June 1, 2001, the packer was deflated with the intent of removing the packer from the borehole. However, the differential water level across the packer remained at about 40 ft with an upward potential, indicating a hydraulic seal remained between zones above and below the packer. In addition, the packer could not be moved vertically in the borehole. Water pumped from just above the packer contained small pieces of rock fragments and fine-grained particles that looked like grout. Collectively, this suggests the grout leaked from behind the casing and produced a seal on top of the packer. On August 6, 2001, the packer was removed forcibly from the borehole.

Heat-pulse flowmeter tests collected on October 18, 2001 (appendix 5B), showed there was no longer measurable leakage from the base of the casing; however, there continued to be minor downflow (0.02 gal/min) from depths of 221 to 301 ft below the top of casing. The fractures at depths of 221 and 301 ft produced water under pumping conditions. Approximately 85 percent of the inflow was attributed to the fracture at a depth of 221 ft and 15 percent of the inflow was produced from the fracture at 301 ft below the top of casing. During the pumping test, which lasted about 4 h, the open-hole water level reached a quasi-steady-state condition. When pumped at 0.30 gal/min, the specific capacity of MW302R was 0.09 gal/min/ft and the related open-hole transmissivity was 15 ft^2/d.

When the open-hole transmissivity is proportioned by the amounts of relative inflow from flowmeter tests, the fracture at the depth of 221 ft has an estimated transmissivity of 12.4 ft^2/d, while the fracture at 301 ft has an estimated transmissivity of 2.2 ft^2/d (table 15).

Using the observed heat-pulse flowmeter profiles, open-hole heads, and Paillet's (2000) program, the transmissivity and heads were determined for the fractures at depths of 221 and 301 ft below top of casing (appendix 5B). The simulated fractures were compared to the measured profiles (fig. 5). The SS error between the observed and simulated values was less than 0.0001. The estimated transmissivity and heads are shown in table 16. The transmissivity values are slightly lower, but consistent with the proportioned transmissivities based on the open-hole pumping and specific-capacity tests. No DZM system was installed and no BAT[3] testing was conducted in this borehole, so the estimated heads could not be compared to any measured heads.

On March 4, 2002, the bottom 20 ft of the borehole was grouted to stop the outflow of water from the fracture at the depth of 301 ft below the top of casing. The total depth of the borehole is now about 275 ft below the top of casing.

Borehole-radar reflectors. Fourteen reflectors were interpreted from the borehole-radar reflection surveys conducted in MW302R (appendix 5G). Four reflectors correlate with features identified using the OTV logs at depths of 138.8, 186.7, 197.5, and 229.0 ft. The reflector at 197.5 ft is the only reflector that correlates with features identified on the ATV logs.

Table 16. Transmissivity and head of fractures determined from modeling heat-pulse flowmeter results in borehole MW302R in the UConn landfill study area, Storrs, Connecticut

Depth, in feet below top of casing	Transmissivity, in feet squared per day	Depth to water, in feet below top of casing	Elevation of head, in feet
221	6.8	24.71	552.49
301	1.2	26.81	554.39

None of the reflectors correlate with the transmissive zones at about 221 and 301 ft. Two of the reflectors project into the PVC-cased interval of the borehole, at depths of 18.0 and 70.9 ft. Another reflector projects below the drilled depth of the borehole and intersects the line of the borehole at 357.0 ft.

The image of the radar data shows a wide range of electromagnetic properties over the length of the borehole (appendix 5D). There are three high-attenuation, low-velocity zones extending from 31 to 53 ft, 95 to 112 ft, and 215 to 230 ft below land surface. The deepest high-attenuation, low-velocity zone coincides with the most transmissive fracture in the borehole. The maximum signal penetration is in the depth interval from 112 to 215 ft, where the radar signal was reflected from up to 65 ft away from the borehole.

Domestic Well W202-NE

Location and construction. Well W202-NE is a domestic bedrock well located about 1,700 ft south and west of the landfill and about 2,000 ft south of the former chemical-waste disposal pits. The borehole was drilled May 5, 1995, to a depth of 325 ft below land surface for a domestic supply. A total of 81 ft of 6-in.-diameter steel casing was set through the overburden and into the bedrock. A submersible pump was set at approximately 280 ft below the top of casing. The water pumped from the well was used for domestic supply until December 2000, when the well was abandoned because of the presence of benzene (1.7 parts per billion, John Kastrinos, Haley and Aldrich, Inc., oral commun., December 2000). On February 26, 2001, the pump was removed from the borehole so that geophysical logs and hydraulic tests could be collected.

The borehole deviates a total of 14 ft towards the southeast. The water level on February 27, 2001, was about 19.77 ft below the top of casing, which extends 2 ft above land surface. All depth measurements were referenced to the top of casing.

Lithologic characterization. Borehole-imaging logs and conventional logs indicate the rock type is coarse-grained biotite-garnet schist to gneiss with quartzo-felspathic layers and augens. The stereoplots in appendix 6I indicate the poles to foliation and felsic layers cluster tightly near the center of the stereoplot, indicating a shallow dip. In general, the foliation strikes southwest and dips at a shallow angle to the northwest.

Fracture characterization. The orientation of all fractures observed on the OTV and ATV logs are provided in appendixes 6E and 6F, respectively. Fractures identified in the OTV and ATV logs are parallel to sub-parallel to the foliation and fabric of the bedrock. The transmissive fractures were identified with the heat-pulse flowmeter at depths of 97 to 105 ft, 197 ft, and 249 ft below the top of casing. The orientations of these transmissive fractures are presented in table 17. The stereoplot and tadpole plots for W202-NE indicate the transmissive fractures at depths of 97.4, 100.3, 197.1, and 248.5 ft below the top of casing had shallow dips (less than 30°) and a wide variation in strike. The fracture at 105.4 ft strikes west-northwest at N249°E and dips steeply north.

Table 17. Transmissive fractures in domestic well W202-NE in the UConn landfill study area, Storrs, Connecticut

[Strike is reported in right-hand-rule in degrees east of true north. The dip is degrees from horizontal. The compass descriptor (N-E-S-W) of the direction of dip is provided, for convenience and clarity.]

Depth, in feet below top of casing	Transmissive fracture zone	Strike	Dip, in degrees	Direction of dip	Proportion of transmissivity, in percent
97.4	1	N118°E	10	SW	50
100.3	1	N339°E	29	E	
105.4	1	N249°E	85	N	
197.1	2	N208 °E	20	NW	25
248.5	3	N347°E	13	E	25

Hydraulic characterization. Heat-pulse flowmeter logs collected on April 24, 2001 indicate the borehole had ambient flow (fig. 6). Water entered the borehole at a depth of 197 ft below the top of casing. Some of the water flowed upward in the borehole and exited the borehole through one or all of the fractures between 97 to 105 ft below the top of casing. The rest of the water flowed downward and exited the borehole at the fracture at a depth of 249 ft below the top of casing. These heat-pulse flowmeter measurements indicate a divergent flow regime at the fracture at 197 ft. On April 26, 2001, under a pumping rate of 0.3 gal/min, water entered the borehole from depths of about 97 to 105 ft, 197 ft, and 249 ft. Table 18 shows the magnitude of the water flowing from each of the boreholes and their relative proportions.

On April 26, 2001, when pumped at 0.30 gal/min for 4 h, the water levels reached steady-state conditions after 30 min of pumping. The specific capacity of the open borehole was 0.18 gal/min/ft of drawdown. Using the methods of Bradbury and Rothschild (1985), the open-hole transmissivity was estimated at 30 ft^2/d. The open-hole transmissivity was proportioned by the amounts of relative inflow identified with the heat-pulse flowmeter (table 19). The uppermost zone from depths of 97 to 105 ft had an estimated transmissivity of 15 ft^2/d while the lower two zones were apportioned at 7.5 ft^2/d.

The ambient and pumped heat-pulse flowmeter were simulated using fitted parameters of transmissivity and head in Paillet's program (2000). The simulated results produced a solution that had an SS error that was less than 0.0001. The ambient measurements and the simulated flow regimes are shown in figure 6. The head and transmissivity of each fracture zone is listed in table 19. The fractures from depths of 97 to 105 ft below the top of casing were treated as a single fracture zone. In this model, the transmissivity was proportioned differently than the interpretation based only on the heat-pulse flowmeter. In this model, the uppermost zone accounted for 40 percent of the transmissivity while the lower two fractures each accounted for 30 percent of the transmissivity. The transmissivity estimates calculated by this method are slightly less, but still consistent with the results obtained with the open-hole transmissivity estimates based on the specific capacity.

Table 18. Transmissive fractures in domestic well W202-NE identified in flowmeter logs collected on June 14, 2001, in the UConn landfill study area, Storrs, Connecticut

Ambient condition and depth	Inflow rate under pumping, in gallon per minute	Flow rate under ambient conditions	Difference in flow rates	Proportion of measured discharge
Receiving fracture at 105 feet	0.10	-0.03	0.13	0.50
Inflowing fracture at 197 feet	0.12	0.054	0.066	0.25
Receiving fracture at 249 feet	0.04	-0.024	0.064	0.25

Table 19. Transmissivity and head of fractures determined from modeling heat-pulse flowmeter data collected on April 24, 2001, in domestic well W202-NE in the UConn landfill study area, Storrs, Connecticut

Depth[1], in feet	Transmissivity, in feet squared per day	Proportion of transmissivity, in percent	Depth to water, in feet	Water-level elevation, in feet
105	9.2	40	20.58	528.62
197	6.9	30	18.78	530.42
247	6.9	30	20.68	528.52

[1]Depth below top of casing.

The integrated head measurement of this borehole is a transmissivity-weighted average of the head from individual fractures. On April 24, 2001, the head was at an elevation of 529.13 ft above NAVD88. The heat-pulse flowmeter measurements (table 19) indicate the head in the inflowing fracture at a depth of 197 ft had a higher head than the heads in both of the fractures that received flow under ambient conditions. The transmissivity-weighted average of the heads shown in table 19 is 529.13 ft above NAVD88.

Discrete-interval testing was conducted on May 14, 2001, with the BAT^3 equipment. Only the fracture at 197 ft was sampled for water-quality testing, because the borehole had been left open prior to testing and the upper and lower fractures were receiving water from the inflowing fracture at 197 ft. On May 18, 2001, packers were set to isolate the zone from 195.4 to 206.2 ft below top of casing. A constant-rate pumping test was conducted to determine the transmissivity and the differential head between the upper and lower test zones. The borehole was pumped at 0.2 gal/min and the water level declined 4.8 ft. The results of the discrete interval test, which were interpreted using the Thiem equation, indicated the transmissivity was 4.7 ft^2/d. This estimate of transmissivity compares fairly well with the modeled profiles of the heat-pulse flowmeter data. The differential-head tests collected at this zone did not correlate with the water levels estimated with the heat-pulse flowmeter data collected on April 24, 2001. The BAT^3 results indicated a downward potential from the upper zone towards the test zone. The potential between the lower zone and the test zone were essentially equal and within measurement error of the tool, so the results are inconclusive.

An additional differential-head test was conducted in the zone at 105 ft. Packers isolated the borehole from 104.4 to 115.2 ft below the top of casing. The results indicated a downward potential (0.69 ft difference) between the upper zone and the test zone. The differential heads of the lower zone were within the measurement error of the transducers. The results are reported in table 20.

Borehole-radar reflectors. Twelve reflectors were interpreted from the borehole-radar reflection survey conducted in W202-NE (appendix 6G). Eight of the reflectors correlated with features identified by the OTV at depths of 120.4, 121.7, 135.5, 156.2, 178.2, 239.2, 248.4, and 302.5 ft. Two of these reflectors, at depths of 120.4 and 156.2 ft, also correlate with the results of the ATV data. The reflector at 248.4 ft correlates with an interpreted transmissive zone. None of the reflectors correlate with the transmissive zone at 197.1 ft or with the fractures in the upper transmissive zone at depths of 97.4, 100.3, or 105.4 ft below the top of casing. One reflector is projected to intercept below the bottom of the borehole, at a depth of 329.4 ft.

There was strong signal penetration throughout most of the radar log (appendix 6D). Radial signal penetration extends up to 85 ft from the borehole. There is a small zone of high attenuation from 118 to 125 ft below the top of casing, which coincides with the fracture identified at a depth of about 120 ft below the top of casing.

Table 20. Differential heads from BAT^3 testing in domestic well W202-NE in the UConn landfill study area, Storrs, Connecticut

[TOC, top of casing in feet]

Well	Date of test	Depth of fracture, in feet	TOC	Hydraulic head, in feet above NAVD88			Head differential[1], in feet		
				Upper	Middle	Lower	Upper-Mid	Mid-Lower	Upper-Lower
W202-NE	5/14/2001	105	549.2	528.87	528.18	528.36	0.69	-0.18[2]	0.51
		197		528.08	524.94	524.93	3.14	0.01[2]	3.15

[1]Head differential—positive number denotes downward potential; negative number denotes upward potential.
[2]Indicates the differential head is less than the resolution of the tool.

RESULTS OF LITHOLOGIC AND FRACTURE CHARACTERIZATION

The distribution of lithology and orientation of foliation that were observed in the six boreholes logged in this investigation were compared to the results of previous investigations. The comparison indicates that the bedrock beneath the study area is fairly uniform with minor variations in the texture and layering of the schist and gneiss. Iron-sulfide layers were observed in image logs and were seen in borehole EM induction and radar logs and in surface EM and resistivity methods (Powers and others, 1999; Johnson and others, 2002a). Igneous intrusions were more commonly observed in MW109R, which is consistent with their presence in upland settings.

The orientation of foliation was determined by integrated interpretation of borehole-geophysical logs from the six boreholes. Stereoplots constructed for the individual boreholes show the poles to the foliation planes form two clusters. One cluster indicates the foliation strikes northeast-southwest and dips at shallow to moderate angles to the southeast and northwest. The other cluster indicates foliation strikes northwest and dips at shallow to moderate angles to the northeast. Tadpole plots of the foliation show some variation in the rock fabric with depth, but no consistent pattern was observed with depth. These results were consistent with borehole-geophysical logs previously collected at the site (Johnson and others, 2002b). The general orientation of the foliation and layering identified in 16 boreholes in the study area and 4 domestic wells is shown in figure 7. The strike of the foliation mapped in the boreholes also is consistent with the bulk fabric identified in the square-array resistivity soundings collected around the landfill (Powers and others, 1999).

The fracture orientations observed in borehole-imaging surveys vary in both strike and dip, and collectively appear to be scattered. The transmissive fractures identified in the six boreholes logged in this investigation were compared to previously logged boreholes (Johnson and others, 2002b). The transmissive fractures identified in the 16 boreholes had a wide variation in orientations. Stereoplots of transmissive fractures constructed for each borehole indicate the fractures generally have one of three different orientations: (1) striking north-northwest and dipping at a shallow angle to the east-northeast; (2) striking southwest and dipping at shallow angles to the northwest; or (3) striking east-west and dipping to the north and south. The generalized direction of the strike of transmissive features in the 16 boreholes at the site is shown in figure 8.

The chances of intersecting a steeply dipping planar feature in a near-vertical borehole are low; thus the fracture information from borehole data is inherently biased. The Terzaghi correction (Terzaghi, 1965) was used to estimate the probable abundance of the transmissive fractures. The underlying assumption in this correction is that if the borehole had been drilled perpendicular to the dip of a specific fracture, then the borehole would have penetrated additional fractures at the same dip angle. The total number of these fractures is proportional to the inverse of the cosine of the dip, and the fractures would be uniformly spaced over the length of the borehole.

For each transmissive fracture, a weighting factor $f = 1/\cos\theta$, where θ is the dip angle, was computed, and additional fractures were added to the data set representing the unbiased fracture population (Terzaghi, 1965). The value of f was rounded to a whole number, and the frequency of the fractures dipping at that specific angle was increased by the weighting factor. At dip angles less than 49°, the frequency of the fracture count does not change. At steep dips, the correction factor has a significant impact on the relative abundance of the fractures (table 21). Terzaghi (1965) indicated that the smaller the angle between the dip of the fracture and the orientation of the borehole, the larger the uncertainty in the predicted bias correction.

Table 21. Weighting factor used to correct for sampling bias of planar features observed in near-vertical boreholes for selected dip angles

[< indicates less than]

Dip θ, in degrees	Count (f) $f = 1/\cos\theta$
<49	1
49	2
67	3
74	4
78	5
80	6
82	7
83	8
84	10
85	11
86	14

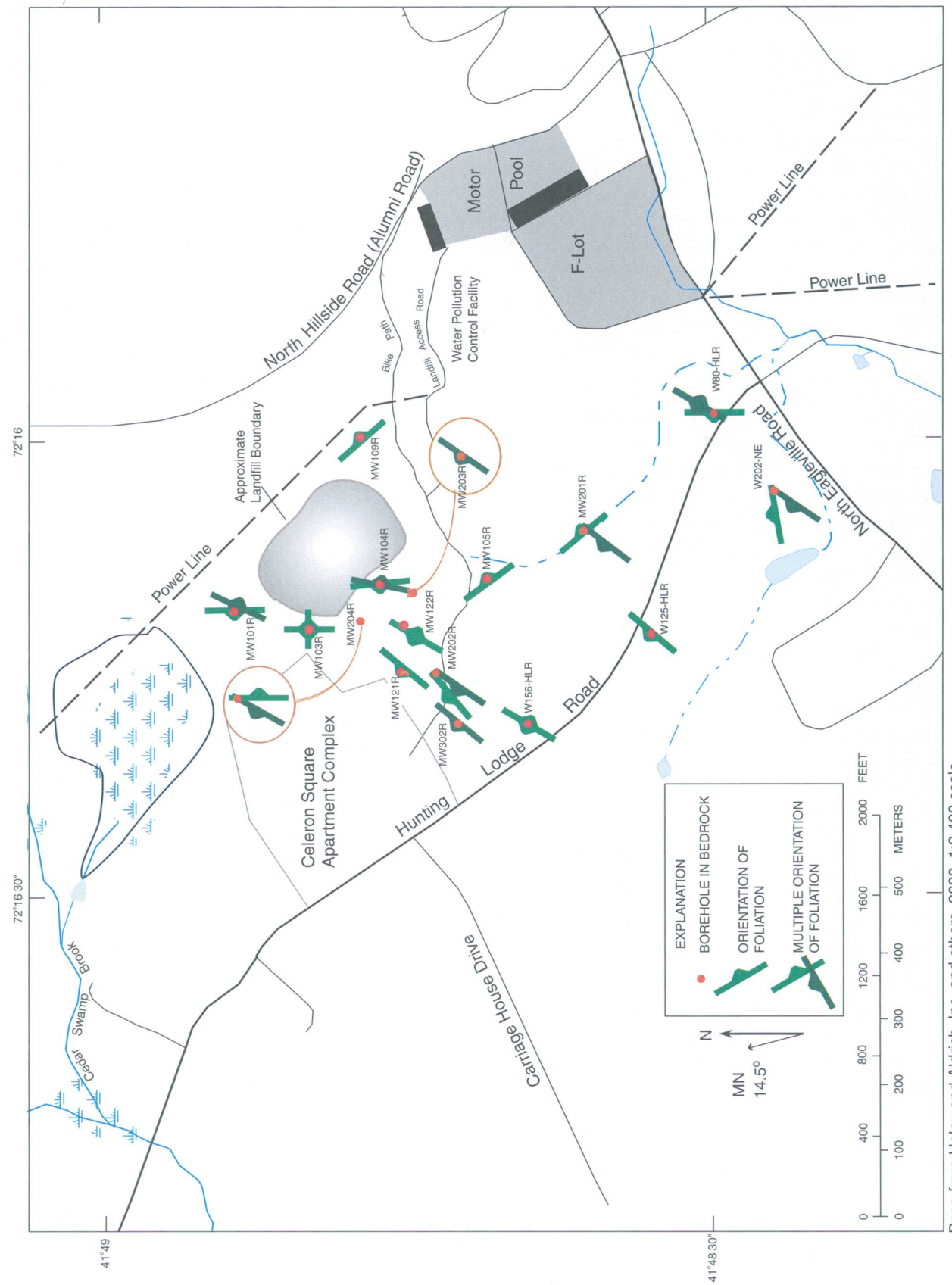

Figure 7. Orientation of foliation in bedrock boreholes, UConn landfill study area, Storrs, Connecticut.

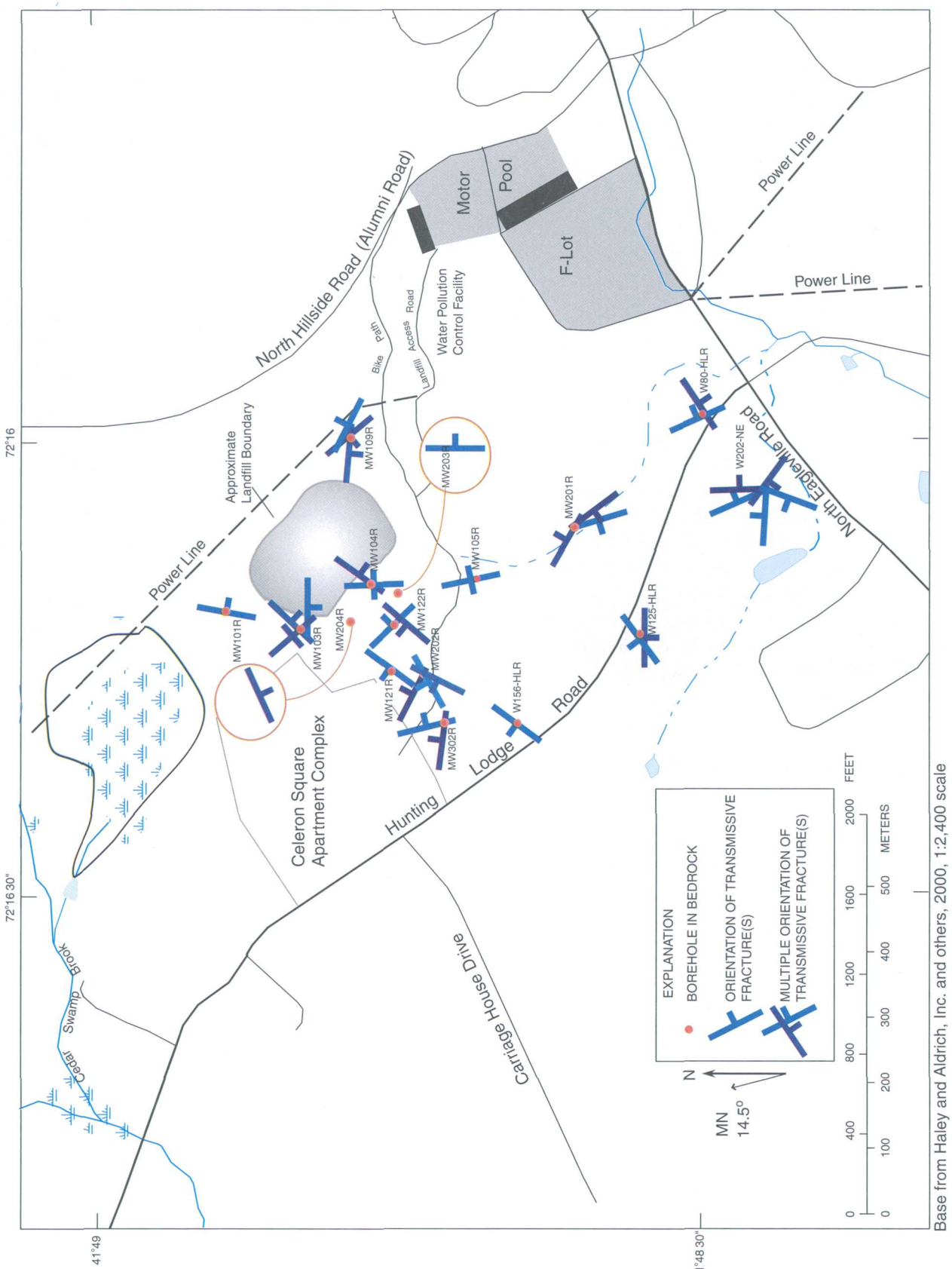

Figure 8. Orientation of transmissive fractures in bedrock boreholes, UConn landfill study area, Storrs, Connecticut.

Composite stereoplots were constructed for all of the transmissive fractures identified with the heat-pulse flowmeter in the 16 boreholes in the study area. The stereoplot in figure 9A, shows the uncorrected population of transmissive fractures, and figure 9B shows the probable distribution of transmissive fractures determined with the Terzaghi correction. The total number of fractures in the bias-corrected data set (126) is nearly double the number of transmissive fractures that were observed in the boreholes (66 fractures). The bias-corrected data set shows a decrease in the relative abundance of the shallow fractures and an increase in the relative abundance of the steeply dipping fractures. Because the original data set had three steeply dipping fractures (two at 81° and one at 84°), the correction for these three fractures alone added 23 fractures to the corrected data set. The population generated by the Terzaghi correction is only a probable distribution, and may overestimate the steep fractures because the analysis does not account for the length and the variation in fracture spacing (Terzaghi, 1965). Because sampling in a near-vertical borehole undersamples vertical features, in reality there are more vertical fractures than what is observed in the boreholes. The actual distribution of transmissive fractures is most likely between the observed distribution (fig. 9A) and the prediction of the distribution from the Terzaghi correction (fig. 9B).

RESULTS OF HYDRAULIC ANALYSES

A comparison of the techniques used in this investigation for estimating hydraulic properties of the fractured-rock aquifer indicates that the BAT^3 provides the most hydraulic information including transmissivity, head, differential head, and a discrete-interval water-quality sample. The field effort to collect the BAT^3 data, however, is the most time consuming and complicated of the three methods. The heat-pulse flowmeter logging and modeling provides information on the transmissive fractures, including the location, transmissivity, and head. The results obtained by this method appear to provide results that are consistent with the open-hole tests and the BAT^3.

Heat-pulse flowmeter analyses were limited in this investigation by the low transmissivity conditions found in most of the boreholes. In MW202R and MW203R, water levels declined in the borehole, preventing measurements of the fractures at the top of the borehole. In both cases, injection tests, rather than pumping tests, would have permitted the characterization of these fractures; however, injection was not feasible at this site. In MW203R and MW204R, all of the inflow to the borehole came from fractures near the top of the borehole below the base of the casing.

Specific-capacity and open-hole transmissivity values were determined in four boreholes where water levels achieved quasi steady-state conditions, including MW201R, MW204R, MW302R, and W202-NE. When pumped at 0.25 to 1 gal/min for 0.7 to 4 h, the specific capacity ranged from 0.03 to 0.09 gal/min/ft. An iterative process described by Bradbury and Rothschild (1985) was used to solve for the transmissivity of the open boreholes where water levels achieved steady-state conditions during pumping. These estimates of open-hole transmissivity ranged from 4.9 to 30 ft^2/d.

For pumping tests where water levels did not achieve quasi steady-state conditions, the Cooper-Jacob straight-line solution was used to interpret the water-level data. These analyses were made for pumping tests in MW201R, MW202R, and MW203R, and the transmissivity ranged from 0.53 to 3.2 ft^2/d. Transmissivity values were plotted to compare the results of the various methods that were used in this investigation (fig. 10). For some boreholes, there were multiple pumping events that permitted multiple estimates of transmissivity. For example, in MW201R, pumping tests were conducted on five occasions. Four times the results could be interpreted with the steady-state solutions (Bradbury and Rothschild, 1985). In the fifth test, the water level in MW201R did not achieve steady-state conditions, and the transmissivity was estimated using the Copper-Jacob straight-line solution and Theis curve-matching techniques.

In figure 10, the transmissivity estimates of the discrete-interval BAT^3 testing were combined so that they could be compared with open-hole transmissivity tests. The BAT^3 results in W202-NE were not included in the comparison, because transmissivity was only determined for one of the three transmissive fractures in the borehole. Figure 10 shows the transmissivity estimates for the various methods are fairly well correlated. In general, the results were reproducible when multiple tests were conducted in the same borehole.

The estimates of open-hole transmissivity may not provide depth-dependent detail; however, they provide valuable information that can be used to

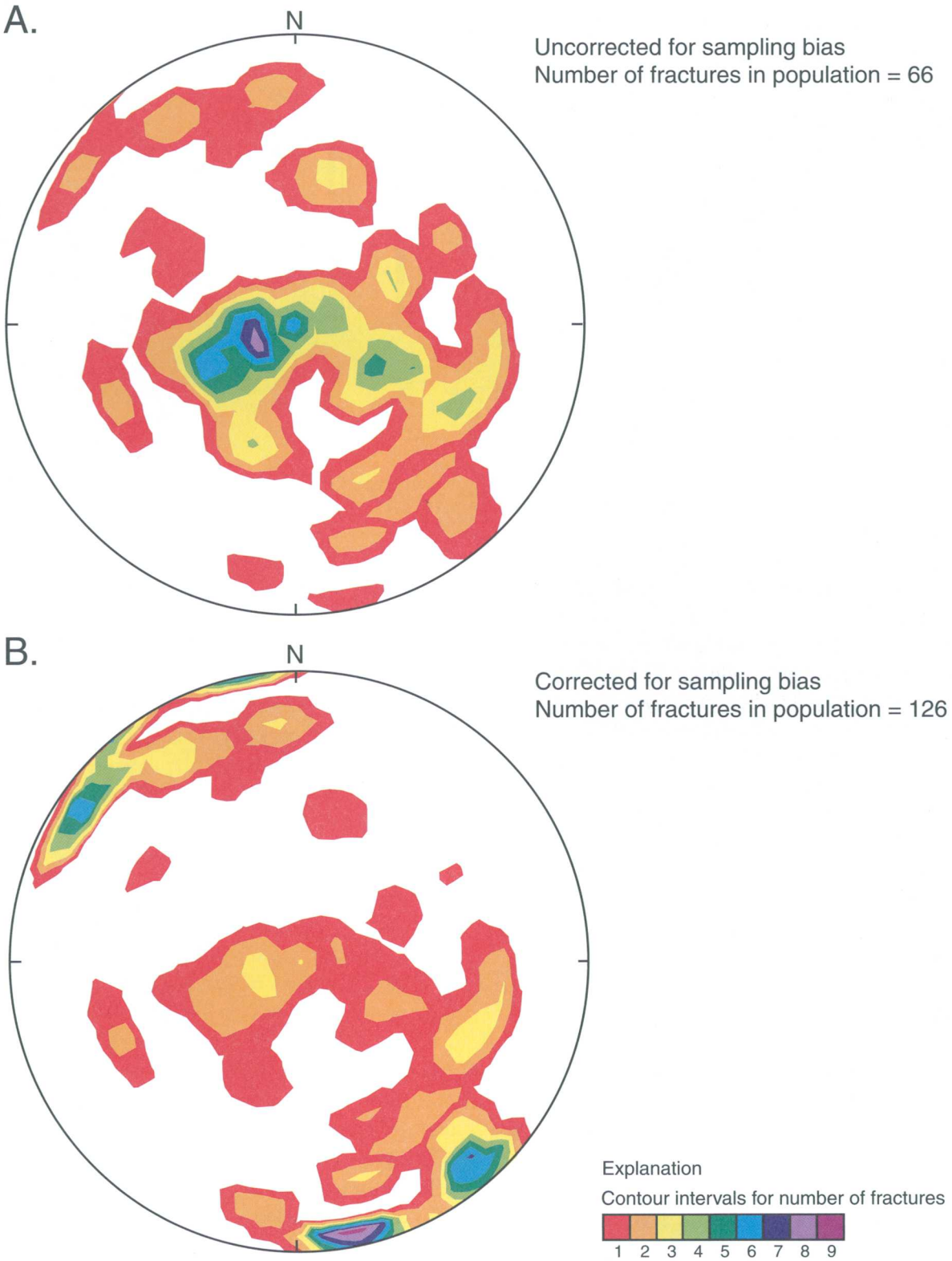

Figure 9. Stereoplots of transmissive fractures observed in 16 boreholes at the UConn landfill study area, Storrs, Connecticut. The plots show contoured pole-to-planes in equal-area, lower-hemisphere projections.

A. Uncorrected for sampling bias.

B. Corrected for sampling bias and represents a probabilistic distribution of transmissive fractures.

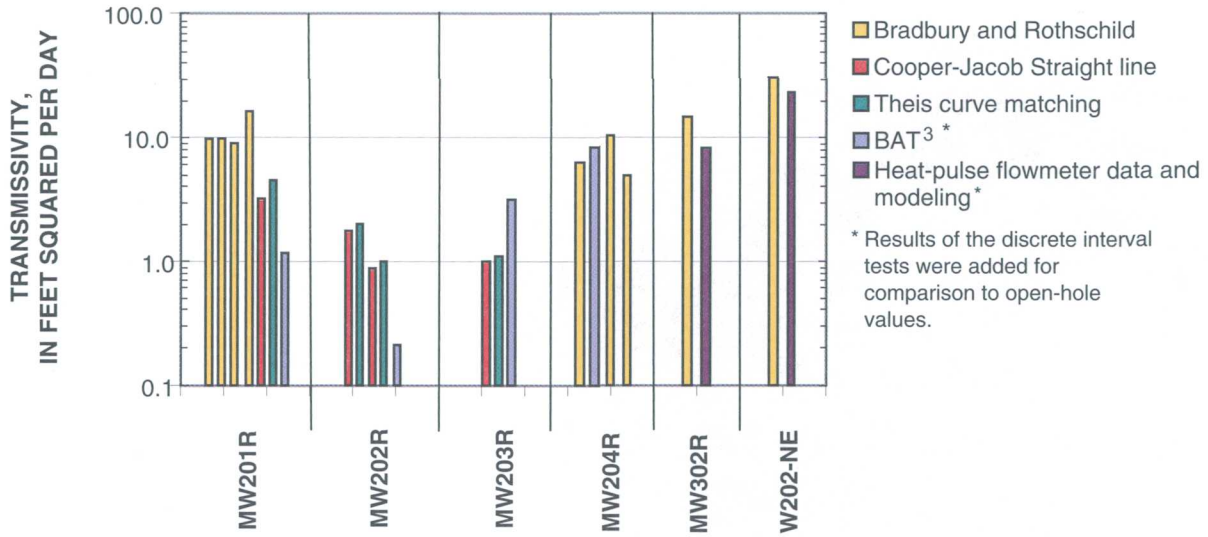

Figure 10. Comparison of open-hole transmissivity estimates from various methods in selected boreholes, UConn landfill study area, Storrs, Connecticut. BAT^3 is the Bedrock Aquifer Transportable Testing Tool.

compare the results of multiple boreholes across the study area. A comparison of all open-hole transmissivity tests, including previously reported values (Johnson and others, 2002b), shows the highest transmissivity estimates were from tests conducted in domestic wells and in MW109R (fig. 11). The boreholes with the lowest measured transmissivity tended to be near the ground-water divide in the area of the former chemical-waste disposal pits. Figure 11 shows that the measured open-hole transmissivities ranged over 2.5 orders of magnitude. The transmissivity in fractured crystalline-rock aquifers typically spans several orders of magnitude. The actual range of transmissivity at the UConn landfill site is much greater than the 2.5 orders of magnitude, but the lower transmissivity fractures were beyond the resolution of the methods used in this investigation.

In boreholes with measurable ambient flow, MW302R and W202-NE, the flow-modeling method described by Paillet (2000) was used to estimate transmissivity and the hydraulic head of each transmissive zone. In MW302R, downflow was detected under ambient conditions, and inflow was identified at two fractures under pumping conditions. The transmissivity was estimated at 15 ft^2/d from an open-hole specific capacity test and at 8.0 ft^2/d from Paillet's method. In abandoned domestic well W202-NE, ambient flow was measured with the heat-pulse flowmeter in April 2001. The results indicated a divergent flow field at a depth of 197 ft where water flowed both upward and downward under ambient conditions. The transmissivity and head of the individual fractures were iteratively varied until an adequate match between the simulated and observed flow profiles was obtained. Transmissivity estimates for individual fracture zones ranged from less than 6.9 to 9.2 ft^2/d in this borehole. The total of these individual zone transmissivities was 23 ft^2/d, which compares fairly well with the open-hole transmissivity measurement of 30 ft^2/d using Bradbury and Rothschild's method (1985).

The identification of the location and proportion of transmissive zones is important for sampling strategies to obtain representative samples or to understand open-hole samples. The results in W202-NE indicate that transmissivity values obtained from open-hole flowmeter testing provide results that are consistent with the results obtained with discrete-interval packer testing. These tests identified three transmissive fractures. Discrete samples were not collected from each of the fractures because the hydraulically active fractures were not isolated prior to sampling. Only the fracture that was producing water under ambient conditions was sampled and the receiving fractures were not sampled. Because the fractures in W202-NE have different transmissivities, the water chemistry of the individual fractures may be different from the water-quality samples collected from the open borehole.

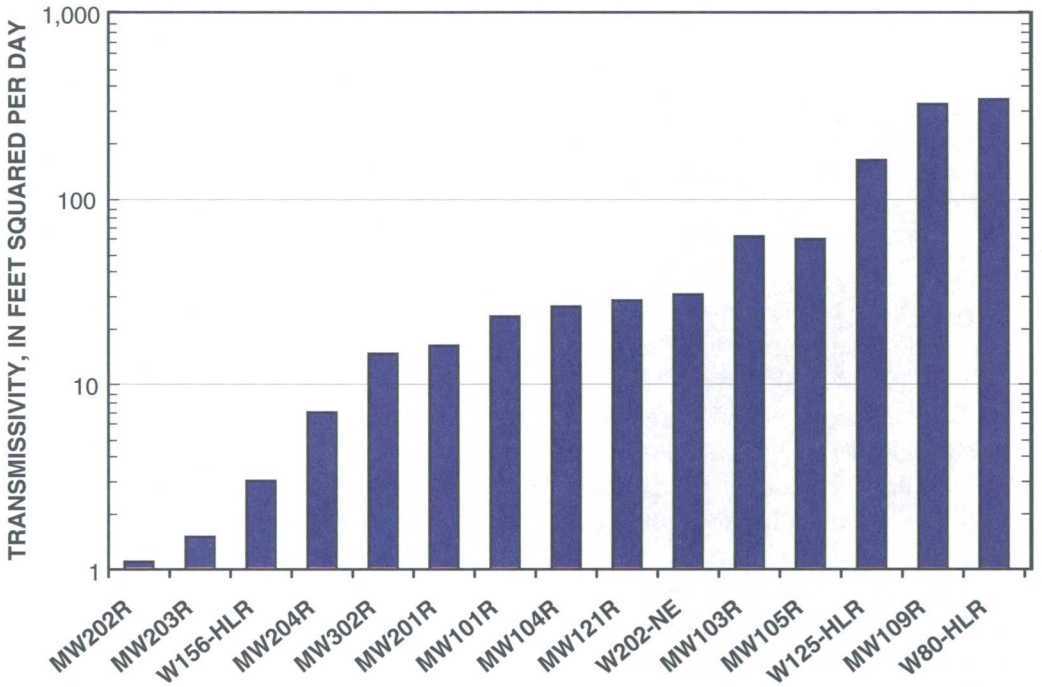

Figure 11. Comparison of open-hole transmissivity estimates from boreholes in the UConn landfill study area, Storrs, Connecticut. To estimate the transmissivity, the Bradbury and Rothschild method was used for boreholes that reached equilibrium, and the Cooper-Jacob method was used for transient responses.

SUMMARY AND CONCLUSIONS

In 2000 and 2001, the USGS, in cooperation with the University of Connecticut, conducted a borehole-geophysical investigation of the fractured-bedrock aquifer near the UConn landfill. Borehole-geophysical methods were used to further characterize the hydrogeology of the fractured-bedrock aquifer as part of an ongoing investigation of the UConn landfill and former chemical-waste disposal pits. The data were collected from August 2000 through October 2001. Six boreholes ranging in depth from 125 to 350 ft were logged to characterize the hydrogeology of the bedrock underlying the landfill and vicinity. Conventional geophysical-logging methods included caliper, deviation, electromagnetic induction, gamma, fluid temperature, and fluid resistivity; and advanced geophysical-logging methods included optical- and acoustic-borehole imaging, heat-pulse flowmeter logging under ambient and pumped conditions, and single-hole directional radar. Open-hole transmissivity estimates were made from pumping-test data. Where conditions permitted, the transmissivity and head were estimated for discrete intervals in the borehole with heat-pulse flowmeter data and with BAT^3 straddle-packer equipment.

The purpose of this investigation was to characterize the site lithology and structure and to identify the orientation, distribution, and hydraulic characteristics of fractures and transmissive zones in the fractured-rock aquifer. This work supported ongoing efforts to develop and refine a conceptual site model of groundwater flow and contaminant distribution and to apply and test the design of a DZM system for long-term water-level monitoring and water sampling. The results of the geophysical and hydraulic investigations conducted at this site and the information obtained from the DZM system will be useful in designing and evaluating remediation alternatives.

Fracture and foliation orientations and distributions were determined by integrated interpretation of borehole-geophysical logs. Stereoplots constructed for the six boreholes logged for this investigation are consistent with the results of previous investigations. Results from all of the boreholes logged in the study area indicate there are two general orientations of foliation. In general, foliation strikes to the northeast-southwest and dips to the southeast and northwest, or strikes to the northwest and dips to the northeast. These results are consistent with geologic maps of the area and with the bulk fabric identified in square-array resis-

tivity soundings collected previously around the landfill.

Numerous fractures were identified in the borehole-imaging surveys. Most of the fractures were identified by optical and acoustic imaging methods; however, some of the fractures were observed by only one of the methods, which underscores the need to collect both types of imaging logs. The orientations of all fractures observed in the boreholes vary in both strike and dip, and collectively appear to be scattered. The transmissive fractures identified in the boreholes logged in this investigation were similar to transmissive fractures previously identified in the study area. The transmissive fractures that were identified in the 16 boreholes at the site showed a wide variation in orientations; however, stereoplots indicate that transmissive fractures generally are oriented in one of three different orientations: (1) striking north-northwest and dipping at a shallow angle to the east-northeast; (2) striking southwest and dipping at shallow angles to the northwest; or (3) striking east-west and dipping to the north and south.

Because near-vertical boreholes undersample steeply dipping fractures, a correction was used to correct for the bias in the population of transmissive fractures. A total of 66 transmissive fractures were identified in 16 boreholes near the landfill. The total number of transmissive fractures resulting from the bias correction was 126. Although the bias correction was intended to increase the relative abundance of steeply dipping fractures, the correction used in this investigation may have disproportionately overestimated the number of steeply dipping fractures. The actual distribution of transmissive fractures is most likely between the observed distribution and the predicted distribution. The analysis highlights the concept that the total population of fractures in the aquifer includes more steeply dipping fractures than were observed in the boreholes.

For this study, heat-pulse flowmeter logging was conducted under ambient and pumping conditions in six boreholes. The specific capacity and transmissivity of the open boreholes were estimated from the discharge and water-level data collected during flowmeter logging. Open-hole transmissivity estimates were made using both steady-state solutions and non-equilibrium solutions. The range of open-hole transmissivity was from less than 1 to 30 ft^2/d. A comparison of the open-hole transmissivity estimates determined for this investigation to estimates from other boreholes in the study area indicates that MW201R, MW202R, MW203R, and MW204R are not very transmissive relative to the other boreholes.

Discrete-zone isolation tests (with the BAT^3) were used in five boreholes (MW201R to MW204R and W202-NE) to obtain water-quality samples from discrete zones while collecting the information to calculate the transmissivity. Thirteen differential-head tests that compared the water levels in the test zones with those above and below the test zone were conducted in the boreholes. Transmissivity was estimated from the discharge and water-level data collected from pumping tests conducted in the isolated portions of the borehole. Depth-specific transmissivity was determined from these tests using the Thiem equation. The transmissivity results ranged from about 0.2 to about 11 ft^2/d.

The heat-pulse flowmeter was used to identify ambient flow in the boreholes MW302R and W202-NE. The data from the ambient flow conditions and the pumping conditions were used along with a numerical method for modeling transmissivity and head of discrete intervals. The transmissivity and head of the individual fractures were iteratively varied in the model until an adequate match between the simulated and observed flow profiles was obtained. The values determined by this method ranged from 1.2 to 9.2 ft^2/d. These depth-specific transmissivity estimates were similar to the results from the BAT^3 testing.

Collectively, the transmissivity tests conducted in the 16 boreholes at the site indicate that transmissivity ranges over 2.5 orders of magnitude. The actual range of the transmissivity is much larger, but lower transmissivity values were beyond the resolution of the methods used in this investigation. The lowest open-hole transmissivity values were observed near the north-south ground-water divide in the area near the former chemical-waste disposal pits. The highest open-hole transmissivity values were observed in the domestic wells and in the background well, MW109R located east of the landfill.

The transmissivity values determined by the three different methods used in this investigation are fairly similar, within an order of magnitude. The open-hole specific capacity and transmissivity tests provided estimates of the transmissive properties of the boreholes, which were used to compare the results across the site. Although the heat-pulse flowmeter data can be

used to proportion the open-hole transmissivity estimates to specific depths of the borehole, the results of the depth-specific measurements were more reliable.

The flowmeter measurements along with numerical modeling provided depth-specific estimates of transmissivity and head; however, the method can be used only in boreholes that have ambient flow and can sustain pumping. Because of this limitation, this method could only be used in two boreholes in this investigation. The depth-specific transmissivity results that were obtained in MW302R and W202-NE were similar to the proportioned open-hole transmissivity results. In W202-NE, where a discrete-interval transmissivity test was conducted, the results were similar. This suggests that where the heat-pulse flowmeter measures ambient flow and low-rate pumping can be sustained, this method can be used to determine the depth-specific transmissivity and head of fractures in the borehole.

The discrete-interval tests that were collected with the straddle packer apparatus (BAT^3) provided the most direct discrete-interval measurement of transmissivity. This method had the additional advantage of obtaining a discrete-interval water-quality sample, the head of the test zone, and the relative head of the zones above and below the test zone. Although this method provided the most depth-specific hydraulic information, the method was the most cost- and labor-intensive and the most complicated of the three methods used to determine transmissivity.

REFERENCES CITED

Bienko, C., Collins, C., Glass, E., McNamara, B., and Welling, T.G., 1980, History of waste disposal at the chemical dump, University of Connecticut, Storrs, Connecticut, *in* Black, R.F., ed., University of Connecticut Geology 344 project: Storrs, Conn., Department of Geology and Geophysics, 7 p.

Bradbury, K.R., and Rothschild, E.R., 1985, A computerized technique for estimating hydraulic conductivity of aquifers from specific capacity data: Ground Water, v. 23, no. 2, p. 240-245.

Connecticut Department of Environmental Protection, 1993, Final site inspection, University of Connecticut Landfill/Waste Pits, Mansfield, Connecticut, CERCLIS no. CTD981894280: Hartford, Conn., 22 p.

Fahey, R.J. and Pease, M.H., Jr., 1977, Preliminary bedrock geologic map of the South Coventry quadrangle, Tolland County, Connecticut: U.S. Geological Survey Open-File Report 77-587, 30 p., 3 plates, scale 1:24,000.

Freeze, R.A. and Cherry, J.A., 1979, Ground water: Englewood Cliffs, N.J., Prentice Hall, Inc., 603 p.

Haley and Aldrich, Inc., 1999, Scope of study for the hydrogeologic investigation, UConn landfill, Storrs, Connecticut, File 91221-400: Storrs, Conn., University of Connecticut, 50 p.

Haley and Aldrich, Inc., Environmental Research Institute; Epona Associates, LLC; Regina Villa Associates, Inc.; and Earth Tech, Inc., 2000, Final preliminary hydrogeologic investigation draft report, UConn landfill, Storrs, Connecticut: Glastonbury, Conn., 267 p. plus attachments and appendixes.

Haley and Aldrich, Inc.; Environmental Research Institute; Epona Associates, LLC; F.P. Haeni, LLC; and Regina Villa Associates, Inc.;with technical oversight by Mitretek Systems, Inc., 2002, Draft comprehensive hydrogeologic investigation and remedial action plan, University of Connecticut, Storrs, Connecticut: Glastonbury, Conn., File No. 91221-513.

Hess, A.E., and Paillet, F.L., 1990, Applications of the thermal-pulse flowmeter in the hydraulic characterization of fractured rocks: West Conshohocken, Penn., American Society for Testing and Materials, Standard Technical Publications 1101, p. 99-112.

Izraeli, R.L., 1985, Water quality and hydrogeological investigations at the University of Connecticut waste disposal area: Storrs, Conn., University of Connecticut, Master's thesis, 108 p.

Johnson, C.D., Dawson, C.B., Belaval, Marcel, and Lane, J.W., Jr., 2002a, An integrated surface-geophysical investigation of the University of Connecticut landfill--2002: U.S. Geological Survey Water-Resources Investigations Report 02-4008, 39 p.

Johnson, C.D., Haeni, F.P., and Lane, J.W., Jr., 2001, Importance of discrete-zone monitoring systems in fractured-bedrock wells—A case study for the University of Connecticut landfill, Storrs, Connecticut, *in* Fractured Rock 2001 Conference, Proceedings: Toronto, Ontario, March 26-28, 2001, CD-ROM.

Johnson, C.D., Haeni, F.P., Lane, J.W., and White, E.A., 2002b, Borehole-geophysical investigation of the University of Connecticut landfill, Storrs, Connecticut: U.S. Geological Survey Water-Resources Investigations Report 01-4033, 187 p.

Johnson, C.D., Kochiss, C.S., and Dawson, C.B., 2005, Use of discrete-zone monitoring systems for hydraulic characterization of a fractured-rock aquifer at the University of Connecticut landfill, Storrs, Connecticut, 1999 to 2002: U.S. Geological Survey Water-Resources Investigations Report 03-4338, 104 p.

Keys, W.S., 1990, Borehole geophysics applied to groundwater investigations: U.S. Geological Survey Techniques of Water-Resources Investigations, book 2, chap. E-2, 149 p.

Lane, J.W., Jr., Haeni, F.P., and Williams, J.H., 1994, Detection of bedrock fractures and lithologic changes using borehole radar at selected sites, *in* Fifth International Conference on Ground-Penetrating Radar, Kitchner, Ontario, Canada, June 12-16, 1993, Proceedings: Kitchner, Ontario, Waterloo Center for Groundwater Research, p. 577-591.

Lohman, S.W., 1979, Ground-water hydraulics: U.S. Geological Survey Professional Paper 708, 70 p.

Olsson, Olle; Falk, Lars; Forslund, Olof; Lundmark, Lars; and Sandberg, Eric, 1992, Borehole radar applied to the characterization of hydraulically conductive fracture zones in crystalline rock: Geophysical Prospecting, v. 40, p. 109-142.

Paillet, F.L., 1998, Flow modeling and permeability estimation using borehole flow logs in heterogeneous fractured formations: Water Resources Research, v. 34, no. 5, p. 997-1010.

Paillet, F.L., 1999, Geophysical reconnaissance in bedrock boreholes—Finding and characterizing the hydraulically active fractures, *in* Morganwalp, D.W., and Buxton, H.T., eds., U.S. Geological Survey Toxic Substance Hydrology Program, Proceedings of the Technical Meeting, Charleston, S.C., March 8-12, 1999: U.S. Geological Survey Water-Resources Investigations Report 99-4018C, v. 3, p. 725-733.

Paillet, F.L., 2000, A field technique for estimating aquifer parameters using flow log data: Ground Water, v. 38, no. 4, p. 510-521.

Powers, C.J., Wilson, Joanna, Haeni, F.P., and Johnson, C.D., 1999, Surface-geophysical investigation of the University of Connecticut landfill, Storrs, Connecticut: U.S. Geological Survey Water-Resources Investigations Report 99-4211, 34 p.

Shapiro, A.M., 2001, Characterizing ground-water chemistry and hydraulic properties of fractured rock aquifers using the multifunction bedrock aquifer transportable testing tool (BAT^3): U.S. Geological Survey Fact Sheet, FS-075-01, 4 p.

Shapiro, A.M., and Hsieh, P.A., 1998, How good are estimates of transmissivity from slug tests in fractured rock?: Ground Water, v. 36, no. 1, p. 37-48.

Terzaghi, R.D., 1965, Sources of error in joint surveys: Geotechnique, v. 15, p. 287-304.

Williams, J.H., and Conger, R.W., 1990, Preliminary delineation of contaminated water-bearing fractures intersected by open-hole bedrock wells: Ground Water Monitoring, v. 10, no. 3, p. 118-126.

Williams, J.H., and Johnson, C.D., 2000, Borehole-wall imaging with acoustic and optical televiewers for fractured-bedrock aquifer investigations, *in* Proceedings of the 7th Minerals and Geotechnical Logging Symposium, Golden, Colo., October 24-26, 2000: Minerals and Geotechnical Logging Society, p. 43-53, CD ROM.

Williams, J.H., Lapham, W.W., and Barringer, T.H., 1993, Application of electromagnetic logging to contamination investigations in glacial sand and gravel aquifers: Ground Water Monitoring and Remediation Review, v. 13, no. 3, p. 129-138.

Appendix 1. Borehole-geophysical logs from borehole MW201R in the UConn landfill study area, Storrs, Connecticut

Appendix 1A. Deviation log of borehole MW201R in the UConn landfill study area, Storrs, Connecticut
[ft, feet]

MW201R

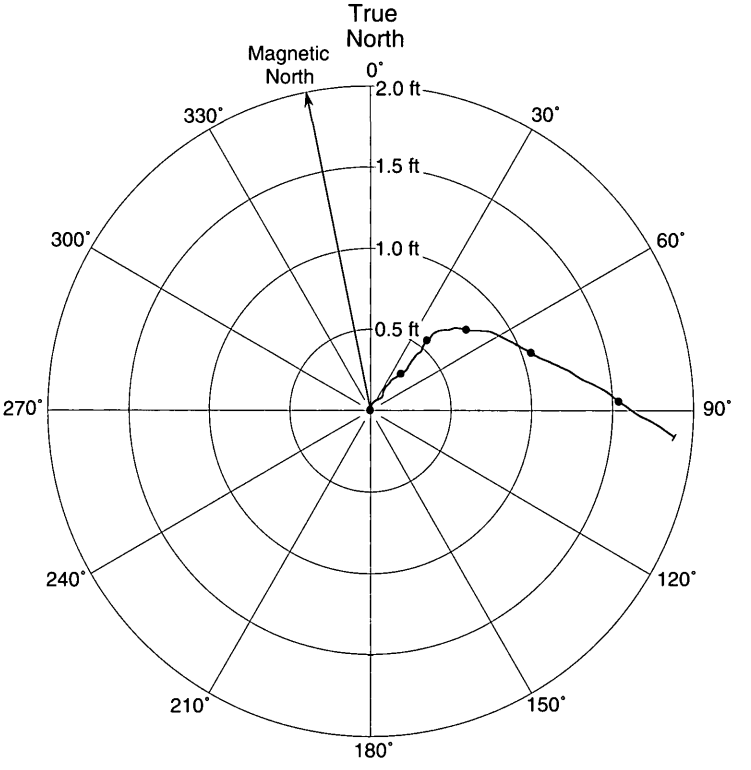

Depth along borehole in 20-foot increments between circles (•)

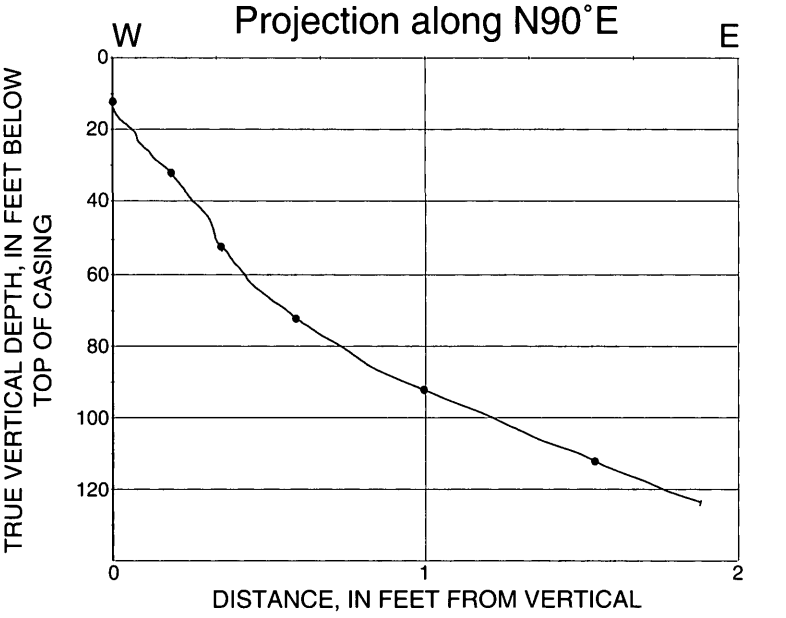

Depth along borehole in 20-foot increments between circles (•)

Appendix 1B. Composite log of natural-gamma, electromagnetic induction, fluid-temperature, specific-conductance, and heat-pulse flowmeter logs from borehole MW201R in the UConn landfill study area, Storrs, Connecticut

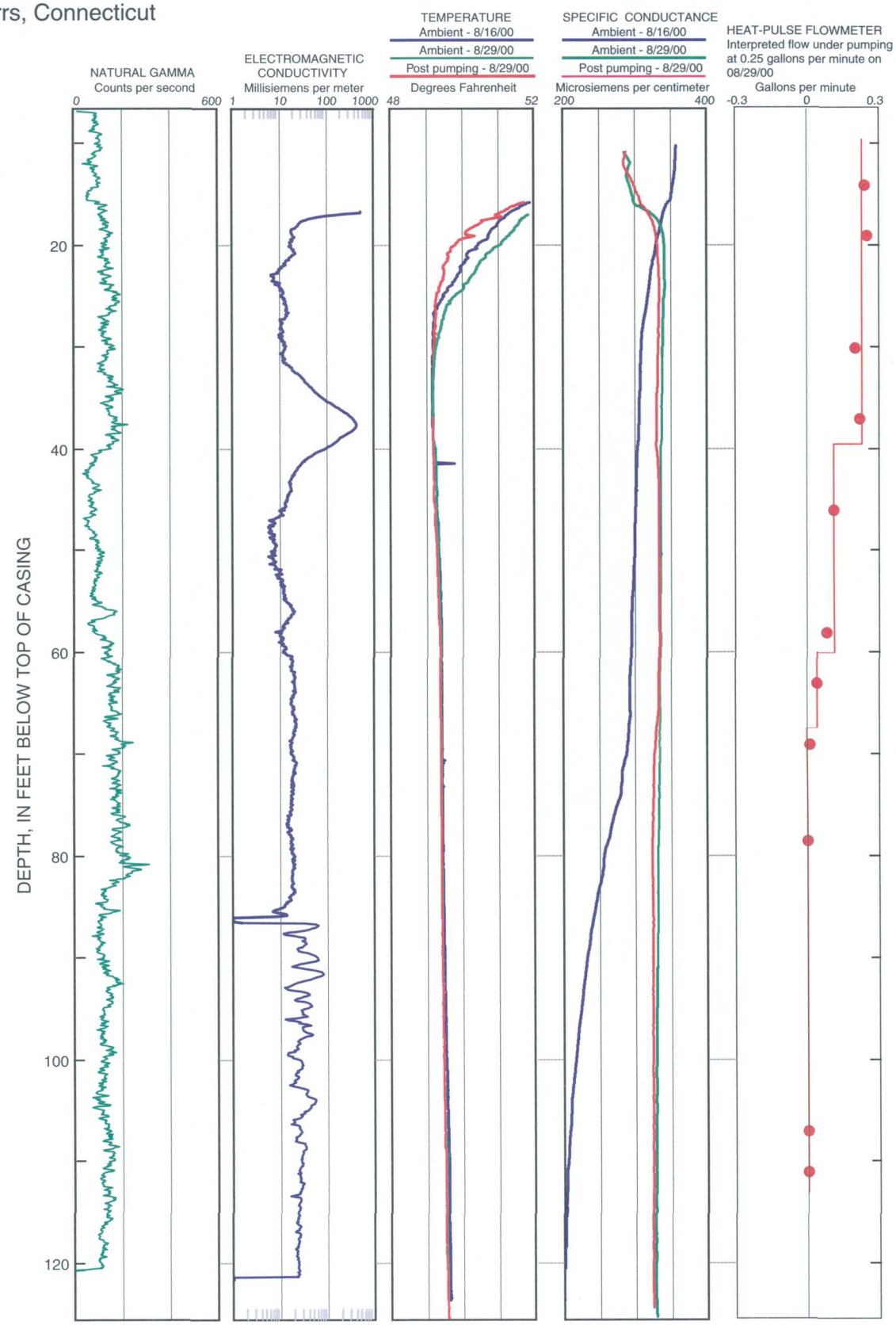

Appendix 1C. Caliper, acoustic-caliper, acoustic-televiewer, and optical-televiewer images and interpreted structures from borehole MW201R in the UConn landfill study area, Storrs, Connecticut

[Interpreted features indicated by color: black - foliation; dark blue - transmissive fracture; red - fracture; light blue - crack or minor fracture; gray - sealed fracture; pink - fracture with modifier, such as "partial" or "oxidized"; blue-gray - parting along foliation; green - fracture along contact; yellow - felsic layer]

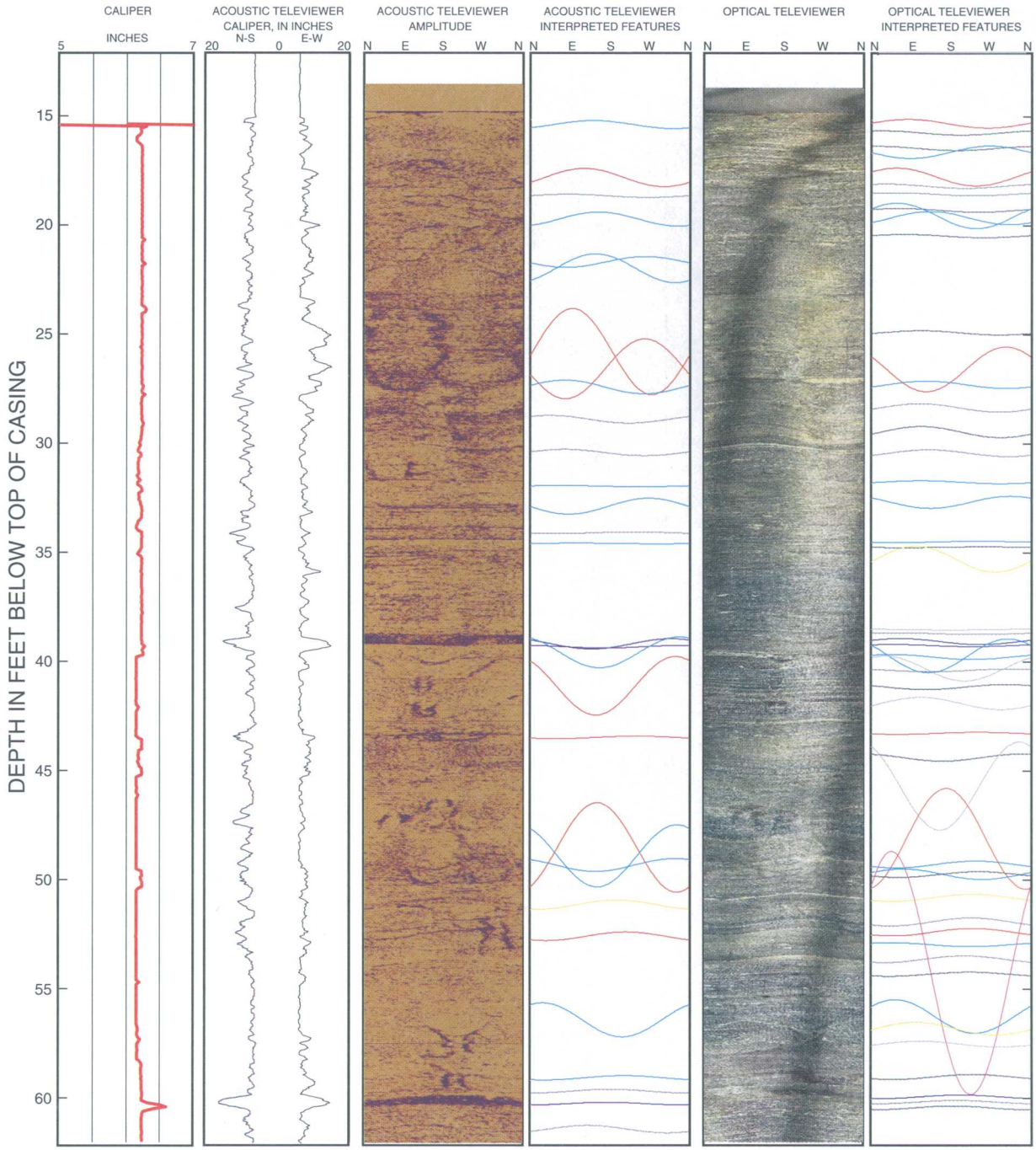

Appendix 1C. Caliper, acoustic-caliper, acoustic-televiewer, and optical-televiewer images and interpreted structures from borehole MW201R in the UConn landfill study area, Storrs, Connecticut--Continued

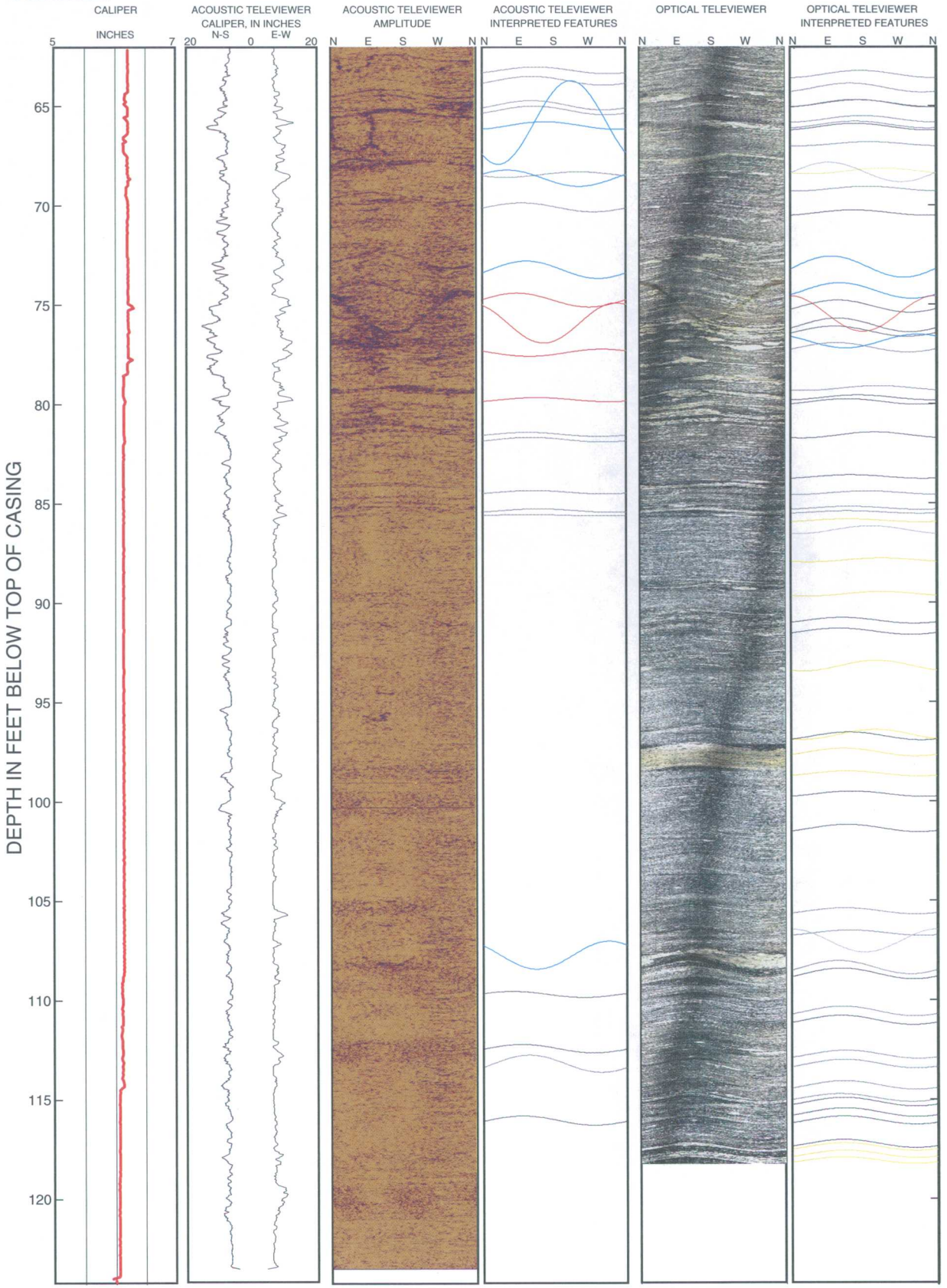

Appendix 1D. Processed borehole-radar reflection logs from borehole MW201R in the UConn landfill study area, Storrs, Connecticut

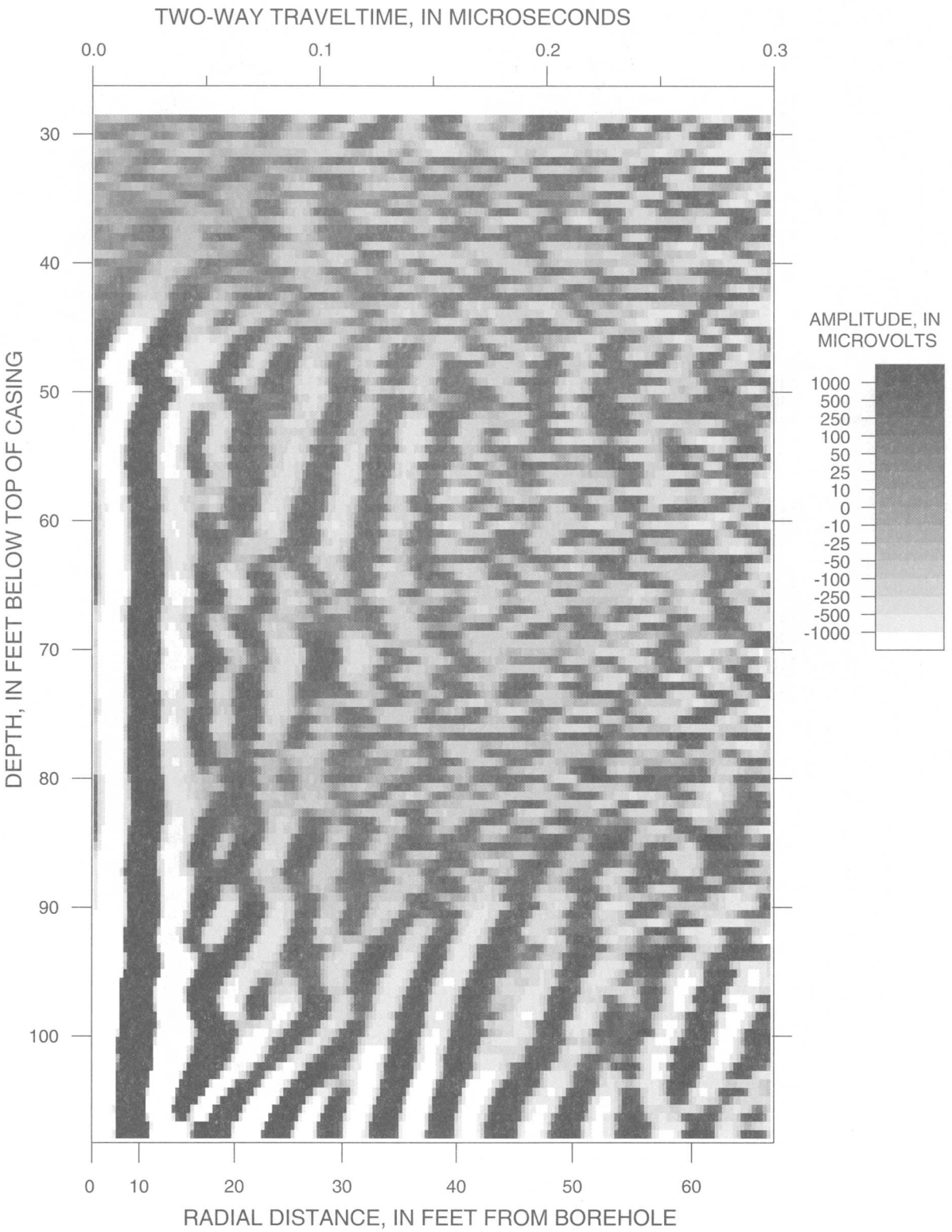

Appendix 1E. Midpoint depth, strike, and dip of features identified in optical-televiewer logs from borehole MW201R in the UConn landfill study area, Storrs, Connecticut

[Depth in feet below top of casing. Strike is reported in "right-hand rule" (RHR) where the direction of dip is to the right of the strike.
-, no measurement]

Midpoint depth, in feet	Dip azimuth, in degrees	Strike, RHR in degrees	Dip, in degrees	Dip direction	Description
15.2	-	-	0	-	bottom of casing
15.4	261	171	38	W	fracture
15.8	203	113	21	SW	foliation
16.5	193	103	21	S	foliation
16.7	87	357	48	E	minor fracture
17.8	235	145	58	SW	fracture
18.2	212	122	21	SW	parting parallel to foliation
18.6	231	141	14	SW	parting parallel to foliation
19.3	242	152	18	SW	foliation
19.6	236	146	66	SW	minor fracture
19.7	311	221	50	NW	minor fracture
20.5	254	164	17	W	foliation
24.9	290	200	21	W	foliation
26.6	123	33	76	SE	fracture
27.4	304	214	33	NW	minor fracture
28.4	289	199	37	W	parting parallel to foliation
29.5	292	202	45	W	foliation
30.5	309	219	31	NW	parting parallel to foliation
31.8	291	201	15	W	minor fracture
32.7	134	44	47	SE	minor fracture
34.5	60	330	6	NE	minor fracture
34.8	73	343	4	E	foliation
35.3	280	190	67	W	lithologic feature
38.5	175	85	4	S	sealed fracture
38.7	237	147	9	SW	parting parallel to foliation
39.1	246	156	28	SW	minor fracture, possible transmissive fracture
39.3	229	139	11	SW	minor fracture, possible transmissive fracture
39.8	129	39	72	SE	minor fracture
39.8	227	137	24	SW	minor fracture
40.3	211	121	66	SW	sealed fracture
40.4	133	43	13	SE	parting parallel to foliation
41.2	123	33	24	SE	foliation
41.9	292	202	48	W	sealed fracture
43.3	58	328	10	NE	fracture
44.4	161	71	32	S	foliation
45.7	154	64	83	SE	sealed fracture
48.1	348	258	84	N	fracture
49.3	55	325	32	NE	minor fracture
49.8	251	161	43	W	minor fracture
49.8	62	332	27	NE	foliation
50.8	47	317	32	NE	lithologic feature
52.0	45	315	36	NE	parting parallel to foliation
52.4	47	317	34	NE	fracture

Appendix 1E. Midpoint depth, strike, and dip of features identified in optical-televiewer logs from borehole MW201R in the UConn landfill study area, Storrs, Connecticut—Continued

[Depth in feet below top of casing. Strike is reported in "right-hand rule" (RHR) where the direction of dip is to the right of the strike. -, no measurement]

Midpoint depth, in feet	Dip azimuth, in degrees	Strike, RHR in degrees	Dip, in degrees	Dip direction	Description
53.0	225	135	19	SW	minor fracture
53.7	30	300	31	NE	parting parallel to foliation
54.3	224	134	87	SW	vertical fracture from 54-60 ft
54.3	40	310	21	NE	foliation
56.3	234	144	72	SW	minor fracture
56.8	280	190	49	W	lithologic feature
57.5	291	201	28	W	sealed fracture
59.0	49	319	24	NE	foliation
59.9	20	290	18	N	transmissive fracture
60.2	11	281	16	N	parting parallel to foliation
60.5	2	272	19	N	foliation
63.4	352	262	36	N	parting parallel to foliation
64.1	327	237	42	NW	parting parallel to foliation
64.8	341	251	38	N	parting parallel to foliation
64.8	347	257	34	N	foliation
65.6	357	267	33	N	parting parallel to foliation
65.9	339	249	34	N	parting parallel to foliation
66.0	338	248	33	N	foliation
66.9	14	284	22	N	parting parallel to foliation
68.2	48	318	29	NE	lithologic feature
68.3	274	184	63	W	sealed fracture
69.2	9	279	24	N	parting parallel to foliation
70.4	334	244	28	NW	foliation
73.1	280	190	65	W	minor fracture
74.3	300	210	57	NW	minor fracture
75.1	295	205	51	NW	foliation
75.4	179	89	74	S	fracture
76.0	295	205	54	NW	foliation
76.3	288	198	46	W	foliation
76.8	135	45	54	SE	minor fracture
77.2	290	200	43	W	parting parallel to foliation
79.2	35	305	25	NE	parting parallel to foliation
79.7	345	255	26	N	foliation
79.9	317	227	29	NW	foliation
81.6	26	296	30	NE	foliation
83.7	327	237	20	NW	foliation
84.5	7	277	19	N	parting parallel to foliation
85.2	322	232	17	NW	parting parallel to foliation
85.4	319	229	15	NW	parting parallel to foliation
85.9	319	229	17	NW	lithologic feature
86.3	17	287	38	N	sealed fracture
87.9	43	313	21	NE	lithologic feature
89.6	43	313	24	NE	lithologic feature

Appendix 1E. Midpoint depth, strike, and dip of features identified in optical-televiewer logs from borehole MW201R in the UConn landfill study area, Storrs, Connecticut—Continued

[Depth in feet below top of casing. Strike is reported in "right-hand rule" (RHR) where the direction of dip is to the right of the strike. -, no measurement]

Midpoint depth, in feet	Dip azimuth, in degrees	Strike, RHR in degrees	Dip, in degrees	Dip direction	Description
90.9	304	214	30	NW	foliation
91.4	297	207	32	NW	foliation
93.2	30	300	46	NE	lithologic feature
96.6	26	296	45	NE	lithologic feature
96.7	320	230	38	NW	foliation
97.5	307	217	38	NW	lithologic feature
98.6	316	226	27	NW	lithologic feature
99.6	327	237	28	NW	foliation
101.4	315	225	37	NW	foliation
105.5	308	218	32	NW	parting parallel to foliation
106.7	322	232	28	NW	parting parallel to foliation
107.1	180	90	66	S	sealed fracture
108.4	293	203	53	NW	parting parallel to foliation
108.7	301	211	47	NW	foliation
110.6	304	214	44	NW	parting parallel to foliation
111.0	299	209	43	NW	foliation
112.8	312	222	39	NW	parting parallel to foliation
113.2	307	217	41	NW	parting parallel to foliation
114.3	307	217	41	NW	parting parallel to foliation
114.9	297	207	38	NW	parting parallel to foliation
115.1	306	216	41	NW	foliation
115.7	308	218	41	NW	foliation
116.1	307	217	39	NW	foliation
117.2	306	216	39	NW	foliation
117.4	307	217	38	NW	lithologic feature
117.8	310	220	37	NW	lithologic feature
118.1	305	215	34	NW	lithologic feature

Appendix 1F. Midpoint depth, strike, and dip of features identified in acoustic-televiewer logs from borehole MW201R in the UConn landfill study area, Storrs, Connecticut

[Depth in feet below top of casing. Strike is reported in "right-hand rule" (RHR) where the direction of dip is to the right of the strike. -, no measurement]

Midpoint depth, in feet	Dip azimuth, in degrees	Strike, RHR in degrees	Dip, in degrees	Dip direction	Description
15.2	-	-	0	-	bottom of casing
15.4	321	231	36	NW	minor fracture
17.9	300	210	59	NW	fracture
18.7	265	175	16	W	parting parallel to foliation
19.8	333	243	52	NW	minor fracture
21.7	79	349	44	E	minor fracture
22.0	327	237	69	NW	minor fracture
25.8	273	183	83	W	fracture
26.6	77	347	79	E	fracture
27.5	257	167	51	W	minor fracture
28.9	223	133	35	SW	parting parallel to foliation
30.4	257	167	30	W	parting parallel to foliation
32.0	249	159	6	W	minor fracture
32.9	87	357	55	E	minor fracture
34.1	52	322	9	NE	parting parallel to foliation
34.6	285	195	4	W	minor fracture
39.2	138	48	43	SE	transmissive fracture
39.3	166	76	14	S	transmissive fracture
39.6	157	67	70	SE	minor fracture
41.1	147	57	79	SE	fracture
43.5	56	326	12	NE	fracture
48.5	330	240	83	NW	fracture
48.9	152	62	80	SE	minor fracture
49.4	147	57	49	SE	minor fracture
51.2	15	285	40	N	lithologic feature
52.6	34	304	38	NE	fracture
56.4	208	118	72	SW	minor fracture
59.1	32	302	21	NE	minor fracture
59.7	0	270	19	N	parting parallel to foliation
60.3	351	261	14	N	transmissive fracture
61.4	310	220	34	NW	parting parallel to foliation
63.2	315	225	34	NW	parting parallel to foliation
63.7	305	215	41	NW	parting parallel to foliation
64.9	304	214	43	NW	parting parallel to foliation
65.2	310	220	41	NW	parting parallel to foliation
65.8	42	312	83	NE	minor fracture
65.9	337	247	37	NW	minor fracture
68.4	60	330	28	NE	parting parallel to foliation
68.6	243	153	58	SW	minor fracture
70.1	279	189	42	W	parting parallel to foliation
73.2	291	201	60	W	minor fracture
74.7	268	178	54	W	fracture
75.9	155	65	76	SE	fracture

Appendix 1F. Midpoint depth, strike, and dip of features identified in acoustic-televiewer logs from borehole MW201R in the UConn landfill study area, Storrs, Connecticut—Continued

[Depth in feet below top of casing. Strike is reported in "right-hand rule" (RHR) where the direction of dip is to the right of the strike. -, no measurement]

Midpoint depth, in feet	Dip azimuth, in degrees	Strike, RHR in degrees	Dip, in degrees	Dip direction	Description
77.4	120	30	35	SE	fracture
79.7	317	227	23	NW	fracture
81.5	292	202	22	W	parting parallel to foliation
81.8	301	211	25	NW	parting parallel to foliation
84.4	307	217	20	NW	parting parallel to foliation
85.3	319	229	19	NW	parting parallel to foliation
85.6	293	203	8	NW	parting parallel to foliation
107.8	135	45	70	SE	minor fracture
109.7	253	163	31	W	foliation
112.5	276	186	40	W	foliation
113.2	295	205	60	NW	parting parallel to foliation
116.1	278	188	43	W	foliation

Appendix 1G. Location, orientation, and length of reflectors interpreted from borehole-radar data from borehole MW201R in the UConn landfill study area, Storrs, Connecticut

[Depth in feet below top of casing. Strike is reported in "right-hand rule" (RHR) where the direction of dip is to the right of the strike. Reflector continuity is on a scale of 1 (good) to 5 (poor)]

Midpoint depth, in feet	Dip azimuth, in degrees	Strike, RHR in degrees	Dip, in degrees	Dip direction	Estimated reflector length, in feet	Reflector continuity
39.7	227	137	24	SW	9.5	5
76.4	252	162	46	W	8.5	4
79.7	317	227	29	NW	16.4	4
84.3	5	275	24	N	12.5	4
112.9	312	222	39	NW	8.5	4
116.1	307	217	39	NW	9.2	4
117.8	310	220	37	NW	15.4	3
130.9	125	35	26	SE	28.2	2
156.2	115	25	71	SE	13.5	4
207.0	335	245	70	NW	21.0	3
228.4	115	25	61	SE	14.8	4

Appendix 1H. Heat-pulse flowmeter measurements in MW201R at the UConn landfill study area, Storrs, Connecticut

[--indicates no flow; for interpretation, if nothing is listed, there is no change in inflow or outflow]

Date	Depth of measurement, in feet below top of casing	Flow direction	Average rate, in gallons per minute	Normalized average rate, in gallons per minute	Interpretation
August 29, 2000	Ambient conditions				No measurable flow
August 29, 2000	Pumping at 0.25 gallon per minute				
	14.0	up	0.115	0.240	
	19.0	up	0.120	0.250	
	30.0	up	0.100	0.208	
	37.0	up	0.108	0.225	Inflow at 38 to 39 feet
	46.0	up	0.053	0.110	
	58.0	up	0.039	0.081	Inflow at 60 feet
	63.0	up	0.020	0.042	Possible inflow at 66 feet
	69.0	up	0.009	0.019	
	78.5	--	0.000	0.000	
	107.0	--	0.000	0.000	
	111.0	--	0.000	0.000	
September 7, 2000	Pumping at 0.25 gallon per minute				
	22.5	up	0.102	0.142	
	23.0	up	0.180	0.250	
	37.0	up	0.159	0.221	Inflow at 38 to 39 feet
	58.0	up	0.068	0.094	Inflow at 60 feet
	74.0	--	0.000	0.000	
	95.0	--	0.000	0.000	
	105.0	--	0.000	0.000	
	122.5	--	0.000	0.000	

Appendix 1I. Tadpole plots and stereoplots of fractures and foliations interpreted in optical-televiewer images from borehole MW201R in the UConn landfill study area, Storrs, Connecticut

[OTV, optical televiewer]

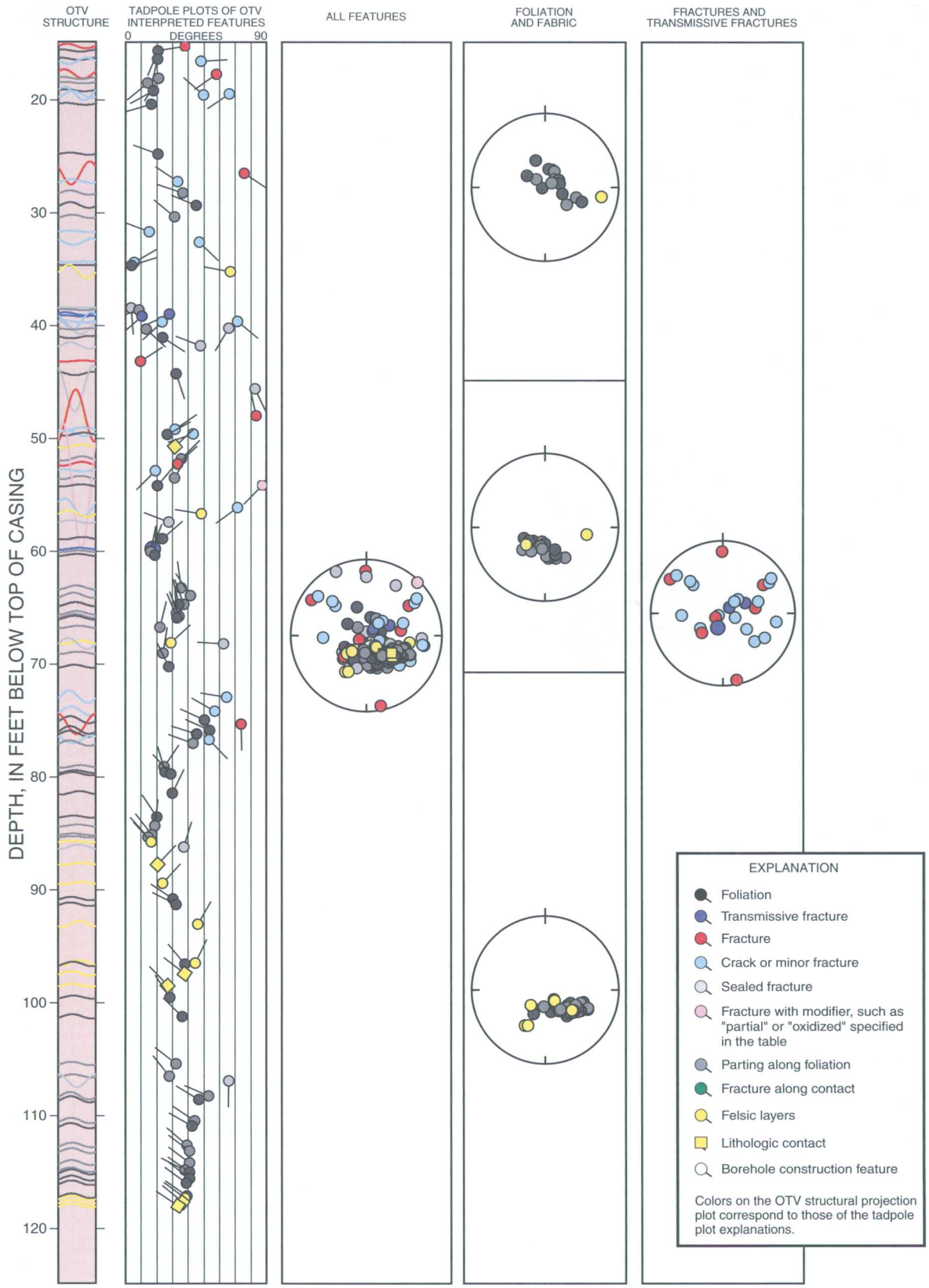

Appendix 1J. Tadpole plots and stereoplots of fractures and foliations interpreted in acoustic-televiewer images from borehole MW201R in the UConn landfill study area, Storrs, Connecticut

[ATV, acoustic televiewer]

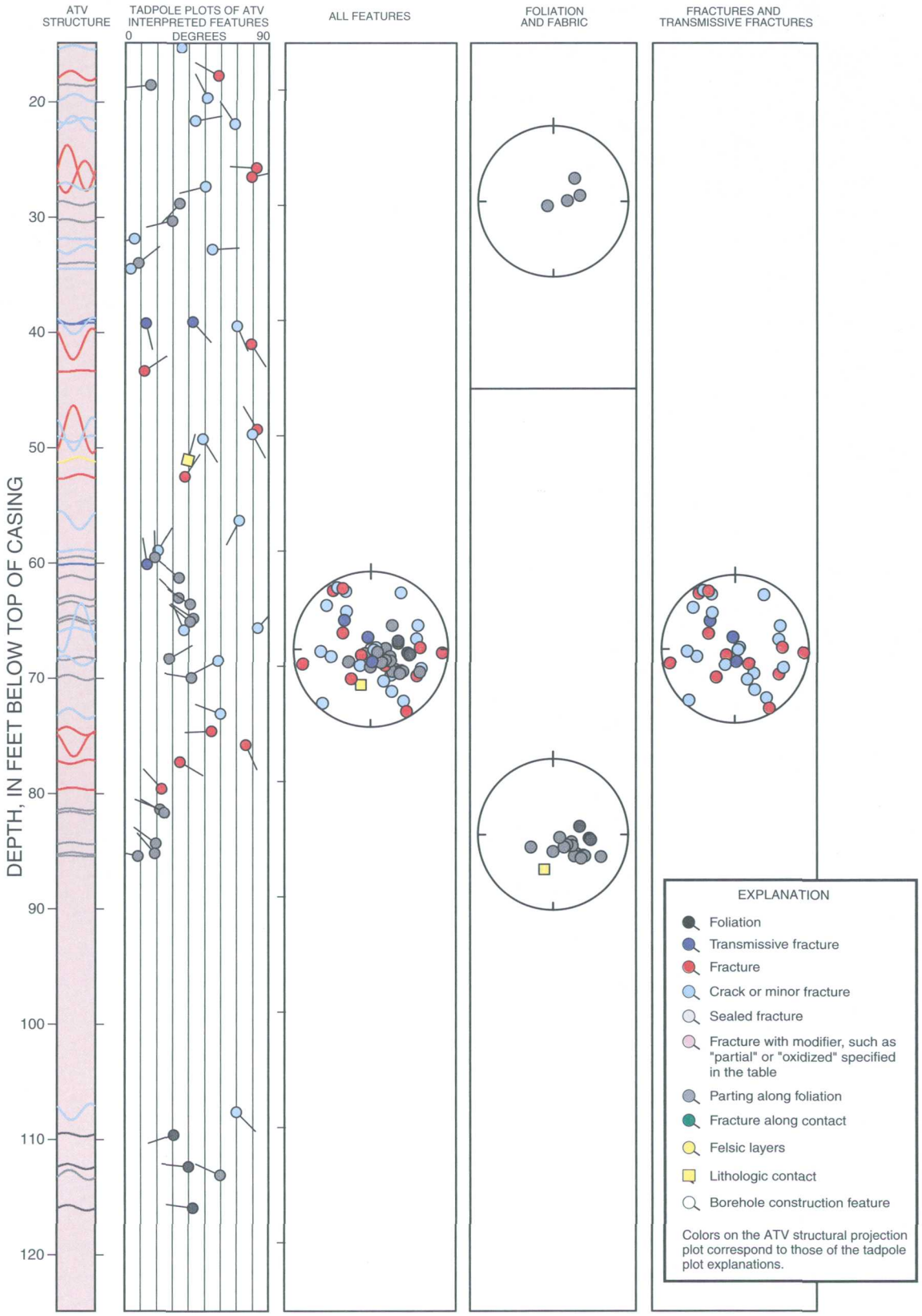

Appendix 2. Borehole-geophysical logs from borehole MW202R in the UConn landfill study area, Storrs, Connecticut

Appendix 2A. Deviation log of borehole MW202R in the UConn landfill study area, Storrs, Connecticut
[ft, feet]

MW202R

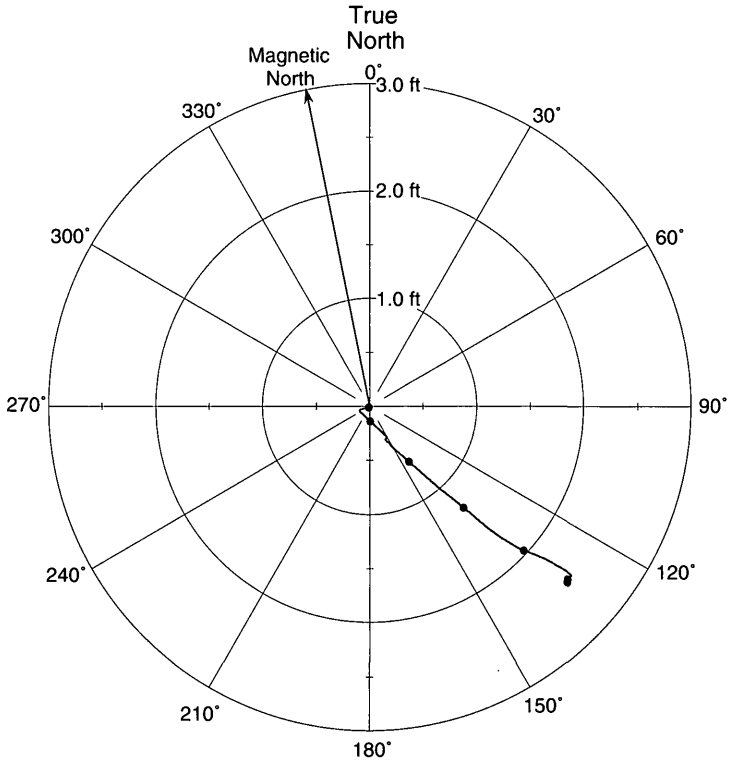

Depth along borehole in 20-foot increments between circles (•)

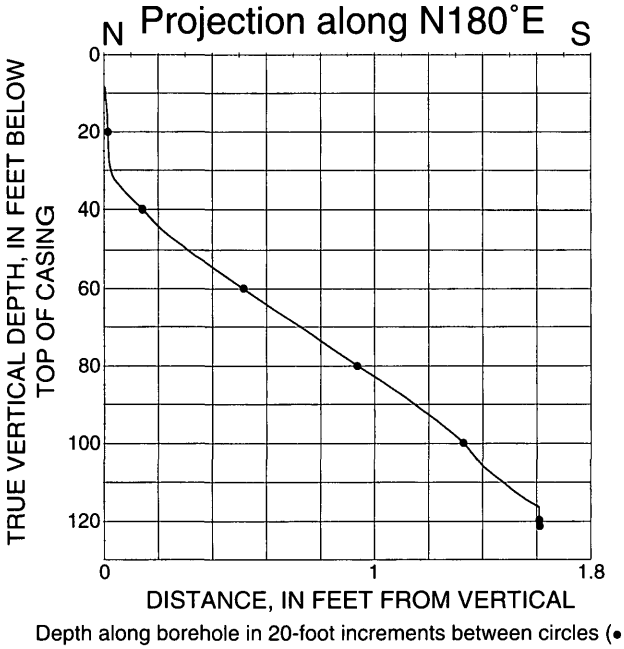

Depth along borehole in 20-foot increments between circles (•)

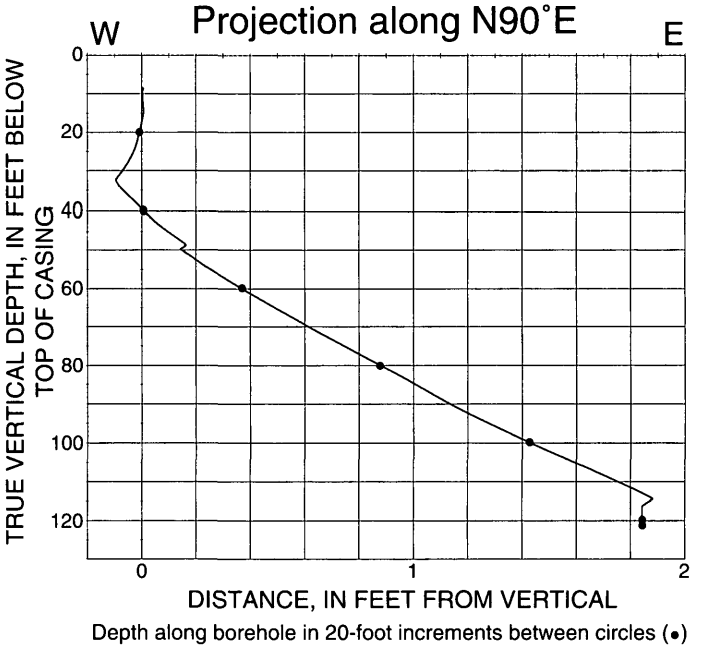

Depth along borehole in 20-foot increments between circles (•)

Appendix 2B. Composite log of natural-gamma, electromagnetic induction, fluid-temperature, specific-conductance, and heat-pulse flowmeter logs from borehole MW202R in the UConn landfill study area, Storrs, Connecticut

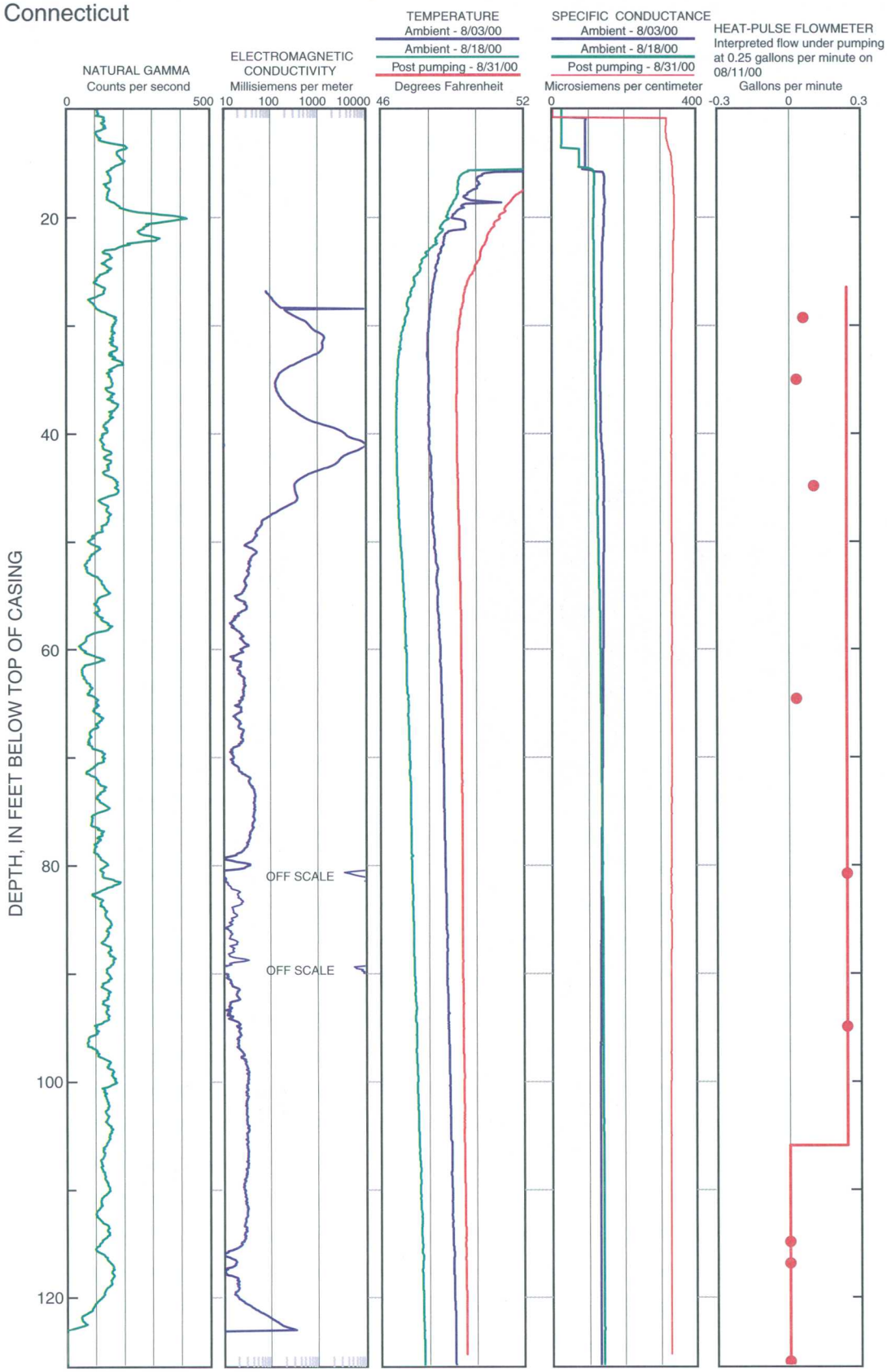

Appendix 2C. Caliper, acoustic-caliper, acoustic-televiewer, and optical-televiewer images and interpreted structures from borehole MW202R in the UConn landfill study area, Storrs, Connecticut

[Interpreted features indicated by color: black - foliation; dark blue - transmissive fracture; red - fracture; light blue - crack or minor fracture; gray - sealed fracture; pink - fracture with modifier, such as "partial" or "oxidized"; blue-gray - parting along foliation; green - fracture along contact; yellow - felsic layer]

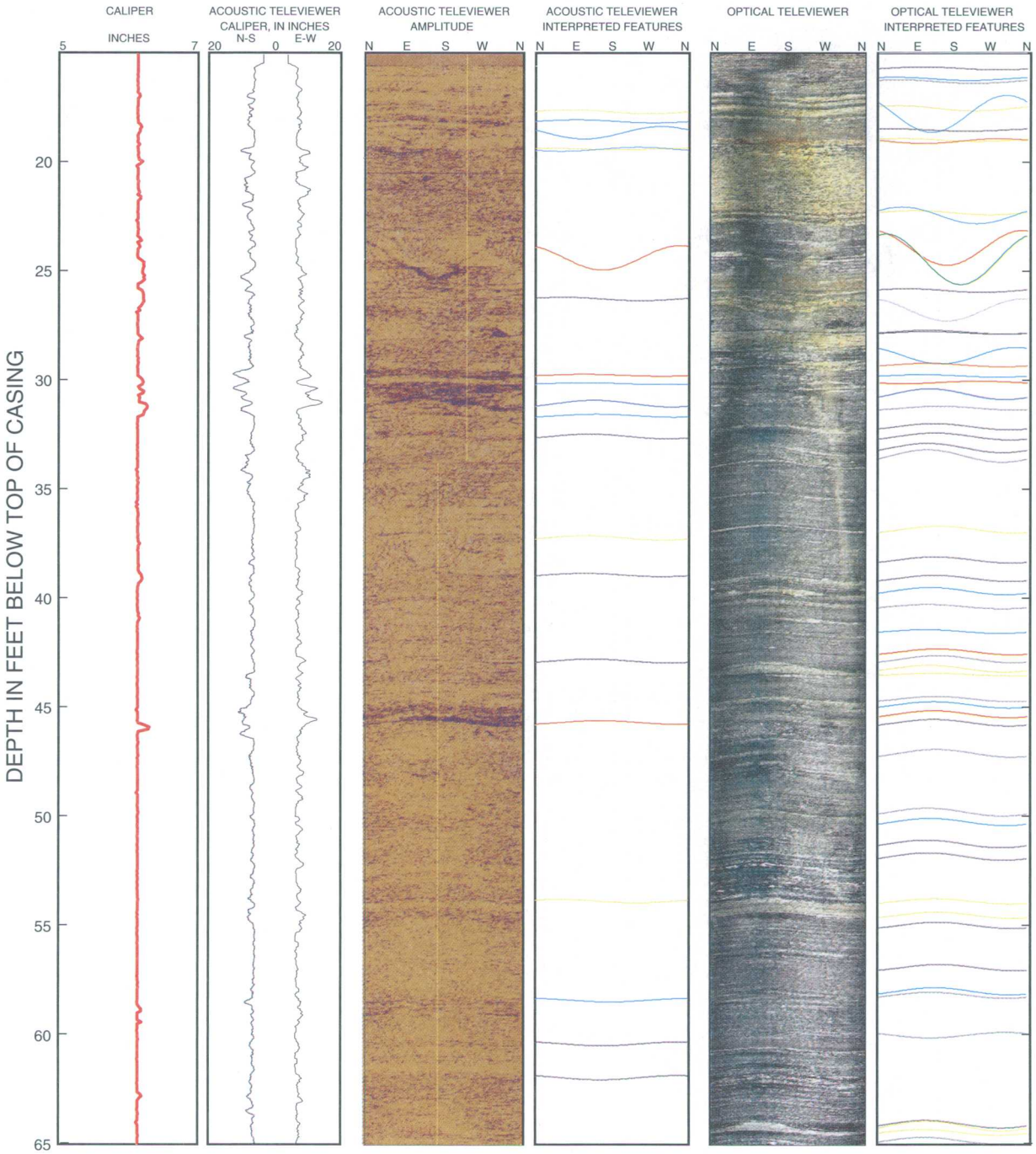

Appendix 2C. Caliper, acoustic-caliper, acoustic-televiewer, and optical-televiewer images and interpreted structures from borehole MW202R in the UConn landfill study area, Storrs, Connecticut-Continued

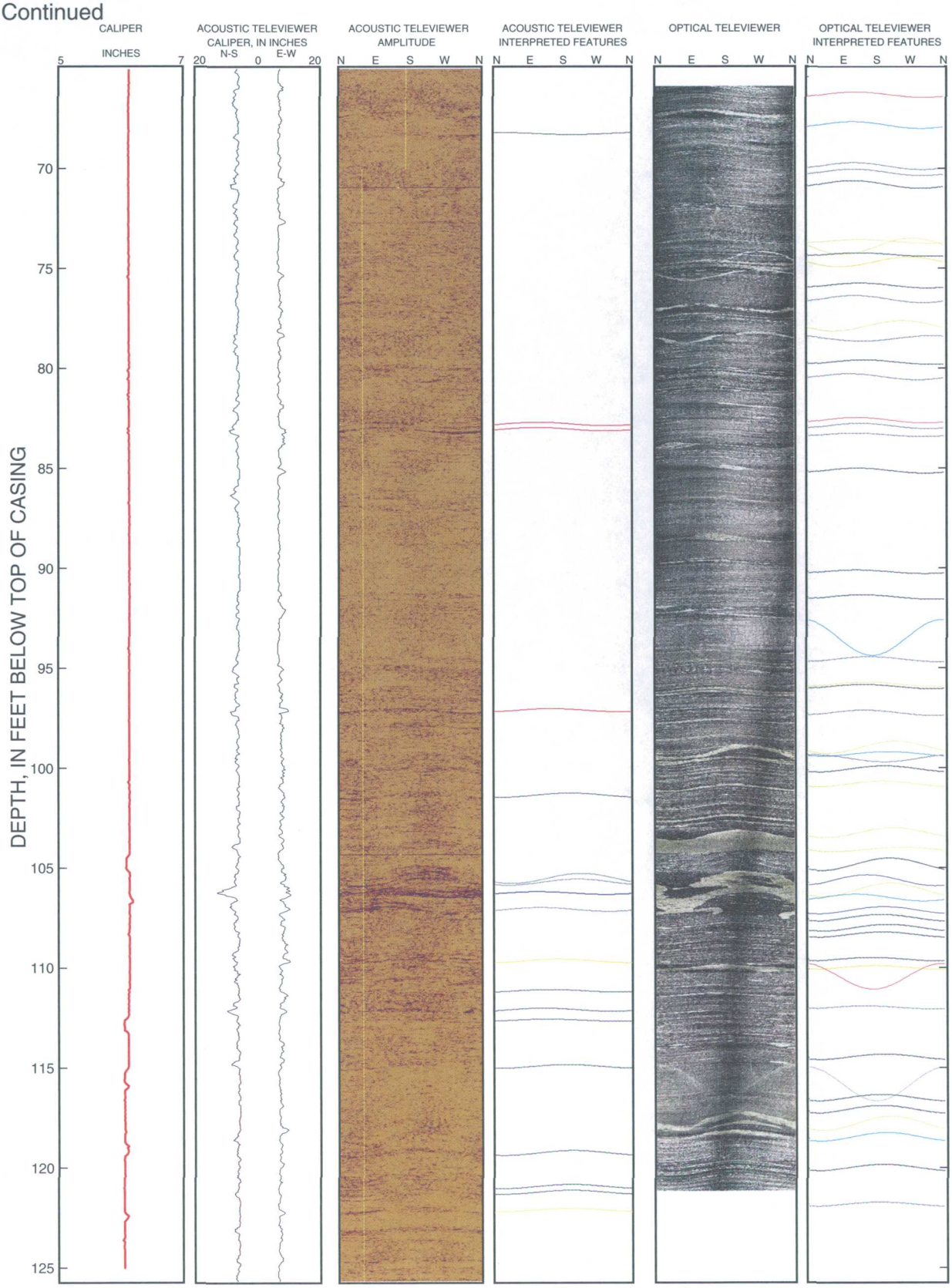

Appendix 2D. Processed borehole-radar reflection logs from borehole MW202R in the UConn landfill study area, Storrs, Connecticut

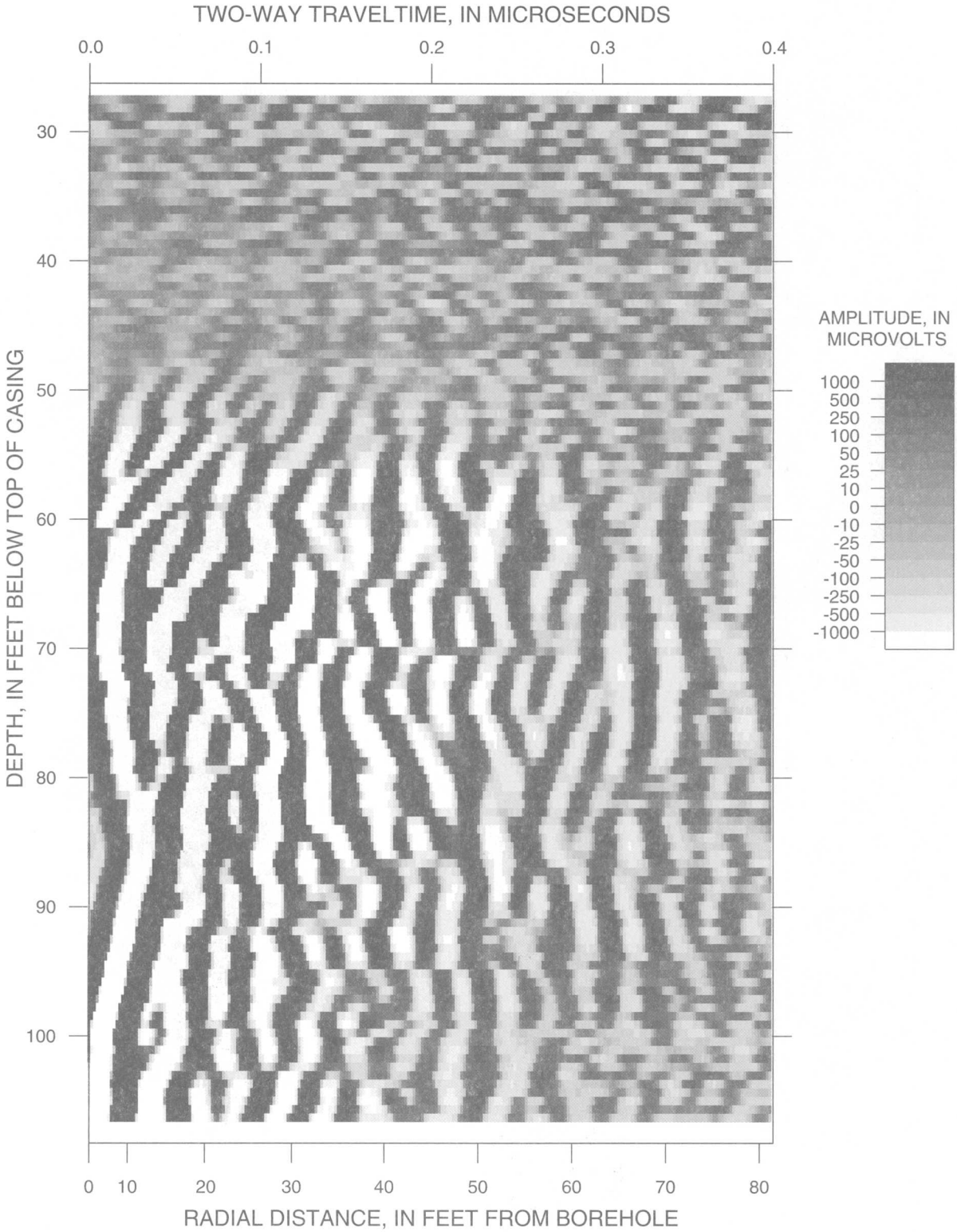

Appendix 2E. Midpoint depth, strike, and dip of features identified in optical-televiewer logs from borehole MW202R in the UConn landfill study area, Storrs, Connecticut

Depth in feet below top of casing. Strike is reported in "right-hand rule" (RHR) where the direction of dip is to the right of the strike. -, no measurement]

Midpoint depth, in feet	Dip azimuth, in degrees	Strike, RHR in degrees	Dip, in degrees	Dip direction	Description
13.2	-	-	0	-	bottom of casing
14.4	219	129	38	SW	minor fracture
14.4	47	317	37	NE	parting parallel to foliation
15.1	211	121	20	SW	foliation
15.5	-	-	0	-	water level
16.1	286	196	14	W	foliation
16.6	220	130	16	SW	minor fracture
16.7	229	139	18	SW	parting parallel to foliation
17.9	230	140	25	SW	lithologic feature
18.2	129	39	73	SE	minor fracture
18.9	211	121	12	SW	foliation
19.4	237	147	15	SW	lithologic feature
19.4	108	18	23	E	fracture
22.6	266	176	20	W	lithologic feature
22.8	238	148	56	SW	minor fracture
24.3	164	74	72	S	fracture
26.2	249	159	17	W	foliation
27.1	165	75	63	S	other
28.1	300	210	17	NW	foliation
28.1	298	208	13	NW	foliation
29.2	151	61	56	SE	minor fracture
29.6	297	207	17	NW	fracture
30.1	288	198	12	W	minor fracture
30.4	61	331	12	NE	fracture
30.9	304	214	44	NW	transmissive fracture
31.5	329	239	19	NW	parting parallel to foliation
32.4	315	225	29	NW	foliation
32.8	317	227	31	NW	foliation
33.4	299	209	39	NW	foliation
33.7	298	208	48	NW	parting parallel to foliation
37.1	326	236	31	NW	lithologic feature
38.5	318	228	28	NW	foliation
39.3	317	227	29	NW	foliation
39.9	308	218	32	NW	minor fracture
40.6	299	209	21	NW	parting parallel to foliation
41.7	295	205	18	NW	minor fracture
42.7	321	231	27	NW	fracture
43.0	325	235	32	NW	parting parallel to foliation
43.4	303	213	31	NW	lithologic feature
43.7	311	221	12	NW	lithologic feature
44.8	321	231	24	NW	parting parallel to foliation
45.0	316	226	30	NW	minor fracture
45.5	312	222	32	NW	fracture
45.9	315	225	30	NW	foliation

Appendix 2E. Midpoint depth, strike, and dip of features identified in optical-televiewer logs from borehole MW202R in the UConn landfill study area, Storrs, Connecticut—Continued

Depth in feet below top of casing. Strike is reported in "right-hand rule" (RHR) where the direction of dip is to the right of the strike. -, no measurement]

Midpoint depth, in feet	Dip azimuth, in degrees	Strike, RHR in degrees	Dip, in degrees	Dip direction	Description
47.2	321	231	34	NW	parting parallel to foliation
49.9	300	210	35	NW	parting parallel to foliation
50.4	308	218	32	NW	minor fracture
51.4	296	206	34	NW	foliation
51.9	301	211	33	NW	foliation
54.0	315	225	25	NW	lithologic feature
54.6	321	231	29	NW	lithologic feature
55.1	323	233	29	NW	foliation
57.0	328	238	28	NW	foliation
58.1	319	229	32	NW	minor fracture
58.2	308	218	28	NW	parting parallel to foliation
60.1	126	36	26	SE	parting parallel to foliation
64.1	295	205	34	NW	foliation
64.2	295	205	41	NW	lithologic feature
64.5	286	196	26	W	lithologic feature
64.9	291	201	32	W	parting parallel to foliation
66.3	307	217	28	NW	fracture
67.8	300	210	34	NW	minor fracture
69.9	302	212	34	NW	parting parallel to foliation
70.2	302	212	33	NW	parting parallel to foliation
70.8	299	209	38	NW	foliation
73.6	318	228	21	NW	lithologic feature
73.9	96	6	58	E	lithologic feature
74.3	316	226	19	NW	foliation
74.7	86	356	43	E	lithologic feature
75.8	317	227	26	NW	foliation
76.5	305	215	35	NW	parting parallel to foliation
77.9	68	338	45	E	lithologic feature
78.5	145	55	28	SE	parting parallel to foliation
79.7	328	238	23	NW	foliation
80.4	290	200	31	W	parting parallel to foliation
82.6	308	218	29	NW	fracture
82.9	317	227	28	NW	parting parallel to foliation
83.3	303	213	19	NW	parting parallel to foliation
85.1	310	220	26	NW	foliation
90.2	307	217	20	NW	foliation
91.4	323	233	23	NW	foliation
93.5	171	81	74	S	minor fracture
94.5	341	251	26	N	parting parallel to foliation
95.8	333	243	24	NW	lithologic feature
95.9	325	235	23	NW	foliation
97.2	329	239	27	NW	parting parallel to foliation
99.0	51	321	50	NE	lithologic feature
99.3	29	299	24	NE	minor fracture

Appendix 2E. Midpoint depth, strike, and dip of features identified in optical-televiewer logs from borehole MW202R in the UConn landfill study area, Storrs, Connecticut—Continued

Depth in feet below top of casing. Strike is reported in "right-hand rule" (RHR) where the direction of dip is to the right of the strike. -, no measurement]

Midpoint depth, in feet	Dip azimuth, in degrees	Strike, RHR in degrees	Dip, in degrees	Dip direction	Description
99.5	202	112	34	S	parting parallel to foliation
100.0	21	291	31	N	foliation
100.8	16	286	30	N	lithologic feature
103.3	43	313	44	NE	lithologic feature
104.1	65	335	23	NE	lithologic feature
104.8	34	304	51	NE	foliation
105.6	335	245	47	NW	transmissive fracture
106.1	36	306	53	NE	lithologic feature
106.5	305	215	34	NW	minor fracture
107.1	20	290	35	N	transmissive fracture
107.5	12	282	33	N	foliation
108.0	29	299	33	NE	foliation
108.3	14	284	27	N	foliation
109.6	346	256	19	N	foliation
110.0	354	264	20	N	lithologic feature
110.5	170	80	68	S	fracture
112.0	328	238	17	NW	parting parallel to foliation
114.5	19	289	28	N	foliation
115.8	179	89	73	S	sealed fracture
116.5	10	280	33	N	foliation
117.1	11	281	38	N	foliation
117.8	36	306	54	NE	lithologic feature
118.5	24	294	40	NE	minor fracture
120.0	16	286	32	N	foliation
121.8	8	278	22	N	parting parallel to foliation

Appendix 2F. Midpoint depth, strike, and dip of features identified in acoustic-televiewer logs from borehole MW202R in the UConn landfill study area, Storrs, Connecticut

[Depth in feet below top of casing. Strike is reported in "right-hand rule" (RHR) where the direction of dip is to the right of the strike. -, no measurement]

Midpoint depth, in feet	Dip azimuth, in degrees	Strike, RHR in degrees	Dip, in degrees	Dip direction	Description
15.6	-	-	0	-	water level
17.7	263	173	29	W	lithologic feature
18.1	276	186	23	W	minor fracture
18.7	114	24	60	SE	minor fracture
19.4	191	101	10	S	lithologic feature
19.4	61	331	30	NE	minor fracture
24.4	156	66	74	SE	fracture
26.3	245	155	26	SW	foliation
29.8	294	204	15	NW	fracture
30.1	297	207	12	NW	minor fracture
31.1	318	228	43	NW	transmissive fracture
31.6	325	235	22	NW	minor fracture
32.6	307	217	33	NW	foliation
37.2	297	207	32	NW	lithologic feature
38.9	293	203	24	NW	foliation
42.9	312	222	28	NW	foliation
45.7	330	240	27	NW	fracture
53.9	235	145	25	SW	lithologic feature
58.4	175	85	26	S	minor fracture
60.4	156	66	28	SE	foliation
61.9	152	62	31	SE	foliation
68.3	205	115	17	SW	foliation
82.8	292	202	29	W	fracture
83.1	291	201	29	W	fracture
97.1	327	237	26	NW	fracture
101.4	16	286	33	N	foliation
105.6	45	315	57	NE	parting parallel to foliation
105.7	35	305	43	NE	parting parallel to foliation
106.3	292	202	23	W	transmissive fracture
107.1	298	208	31	NW	parting parallel to foliation
109.7	346	256	30	N	lithologic feature
111.2	323	233	21	NW	foliation
112.1	306	216	26	NW	foliation
112.7	315	225	18	NW	foliation
115.0	7	277	29	N	foliation
119.3	23	293	36	NE	foliation
121.0	20	290	32	N	foliation
121.3	19	289	32	N	foliation
122.1	15	285	26	N	lithologic feature

Appendix 2G. Location, orientation, and length of reflectors interpreted from borehole-radar data from borehole MW202R in the UConn landfill study area, Storrs, Connecticut

[Depth in feet below top of casing. Strike is reported in "right-hand rule" (RHR) where the direction of dip is to the right of the strike. Reflector continuity is on a scale of 1 (good) to 5 (poor); --, cannot be determined]

Midpoint depth, in feet	Dip azimuth, in degrees	Strike, RHR in degrees	Dip, in degrees	Dip direction	Estimated reflector length, in feet	Reflector continuity
-38.1	75	345	61	E	28.0	3
30.8	283	193	44	W	22.2	4
39.0	75	345	17	E	25.1	3
39.7	265	175	42	W	41.2	4
49.9	300	210	35	NW	14.4	5
[1]76.4	--	--	0	--	--	4
98.8	202	112	38	S	24.7	4
143.7	265	175	18	W	22.5	4

[1]Horizontal fracture—Reflector dip azimuth, strike, dip direction, and length cannot be determined.

Appendix 2H. Heat-pulse flowmeter measurements in MW202R at the UConn landfill study area, Storrs, Connecticut

[-- indicates no flow; for interpretation, if nothing is listed, there is no change in inflow or outflow]

Date	Depth of measurement, in feet below top of casing	Flow direction	Average rate, in gallons per minute	Normalized average rate, in gallons per minute	Interpretation
August 4, 2000	Ambient conditions				No measurable flow
September 9, 2000	Ambient conditions				No measurable flow
August 11, 2000	Pumping at 0.25 gallon per minute				
	29.3	up	0.035	0.054	Possible inflow at 30 feet
	35.0	up	0.022	0.034	
	44.9	up	0.069	0.106	
	64.6	up	0.020	0.031	
	80.9	up	0.164	0.250	
	95.0	up	0.164	0.250	Inflow between 105 and 107 feet
	115.0	--	0.000	0.000	
	117.0	--	0.000	0.000	
	126.1	--	0.000	0.000	
August 16, 2000[1]	Pumping at 0.25 gallon per minute				
	44.9	up	0.021	0.250	
	64.9	up	0.021	0.250	
	80.9	up	0.020	0.238	
	95.0	up	0.020	0.238	Inflow at 97 or 105 feet
	115.1	--	0.000	0.000	
	117.0	--	0.000	0.000	
	125.0	--	0.000	0.000	
September 6, 2000[1]	Pumping at 0.25 gallon per minute				
	50.0	up	0.030	0.242	
	56.0	up	0.024	0.194	
	80.0	up	0.031	0.250	
	94.0	up	0.031	0.250	Possible inflow at 97 feet
	103.0	up	0.026	0.210	Inflow at 105-107 feet
	117.0	--	0.000	0.000	
	120.0	--	0.000	0.000	

[1]Log was rerun because of poor tool response relative to the total pumping.

Appendix 2I. Tadpole plots and stereoplots of fractures and foliations interpreted in optical-televiewer images from borehole MW202R in the UConn landfill study area, Storrs, Connecticut

[OTV, optical televiewer]

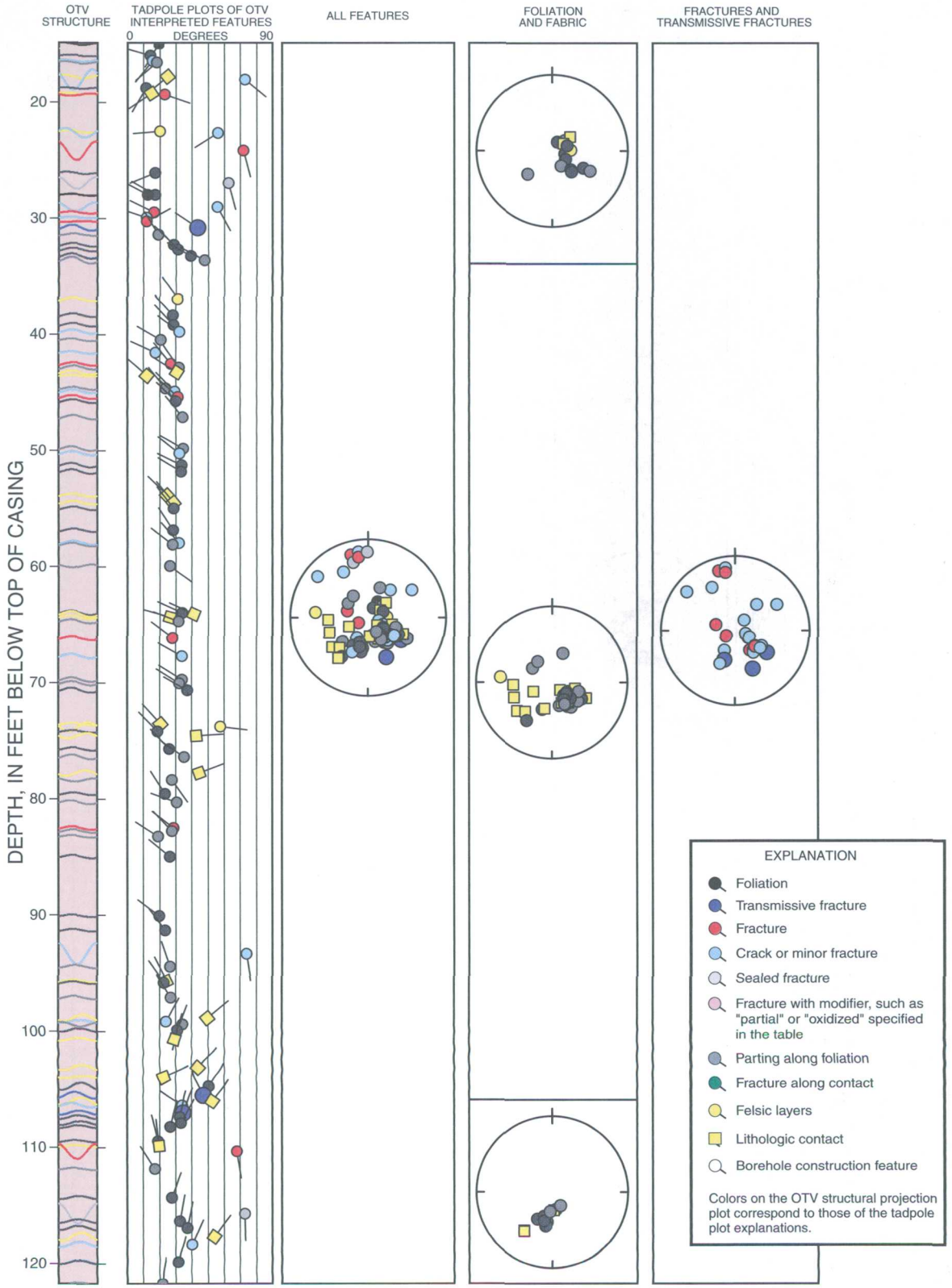

Appendix 2J. Tadpole plots and stereoplots of fractures and foliations interpreted in acoustic-televiewer images from borehole MW202R in the UConn landfill study area, Storrs, Connecticut

[ATV, acoustic televiewer]

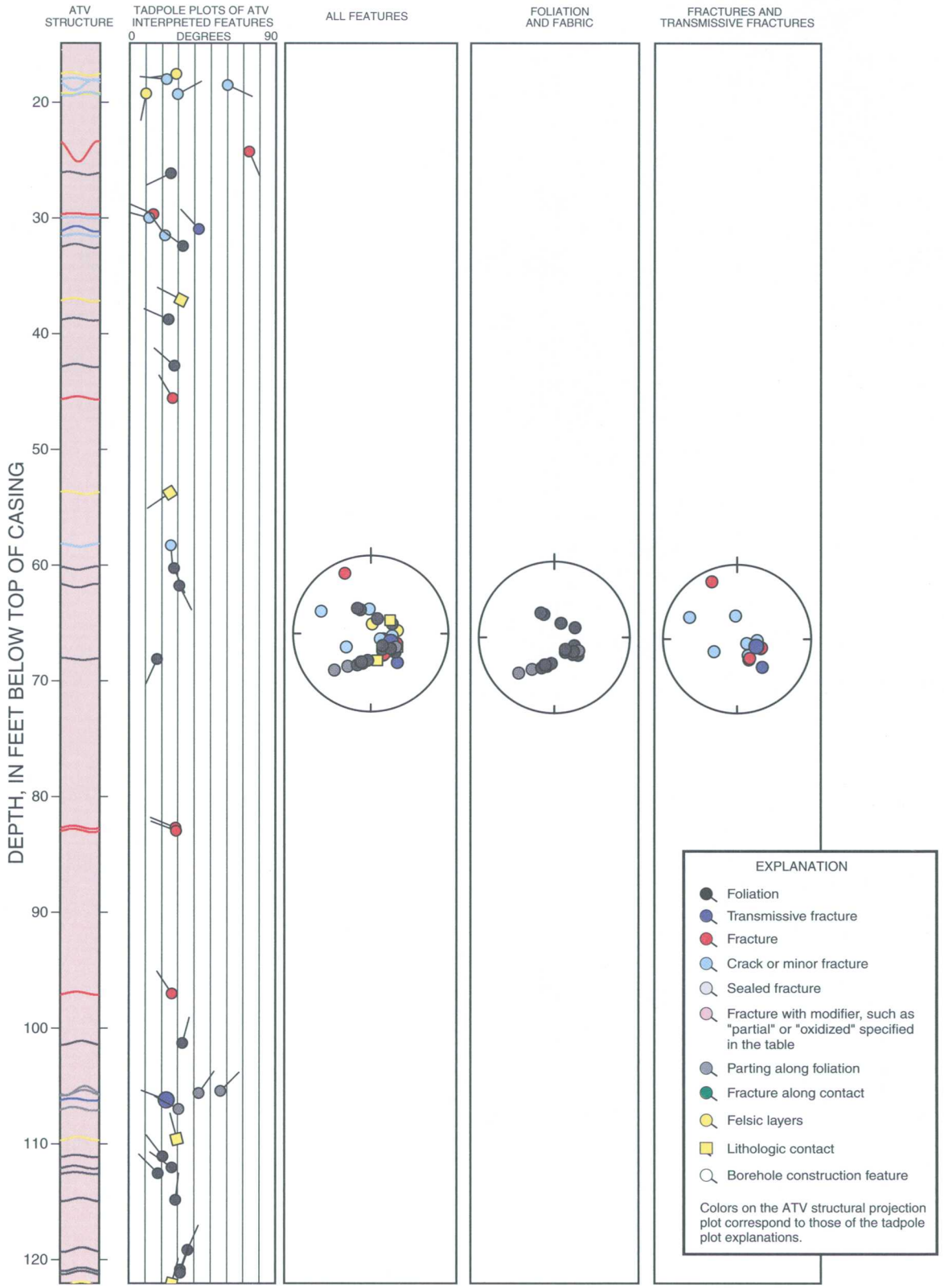

Appendix 3. Borehole-geophysical logs from borehole MW203R in the UConn landfill study area, Storrs, Connecticut

Appendix 3A. Deviation log of borehole MW203R in the UConn landfill study area, Storrs, Connecticut
[ft, feet]

MW203R

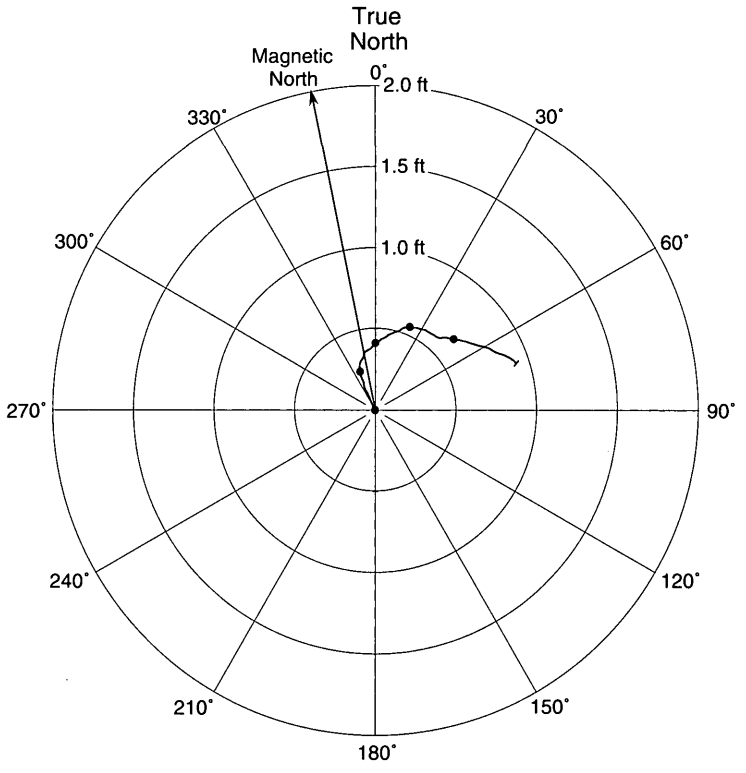

Depth along borehole in 20-foot increments between circles (•)

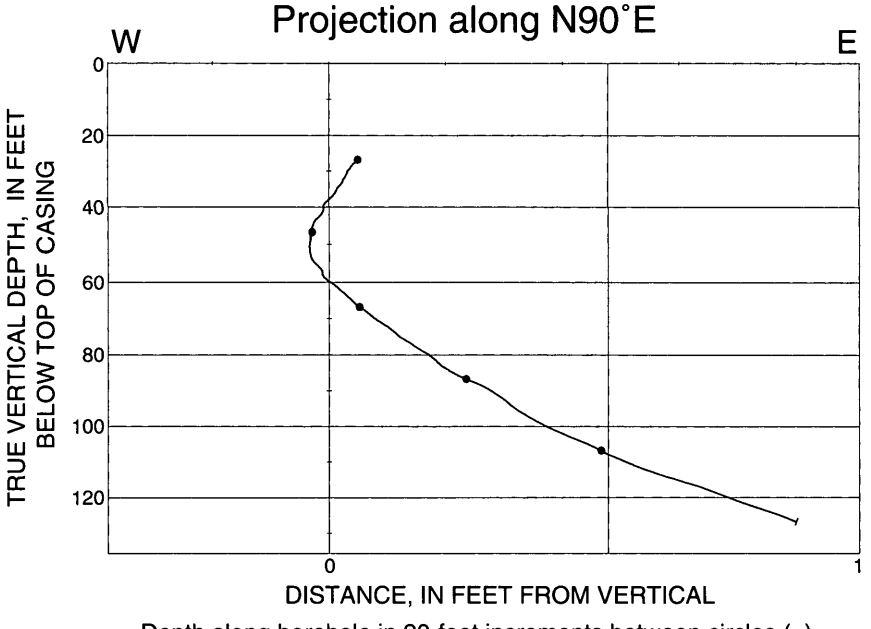

Depth along borehole in 20-foot increments between circles (•)

Appendix 3B. Composite log of natural-gamma, electromagnetic induction, fluid-temperature, specific-conductance, and heat-pulse flowmeter logs from borehole MW203R in the UConn landfill study area, Storrs, Connecticut

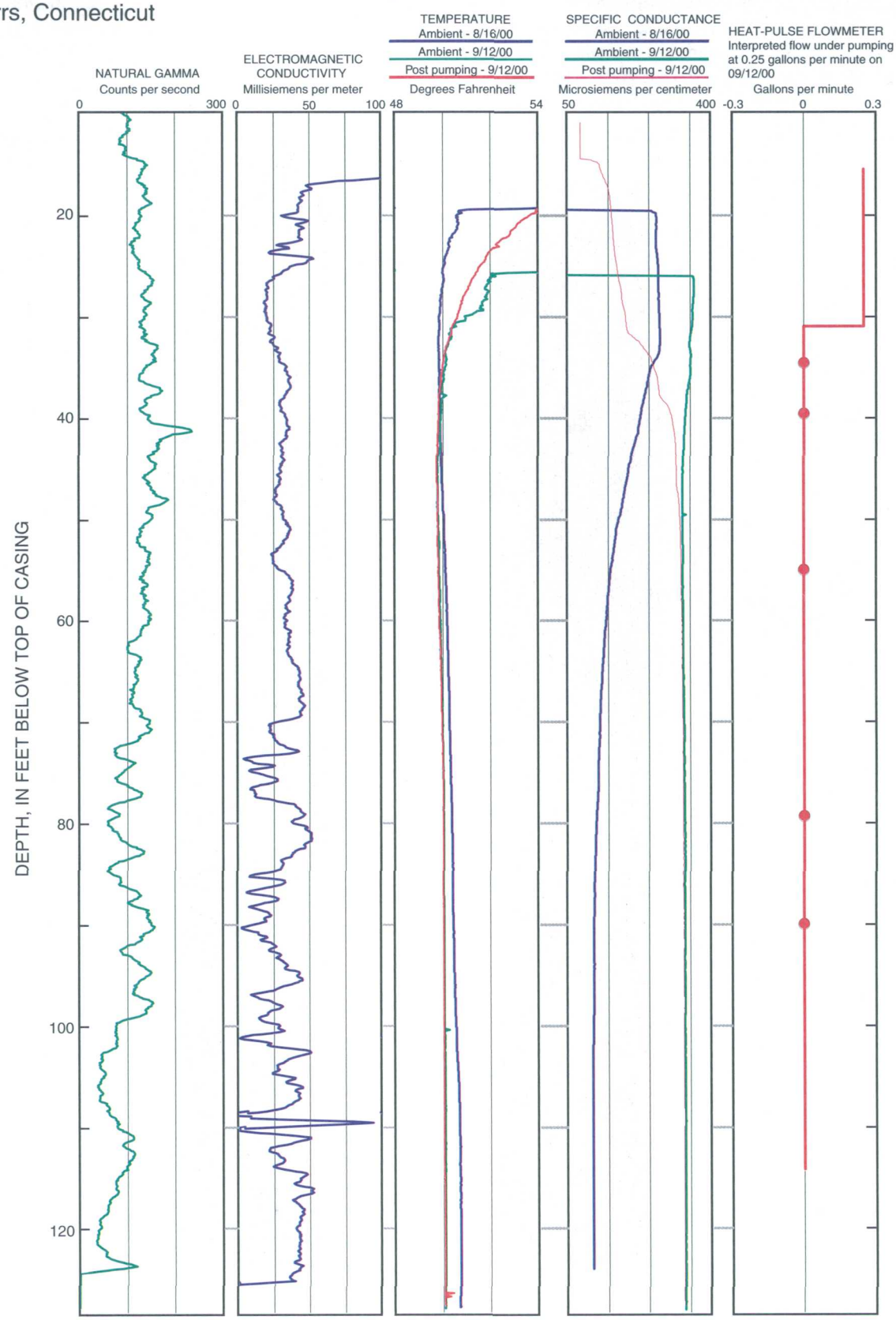

Appendix 3C. Caliper, acoustic-caliper, acoustic-televiewer, and optical-televiewer images and interpreted structures from borehole MW203R in the UConn landfill study area, Storrs, Connecticut

[Interpreted features indicated by color: black - foliation; dark blue - transmissive fracture; red - fracture; light blue - crack or minor fracture; gray - sealed fracture; pink - fracture with modifier, such as "partial" or "oxidized"; blue-gray - parting along foliation; green - fracture along contact; yellow - felsic layer]

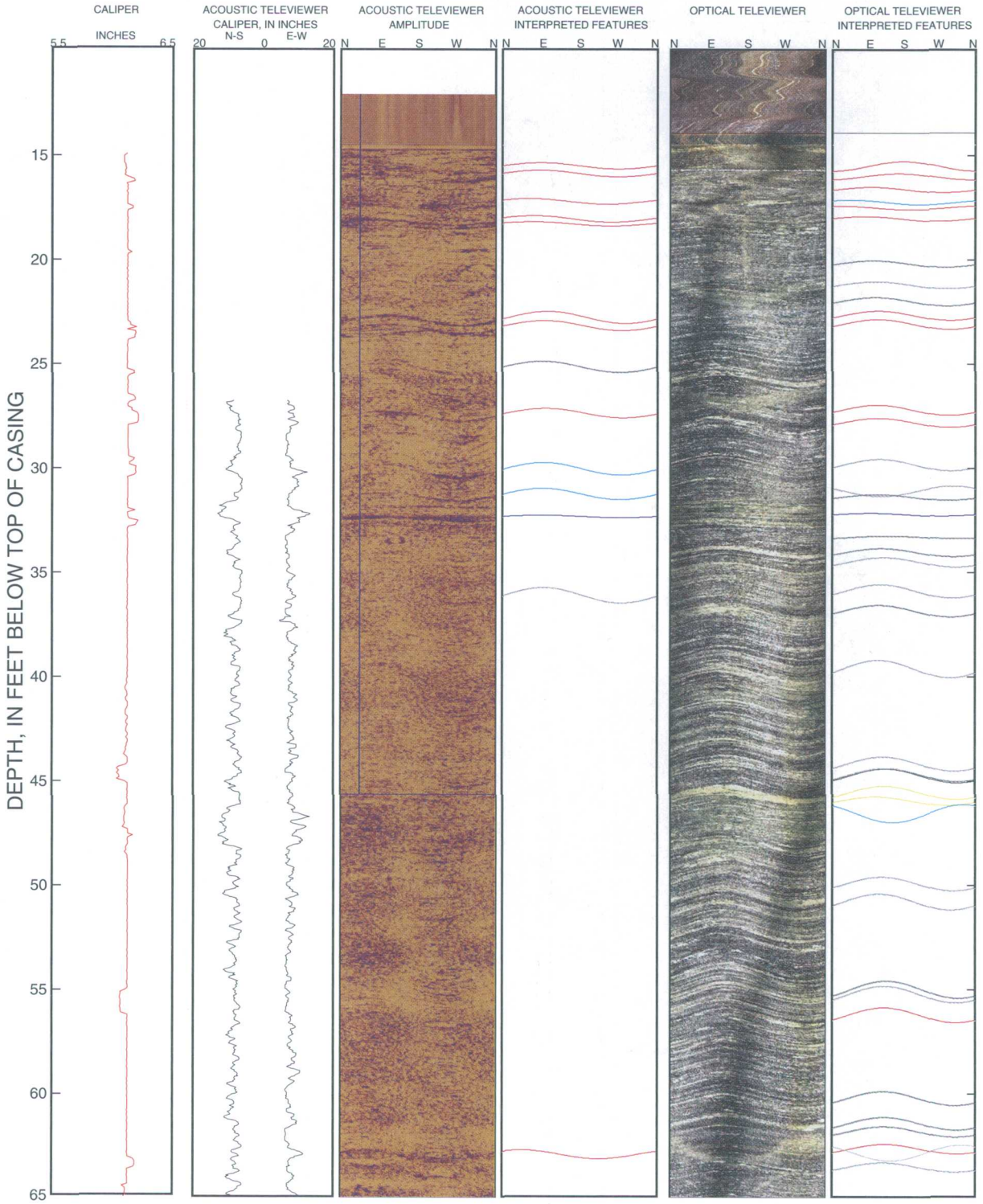

Appendix 3C. Caliper, acoustic-caliper, acoustic-televiewer, and optical-televiewer images and interpreted structures from borehole MW203R in the UConn landfill study area, Storrs, Connecticut--Continued

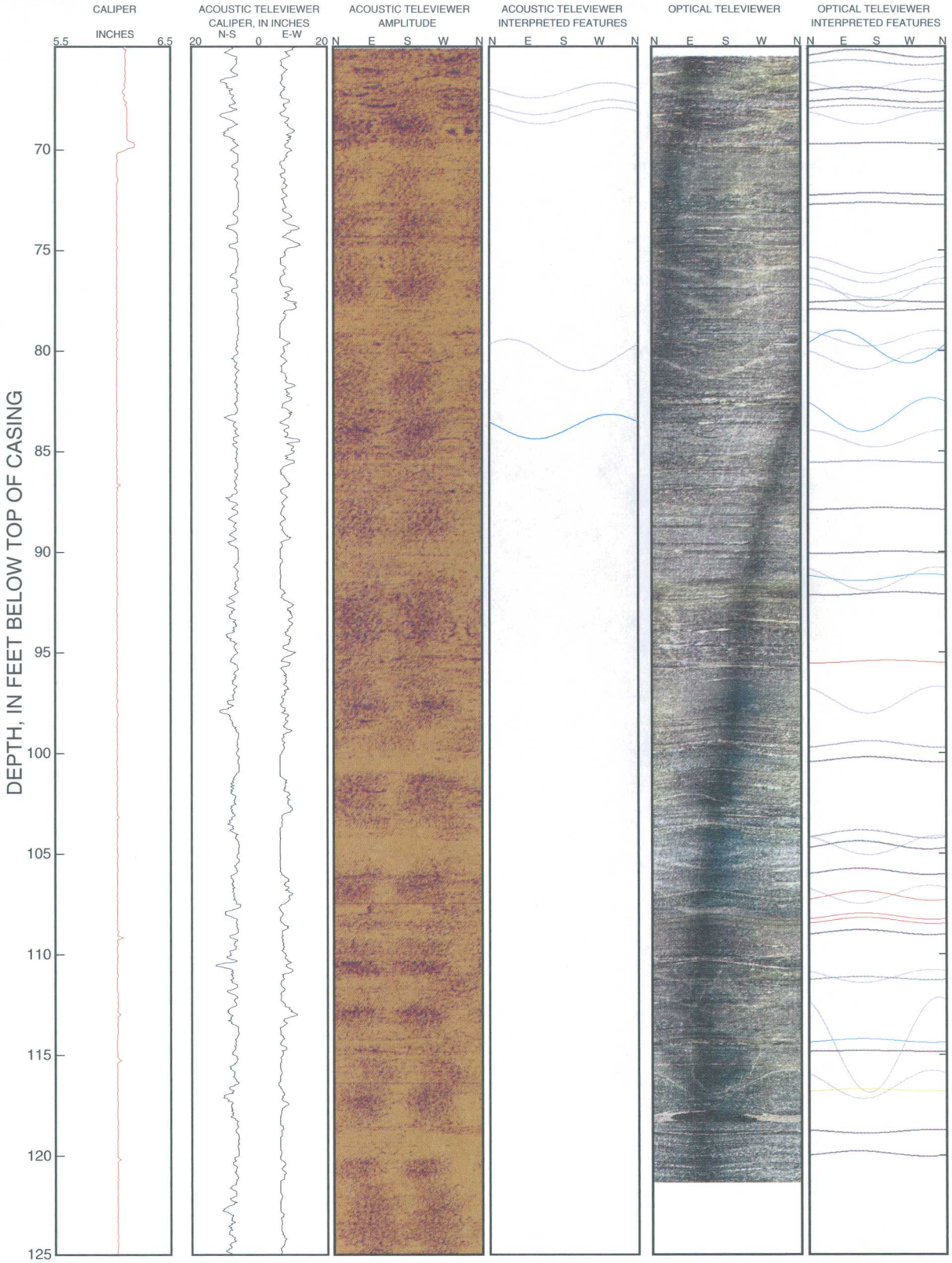

Appendix 3D. Processed borehole-radar reflection logs from borehole MW203R in the UConn landfill study area, Storrs, Connecticut

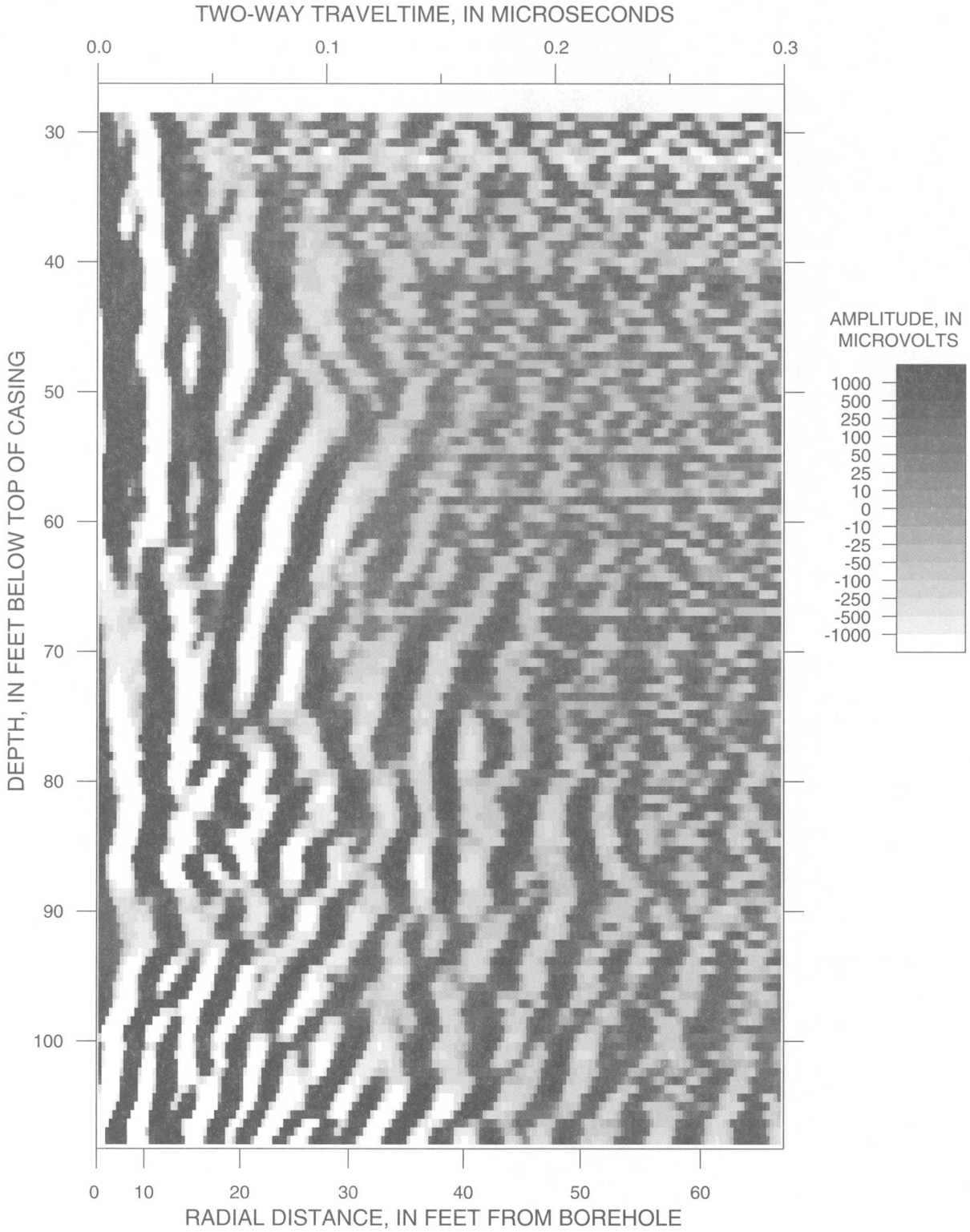

Appendix 3E. Midpoint depth, strike, and dip of features identified in optical-televiewer logs from borehole MW203R in the UConn landfill study area, Storrs, Connecticut

[Depth in feet below top of casing. Strike is reported in "right-hand rule" (RHR) where the direction of dip is to the right of the strike. -, no measurement]

Midpoint depth, in feet	Dip azimuth, in degrees	Strike, RHR in degrees	Dip, in degrees	Dip direction	Description
14.5	-	-	0	-	bottom of casing
15.6	359	269	43	N	fracture
16.1	346	256	31	NW	fracture
16.7	278	188	27	W	fracture
17.3	226	136	24	SW	minor fracture
17.6	198	108	20	S	fracture
18.1	263	173	24	W	fracture
20.2	284	194	32	W	foliation
21.3	289	199	34	W	parting parallel to foliation
22.1	289	199	39	W	foliation
22.7	296	206	42	NW	fracture
23.1	296	206	44	NW	fracture
27.3	293	203	45	NW	fracture
27.9	295	205	42	NW	fracture
29.9	297	207	48	NW	parting parallel to foliation
31.2	121	31	45	SE	parting parallel to foliation
31.5	291	201	28	W	foliation
32.3	275	185	15	W	transmissive fracture
33.4	318	228	15	NW	foliation
34.1	302	212	39	NW	foliation
34.6	309	219	43	NW	parting parallel to foliation
36.0	301	211	52	NW	parting parallel to foliation
36.9	296	206	48	NW	foliation
39.7	296	206	59	NW	parting parallel to foliation
44.2	307	217	54	NW	parting parallel to foliation
44.8	313	223	52	NW	foliation
44.8	313	223	54	NW	foliation
45.7	311	221	52	NW	lithologic feature
46.0	288	198	39	W	lithologic feature
46.7	150	60	60	SE	minor fracture
50.0	303	213	53	NW	parting parallel to foliation
50.9	297	207	57	NW	parting parallel to foliation
55.1	316	226	59	NW	foliation
55.3	310	220	58	NW	parting parallel to foliation
56.3	310	220	56	NW	fracture
60.3	307	217	54	NW	foliation
61.5	310	220	51	NW	foliation
61.9	308	218	45	NW	foliation
62.7	313	223	44	NW	fracture
62.9	145	55	56	SE	sealed fracture
63.6	306	216	43	NW	parting parallel to foliation
65.3	303	213	38	NW	foliation

Appendix 3E. Midpoint depth, strike, and dip of features identified in optical-televiewer logs from borehole MW203R in the UConn landfill study area, Storrs, Connecticut—Continued

[Depth in feet below top of casing. Strike is reported in "right-hand rule" (RHR) where the direction of dip is to the right of the strike. -, no measurement]

Midpoint depth, in feet	Dip azimuth, in degrees	Strike, RHR in degrees	Dip, in degrees	Dip direction	Description
65.8	289	199	27	W	parting parallel to foliation
66.9	126	36	49	SE	sealed fracture
67.1	307	217	26	NW	foliation
67.7	300	210	21	NW	foliation
68.0	311	221	19	NW	parting parallel to foliation
68.5	151	61	53	SE	sealed fracture
69.8	18	288	6	N	foliation
72.3	348	258	12	N	foliation
72.8	338	248	11	N	foliation
75.9	183	93	59	S	sealed fracture
76.3	162	72	58	S	sealed fracture
77.1	164	74	55	S	sealed fracture
77.2	178	88	71	S	sealed fracture
77.6	337	247	12	NW	foliation
78.1	179	89	14	S	foliation
79.5	157	67	57	SE	sealed fracture
79.9	261	171	73	W	minor fracture
80.5	144	54	65	SE	sealed fracture
83.3	141	51	73	SE	minor fracture
84.4	176	86	60	S	sealed fracture
85.6	344	254	10	N	parting parallel to foliation
87.9	14	284	10	N	foliation
90.1	44	314	11	NE	foliation
91.4	128	38	34	SE	minor fracture
91.4	156	66	67	SE	sealed fracture
92.2	58	328	16	NE	foliation
95.5	28	298	16	NE	fracture
97.4	156	66	70	SE	sealed fracture
99.7	340	250	33	N	parting parallel to foliation
100.4	337	247	27	NW	foliation
104.1	317	227	40	NW	parting parallel to foliation
104.7	310	220	39	NW	foliation
104.7	157	67	62	SE	sealed fracture
106.0	313	223	32	NW	foliation
107.1	135	45	61	SE	sealed fracture
107.1	321	231	43	NW	fracture
108.2	324	234	32	NW	fracture
108.4	326	236	32	NW	fracture
109.0	316	226	27	NW	foliation
111.2	142	52	52	SE	sealed fracture
111.3	318	228	17	NW	parting parallel to foliation
114.4	322	232	21	NW	minor fracture

Appendix 3E. Midpoint depth, strike, and dip of features identified in optical-televiewer logs from borehole MW203R in the UConn landfill study area, Storrs, Connecticut—Continued

[Depth in feet below top of casing. Strike is reported in "right-hand rule" (RHR) where the direction of dip is to the right of the strike. -, no measurement]

Midpoint depth, in feet	Dip azimuth, in degrees	Strike, RHR in degrees	Dip, in degrees	Dip direction	Description
114.6	159	69	84	S	sealed fracture
114.9	319	229	4	NW	foliation
116.5	143	53	70	SE	sealed fracture
116.8	318	228	15	NW	lithologic feature
118.9	147	57	18	SE	foliation
120.0	308	218	28	NW	foliation

Appendix 3F. Midpoint depth, strike, and dip of features identified in acoustic-televiewer logs from borehole MW203R in the UConn landfill study area, Storrs, Connecticut

[Depth in feet below top of casing. Strike is reported in "right-hand rule" (RHR) where the direction of dip is to the right of the strike. -, no measurement]

Midpoint depth, in feet	Dip azimuth, in degrees	Strike, RHR in degrees	Dip, in degrees	Dip direction	Description
14.5	-	-	0	-	bottom of casing
15.6	270	180	31	W	fracture
15.9	269	179	32	W	fracture
17.3	244	154	28	SW	fracture
18.1	254	164	32	W	fracture
18.3	252	162	22	W	fracture
22.8	286	196	49	W	fracture
23.2	278	188	44	W	fracture
25.2	273	183	47	W	foliation
27.4	280	190	42	W	fracture
30.1	275	185	50	W	minor fracture
31.3	273	183	47	W	minor fracture
32.4	273	183	13	W	transmissive fracture
36.2	275	185	56	W	parting parallel to foliation
63.0	225	135	40	SW	fracture
67.1	106	16	57	E	possible fracture
68.0	114	24	55	SE	possible fracture
68.4	122	32	58	SE	possible fracture
80.3	228	138	72	SW	possible fracture
83.9	112	22	68	E	minor fracture
126.1	136	46	35	SE	minor fracture

Appendix 3G. Location, orientation, and length of reflectors interpreted from borehole-radar data from borehole MW203R in the UConn landfill study area, Storrs, Connecticut

[Depth in feet below top of casing. Strike is reported in "right-hand rule" (RHR) where the direction of dip is to the right of the strike. Reflector continuity is on a scale of 1 (good) to 5 (poor)]

Midpoint depth, in feet	Dip azimuth, in degrees	Strike, RHR in degrees	Dip, in degrees	Dip direction	Estimated reflector length, in feet	Reflector continuity
16.7	278	188	27	W	24.6	5
17.7	198	108	20	S	24.6	5
34.5	309	219	43	NW	40.6	5
69.9	183	93	51	S	12.2	4
83.3	141	51	73	SE	7.6	5
93.8	145	55	50	SE	7.9	3
111.2	318	228	17	NW	13.5	4
117.1	195	105	0	S	0.0	4
128.9	295	205	0	NW	0.0	4
149.3	5	275	74	N	59.7	2
181.8	5	275	46	N	23.3	3

Appendix 3H. Heat-pulse flowmeter measurements in MW203R at the UConn landfill study area, Storrs, Connecticut

[--indicates no flow; for interpretation, if nothing is listed, there is no change in inflow or outflow]

Date	Depth of measurement, in feet below top of casing	Flow direction	Average rate, in gallons per minute	Normalized average rate, in gallons per minute	Interpretation
September 12, 2000	Ambient conditions				No measurable flow
September 12, 2000	Pumping at 0.25 gallon per minute				
	35.0	--	0.000	0.000	Inflow above 35.0 feet
	40.0	--	0.000	0.000	
	55.0	--	0.000	0.000	
	79.9	--	0.000	0.000	
	90.0	--	0.000	0.000	

Appendix 3I. Tadpole plots and stereoplots of fractures and foliations interpreted in optical-televiewer images from borehole MW203R in the UConn landfill study area, Storrs, Connecticut

[OTV, optical televiewer]

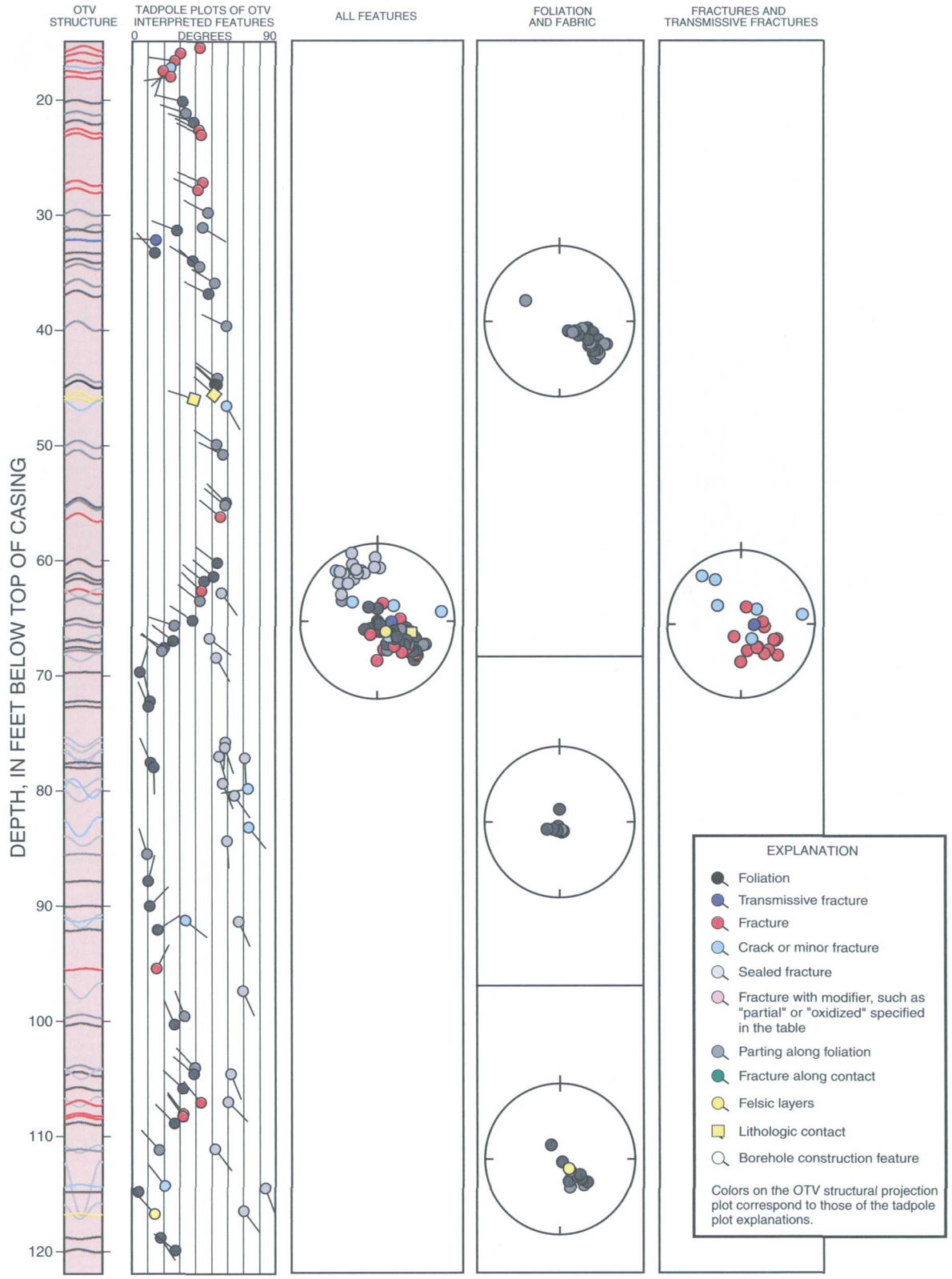

Appendix 3J. Tadpole plots and stereoplots of fractures and foliations interpreted in acoustic-televiewer images from borehole MW203R in the UConn landfill study area, Storrs, Connecticut

[ATV, acoustic televiewer]

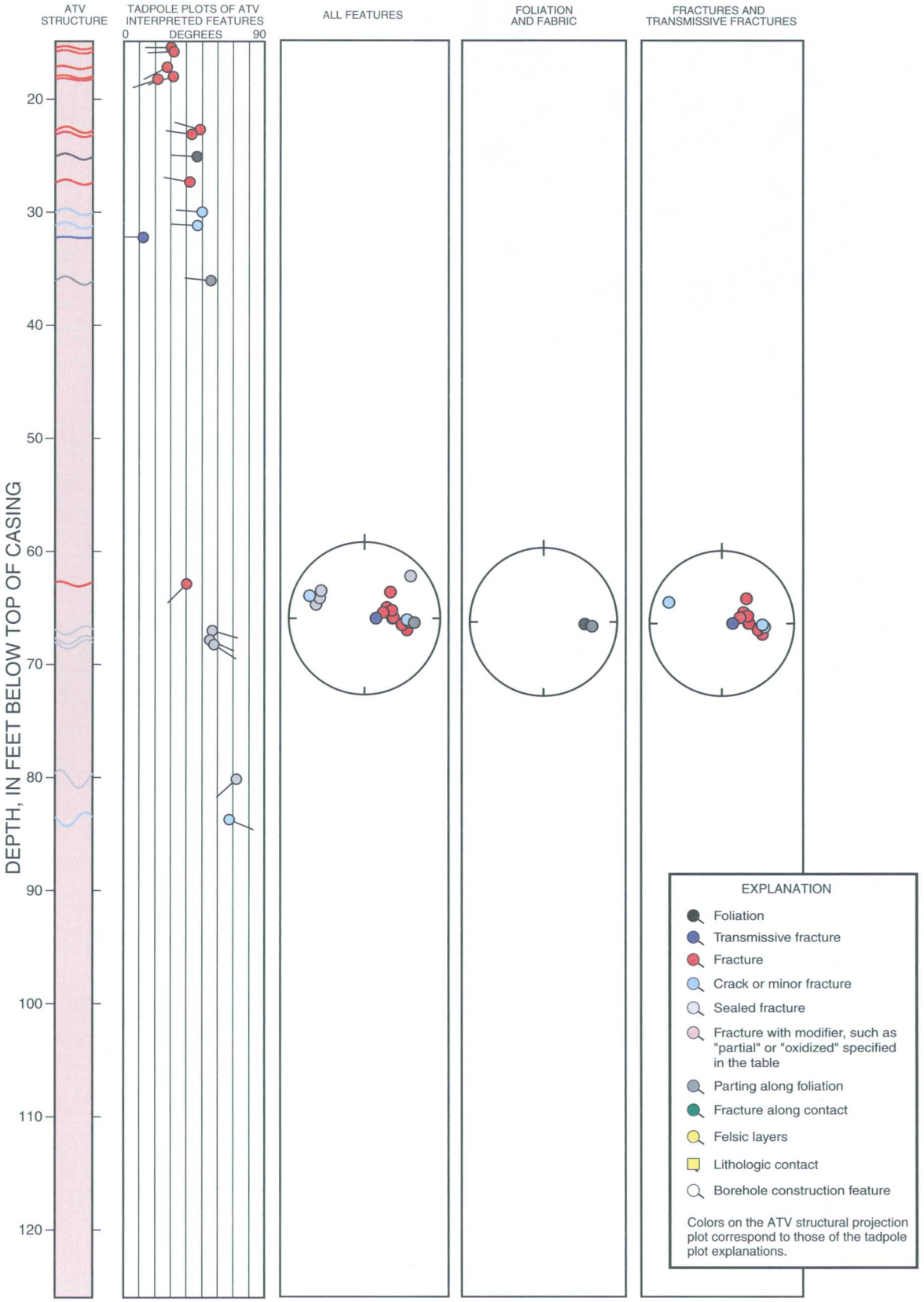

Appendix 4. Borehole-geophysical logs from borehole MW204R in the UConn landfill study area, Storrs, Connecticut

Appendix 4A. Deviation log of borehole MW204R in the UConn landfill study area, Storrs, Connecticut

[ft, feet]

MW204R

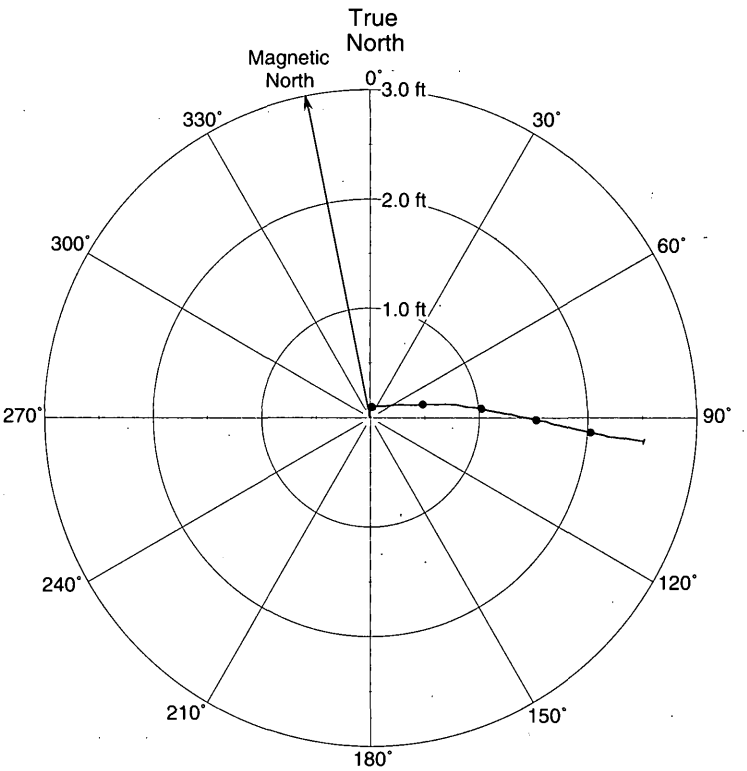

Depth along borehole in 20-foot increments between circles (•)

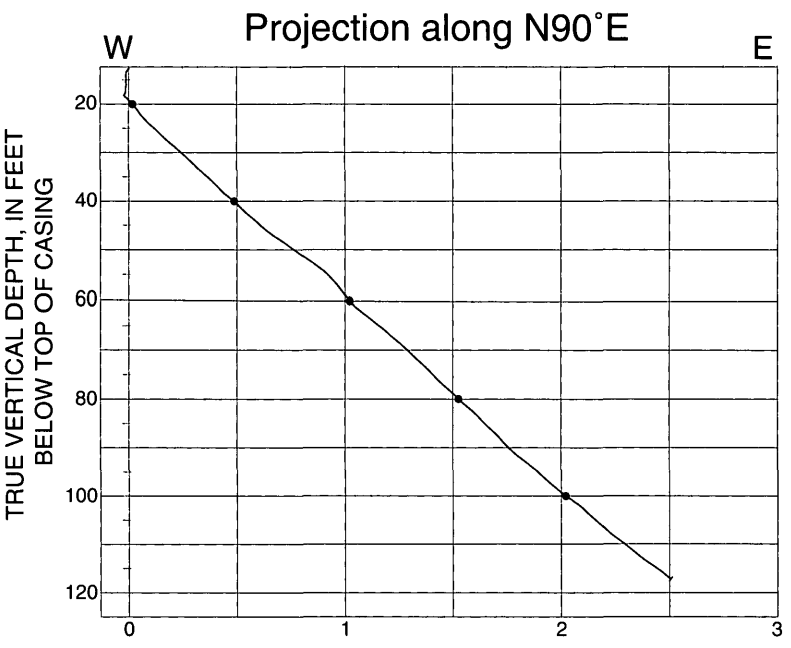

Depth along borehole in 20-foot increments between circles (•)

Appendix 4B. Composite log of natural-gamma, electromagnetic induction, fluid-temperature, specific-conductance, and heat-pulse flowmeter logs from borehole MW204R in the UConn landfill study area, Storrs, Connecticut

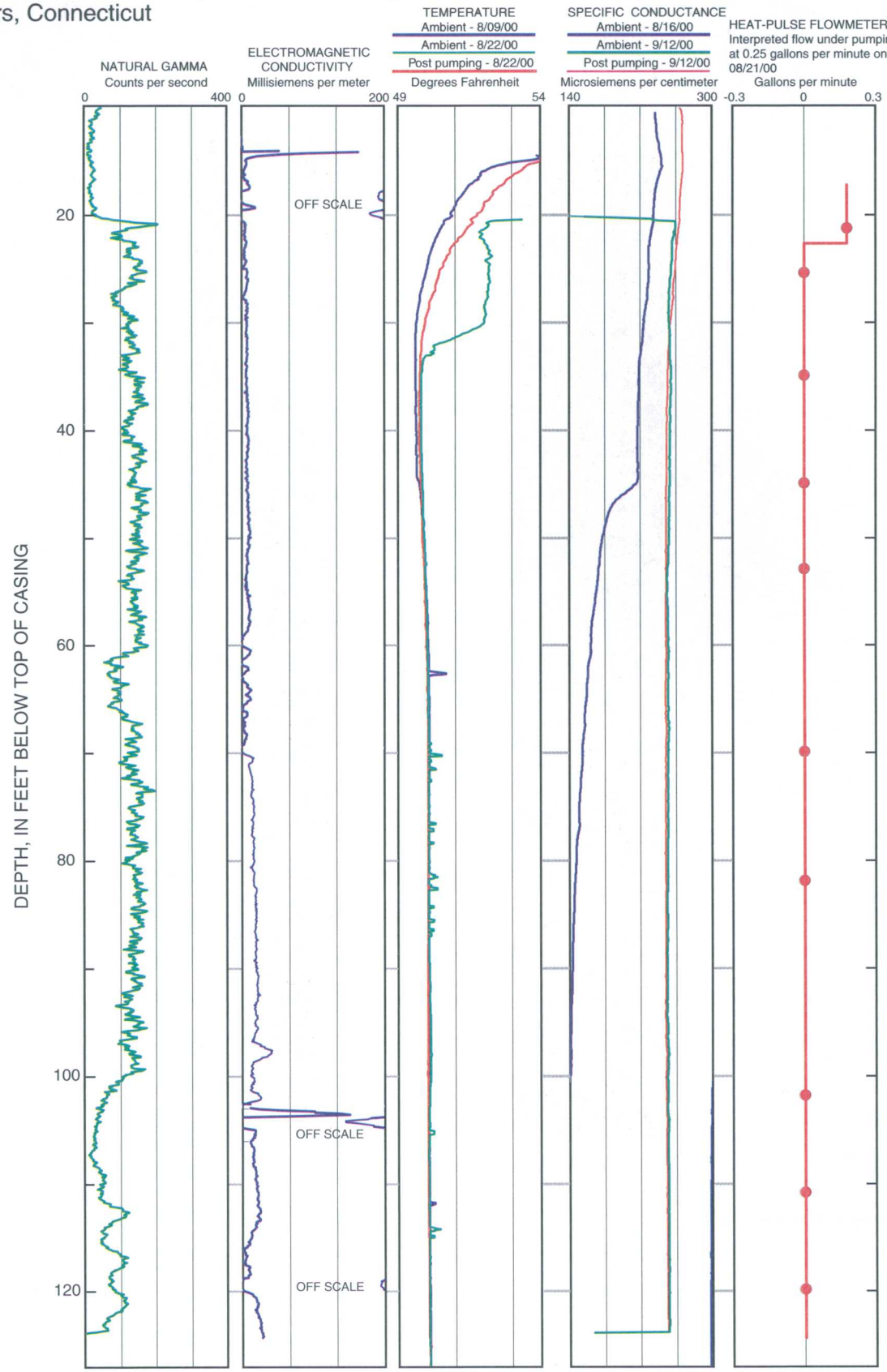

Appendix 4C. Caliper, acoustic-caliper, acoustic-televiewer, and optical-televiewer images and interpreted structures from borehole MW204R in the UConn landfill study area, Storrs, Connecticut

[Interpreted features indicated by color: black - foliation; dark blue - transmissive fracture; red - fracture; light blue - crack or minor fracture; gray - sealed fracture; pink - fracturewith modifier, such as "partial" or "oxidized"; blue-gray - parting along foliation; green - fracture along contact; yellow - felsic layer]

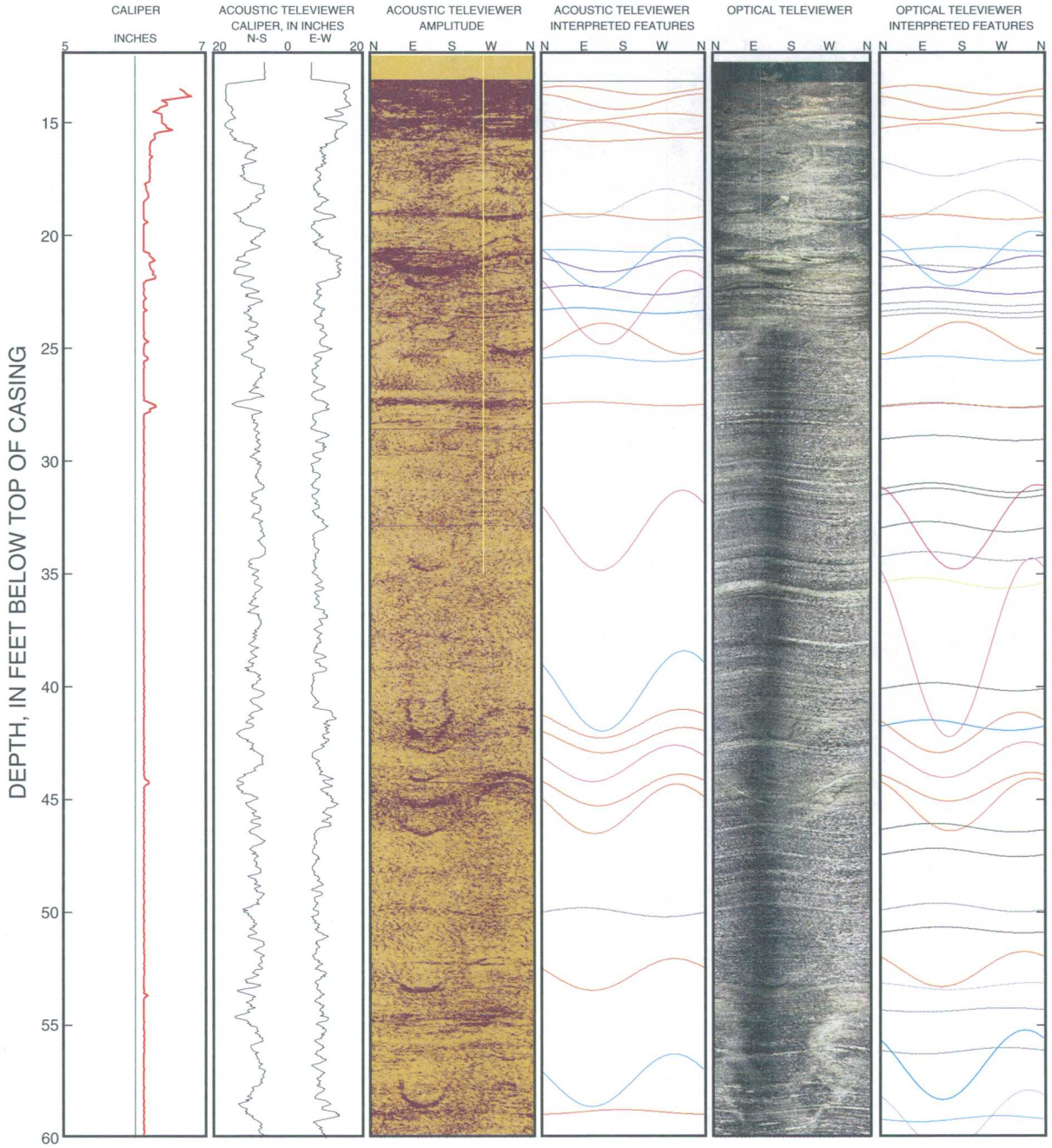

Appendix 4C. Caliper, acoustic-caliper, acoustic-televiewer, and optical-televiewer images and interpreted structures from borehole MW204R in the UConn landfill study area, Storrs, Connecticut--Continued

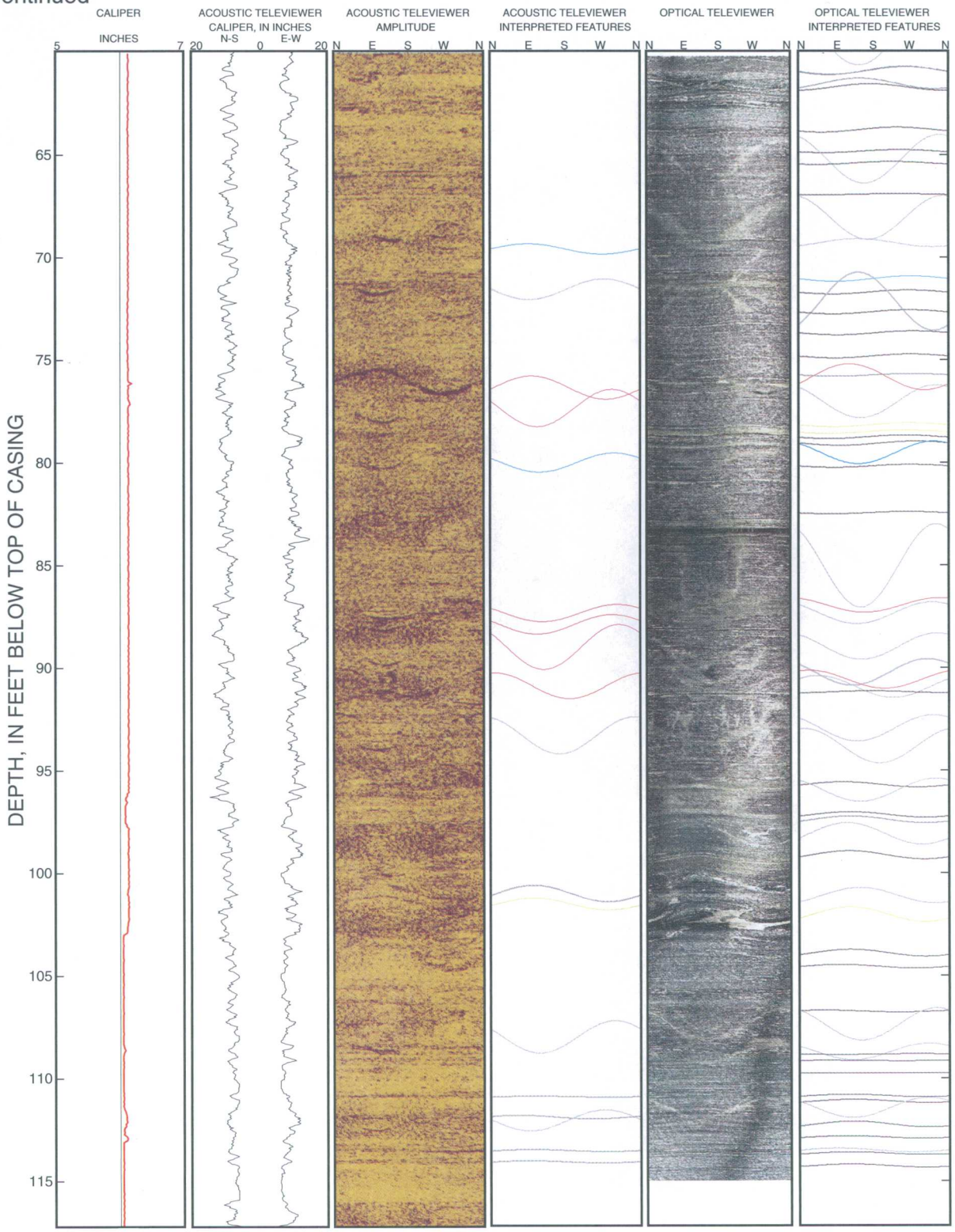

Appendix 4D. Processed borehole-radar reflection logs from borehole MW204R in the UConn landfill study area, Storrs, Connecticut

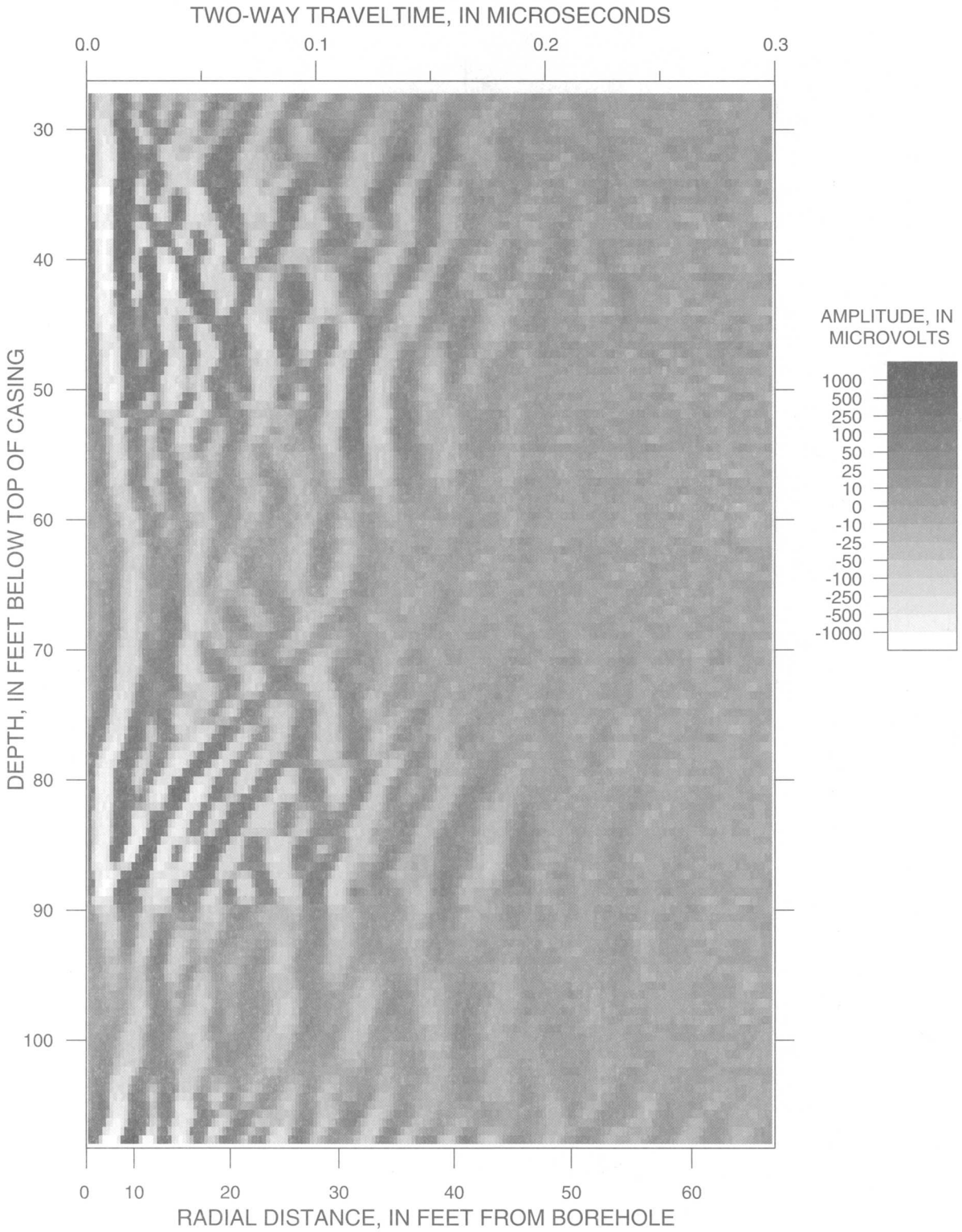

Appendix 4E. Midpoint depth, strike, and dip of features identified in optical-televiewer logs from borehole MW204R in the UConn landfill study area, Storrs, Connecticut

[Depth in feet below top of casing. Strike is reported in "right-hand rule" (RHR) where the direction of dip is to the right of the strike.
-, no measurement]

Midpoint depth, in feet	Dip azimuth, in degrees	Strike, RHR in degrees	Dip, in degrees	Dip direction	Description
13.2	-	-	0	-	bottom of casing
13.5	252	162	39	W	fracture
14.1	165	75	50	S	fracture
14.7	98	8	30	E	fracture
15.2	293	203	33	NW	fracture
17.0	140	50	56	SE	sealed fracture
18.6	51	321	68	NE	sealed fracture
19.2	279	189	25	W	fracture
20.6	346	256	22	N	minor fracture
21.0	157	67	78	SE	minor fracture
21.3	158	68	55	S	transmissive fracture
21.4	266	176	17	W	parting parallel to foliation
22.4	282	192	30	W	transmissive fracture
23.0	284	194	21	W	parting parallel to foliation
23.3	286	196	21	W	parting parallel to foliation
23.6	294	204	24	NW	parting parallel to foliation
24.5	356	266	71	N	fracture
25.5	298	208	21	NW	minor fracture
27.5	294	204	22	NW	parting parallel to foliation
27.5	304	214	21	NW	fracture
29.0	297	207	25	NW	foliation
31.2	291	201	39	W	foliation
31.4	295	205	40	NW	foliation
32.9	164	74	82	S	partial fracture trace, the bottom of
32.9	284	194	42	W	foliation
34.2	280	190	38	W	parting parallel to foliation
35.4	267	177	43	W	lithologic feature
38.3	152	62	86	SE	partial fracture trace, the bottom of
40.0	298	208	35	NW	foliation
41.7	284	194	43	W	minor fracture
42.1	128	38	74	SE	fracture
43.3	142	52	72	SE	partial fracture trace, the bottom of
44.5	151	61	68	SE	fracture
45.3	154	64	78	SE	fracture
46.3	296	206	37	NW	foliation
47.4	301	211	36	NW	foliation
49.8	306	216	38	NW	parting parallel to foliation
50.8	314	224	27	NW	foliation
52.6	135	45	72	SE	fracture
53.3	153	63	31	SE	sealed fracture
54.4	94	4	20	E	parting parallel to foliation
56.2	95	5	29	E	parting parallel to foliation
56.8	139	49	81	SE	minor fracture

Appendix 4E. Midpoint depth, strike, and dip of features identified in optical-televiewer logs from borehole MW204R in the UConn landfill study area, Storrs, Connecticut—Continued

[Depth in feet below top of casing. Strike is reported in "right-hand rule" (RHR) where the direction of dip is to the right of the strike. -, no measurement]

Midpoint depth, in feet	Dip azimuth, in degrees	Strike, RHR in degrees	Dip, in degrees	Dip direction	Description
59.2	85	355	27	E	minor fracture
59.3	145	55	79	SE	sealed fracture
60.9	78	348	36	E	parting parallel to foliation
60.9	73	343	39	E	parting parallel to foliation
61.5	327	237	45	NW	parting parallel to foliation
61.7	351	261	32	N	foliation
63.8	56	326	26	NE	foliation
64.8	61	331	16	NE	foliation
65.2	158	68	78	S	sealed fracture
65.4	43	313	16	NE	foliation
66.9	52	322	6	NE	foliation
68.1	167	77	77	S	sealed fracture
69.3	320	230	38	NW	sealed fracture
71.1	88	358	27	E	minor fracture
71.7	81	351	21	E	foliation
72.2	324	234	80	NW	sealed fracture
72.7	84	354	21	E	foliation
73.7	93	3	21	E	foliation
74.8	87	357	21	E	foliation
75.7	90	360	13	E	parting parallel to foliation
75.8	302	212	68	NW	fracture
77.0	148	58	72	SE	sealed fracture
78.2	84	354	21	E	lithologic feature
78.5	74	344	17	E	lithologic feature
78.8	73	343	18	E	foliation
79.1	100	10	22	E	foliation
79.5	143	53	65	SE	minor fracture
80.2	86	356	15	E	foliation
82.5	78	348	12	E	foliation
85.1	149	59	83	SE	sealed fracture
86.9	158	68	54	S	fracture
87.4	139	49	64	SE	sealed fracture
89.0	151	61	68	SE	sealed fracture
90.2	128	38	68	SE	sealed fracture
90.6	205	115	60	SW	fracture
91.0	226	136	65	SW	sealed fracture
91.2	350	260	11	N	foliation
93.0	140	50	68	SE	sealed fracture
93.8	193	103	73	S	sealed fracture
95.7	285	195	27	W	foliation
96.0	147	57	66	SE	sealed fracture
97.2	302	212	28	NW	foliation
97.4	302	212	33	NW	parting parallel to foliation

Appendix 4E. Midpoint depth, strike, and dip of features identified in optical-televiewer logs from borehole MW204R in the UConn landfill study area, Storrs, Connecticut—Continued

[Depth in feet below top of casing. Strike is reported in "right-hand rule" (RHR) where the direction of dip is to the right of the strike. -, no measurement]

Midpoint depth, in feet	Dip azimuth, in degrees	Strike, RHR in degrees	Dip, in degrees	Dip direction	Description
98.1	295	205	64	NW	sealed fracture
99.2	299	209	38	NW	foliation
101.1	325	235	56	NW	sealed fracture
102.1	302	212	55	NW	lithologic feature
103.9	302	212	34	NW	foliation
104.6	278	188	19	W	foliation
106.8	239	149	11	SW	foliation
107.4	149	59	72	SE	sealed fracture
108.7	129	39	58	SE	sealed fracture
108.9	100	10	4	E	foliation
109.2	245	155	4	SW	foliation
109.8	306	216	3	NW	foliation
110.9	298	208	14	NW	foliation
111.2	309	219	17	NW	foliation
111.5	127	37	62	SE	sealed fracture
112.3	308	218	29	NW	foliation
112.9	294	204	13	NW	foliation
113.5	272	182	21	W	sealed fracture
113.7	303	213	14	NW	foliation
114.3	302	212	17	NW	foliation

Appendix 4F. Midpoint depth, strike, and dip of features identified in acoustic-televiewer logs from borehole MW204R in the UConn landfill study area, Storrs, Connecticut

[Depth in feet below top of casing. Strike is reported in "right-hand rule" (RHR) where the direction of dip is to the right of the strike. -, no measurement]

Midpoint depth, in feet	Dip azimuth, in degrees	Strike, RHR in degrees	Dip, in degrees	Dip direction	Description
13.1	-	-	0	-	bottom of casing
13.6	234	144	37	SW	fracture
14.1	171	81	53	S	fracture
14.7	96	6	32	E	fracture
15.2	307	217	46	NW	fracture
15.7	126	36	16	SE	fracture
18.6	94	4	68	E	sealed fracture
19.2	267	177	30	W	fracture
20.7	229	139	13	SW	minor fracture
21.2	123	33	77	SE	minor fracture
21.3	142	52	54	SE	transmissive fracture
22.4	251	161	39	W	transmissive fracture
23.2	138	48	81	SE	partial fracture trace (bottom of fracture)
23.3	260	170	26	W	minor fracture
24.6	315	225	70	NW	fracture
25.5	263	173	26	W	minor fracture
27.5	281	191	18	W	fracture
33.1	129	39	82	SE	partial fracture trace (bottom of fracture)
40.2	133	43	82	SE	minor fracture
41.7	129	39	68	SE	fracture
42.4	135	45	66	SE	fracture
43.4	112	22	73	E	partial fracture trace (bottom of fracture)
44.6	124	34	70	SE	fracture
45.5	116	26	77	SE	fracture
50.0	269	179	38	W	parting parallel to foliation
52.8	112	22	70	E	fracture
57.5	111	21	78	E	minor fracture
58.9	354	264	21	N	fracture
69.6	270	180	45	W	minor fracture
71.6	93	3	63	E	sealed fracture
76.3	279	189	66	W	fracture
77.3	113	23	74	SE	partial fracture trace (bottom of fracture)
80.0	118	28	61	SE	minor fracture
87.3	125	35	59	SE	fracture
87.9	112	22	62	E	fracture
89.0	128	38	77	SE	partial fracture trace (bottom of fracture)
90.9	190	100	68	S	fracture
93.3	165	75	74	S	sealed fracture
101.0	282	192	58	W	parting parallel to foliation
101.5	283	193	49	W	lithologic feature

Appendix 4F. Midpoint depth, strike, and dip of features identified in acoustic-televiewer logs from borehole MW204R in the UConn landfill study area, Storrs, Connecticut—Continued

[Depth in feet below top of casing. Strike is reported in "right-hand rule" (RHR) where the direction of dip is to the right of the strike. -, no measurement]

Midpoint depth, in feet	Dip azimuth, in degrees	Strike, RHR in degrees	Dip, in degrees	Dip direction	Description
108.0	118	28	72	SE	sealed fracture
110.9	283	193	5	W	parting parallel to foliation
111.9	246	156	19	SW	parting parallel to foliation
112.1	93	3	63	E	sealed fracture
113.5	278	188	11	W	parting parallel to foliation
114.1	269	179	12	W	parting parallel to foliation

Appendix 4G. Location, orientation, and length of reflectors interpreted from borehole-radar data from borehole MW204R in the UConn landfill study area, Storrs, Connecticut

[Depth in feet below top of casing. Strike is reported in "right-hand rule" (RHR) where the direction of dip is to the right of the strike. Reflector continuity is on a scale of 1 (good) to 5 (poor)]

Midpoint depth, in feet	Dip azimuth, in degrees	Strike, RHR in degrees	Dip, in degrees	Dip direction	Estimated reflector length, in feet	Reflector continuity
-54.1	275	185	77	W	19.4	3
22.4	288	198	33	W	12.5	4
50.9	314	224	27	NW	10.8	5
56.1	95	5	29	E	12.8	5
61.4	327	237	45	NW	11.3	5
63.7	56	326	26	NE	33.1	4
99.1	5	275	17	N	35.0	4
104.0	195	105	60	S	25.9	4
143.7	5	275	59	N	10.6	5
266.7	185	95	82	S	18.0	4

Appendix 4H. Heat-pulse flowmeter measurements in MW204R at the UConn landfill study area, Storrs, Connecticut

[--indicates no flow; for interpretation, if nothing is listed, there is no change in inflow or outflow]

Date	Depth of measurement, in feet below top of casing	Flow direction	Average rate, in gallons per minute	Normalized average rate, in gallons per minute	Interpretation
August 10, 2000	Ambient conditions				No measurable flow
August 21, 2000	Pumping at 0.25 gallon per minute				Inflow between 21.3 and 25.5 feet
	21.3	up	0.036	0.250	
	25.5	--	0.000	0.000	
	35.0	--	0.000	0.000	
	45.0	--	0.000	0.000	
	53.0	--	0.000	0.000	
	70.0	--	0.000	0.000	
	82.0	--	0.000	0.000	
	102.0	--	0.000	0.000	
	111.0	--	0.000	0.000	
	120.0	--	0.000	0.000	
August 30, 2000	Pumping at 0.25 gallon per minute				Inflow between 21.3 and 25.5 feet
	18.0	up	0.056	0.250	
	24.0	--	0.000	0.000	
	29.0	--	0.000	0.000	
	39.0	--	0.000	0.000	
	49.0	--	0.000	0.000	
	60.0	--	0.000	0.000	
	74.0	--	0.000	0.000	
	105.0	--	0.000	0.000	
September 11, 2000	Pumping at 0.25 gallon per minute				Inflow between 21.3 and 25.5 feet
	24.0	up	0.008	0.250	
	39.0	--	0.000	0.000	
	50.0	--	0.000	0.000	
	74.0	--	0.000	0.000	
	90.0	--	0.000	0.000	
	105.0	--	0.000	0.000	

Appendix 4I. Tadpole plots and stereoplots of fractures and foliations interpreted in optical-televiewer images from borehole MW204R in the UConn landfill study area, Storrs, Connecticut

[OTV, optical televiewer]

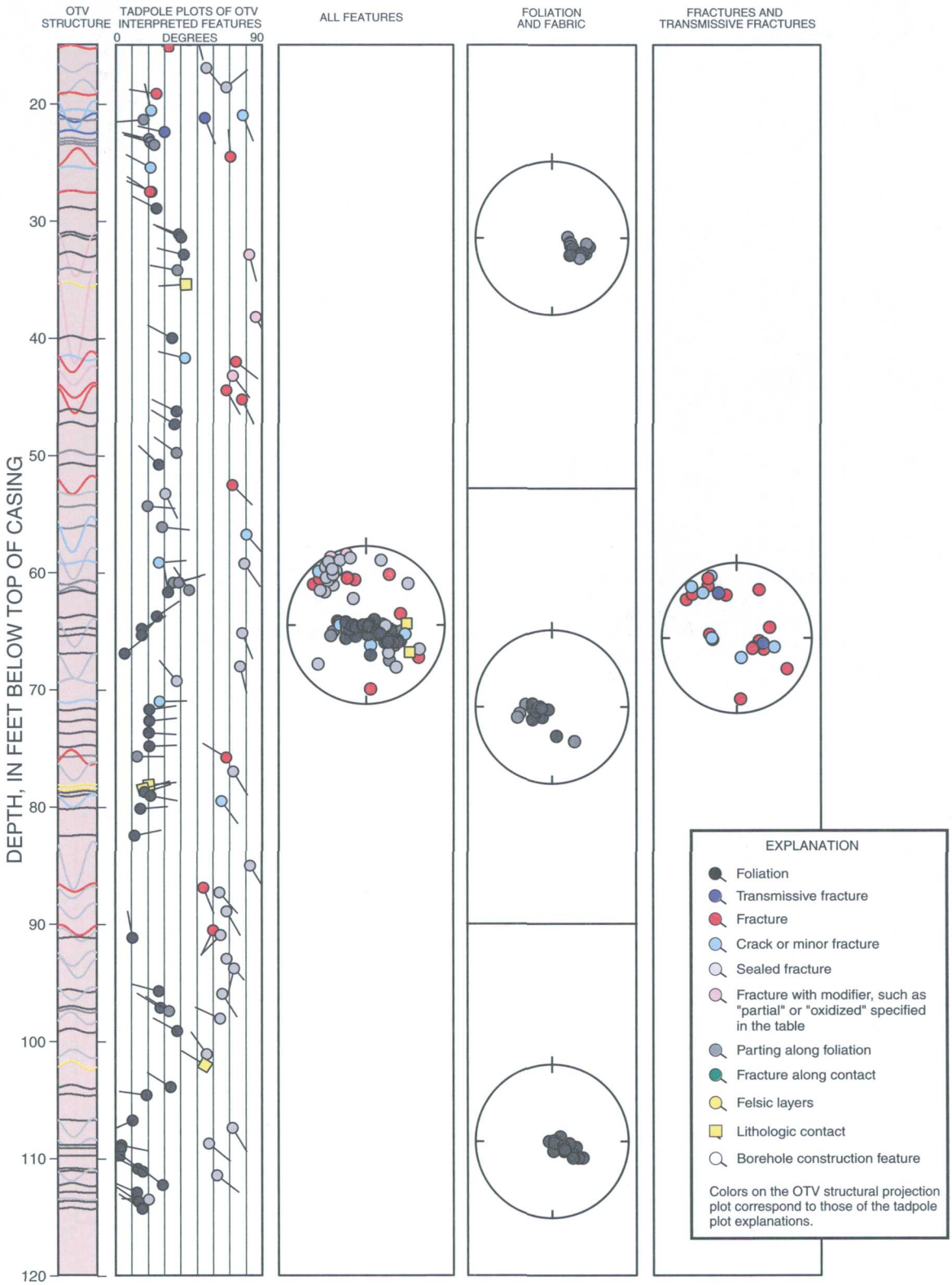

Appendix 4J. Tadpole plots and stereoplots of fractures and foliations interpreted in acoustic-televiewer images from borehole MW204R in the UConn landfill study area, Storrs, Connecticut

[ATV, acoustic televiewer]

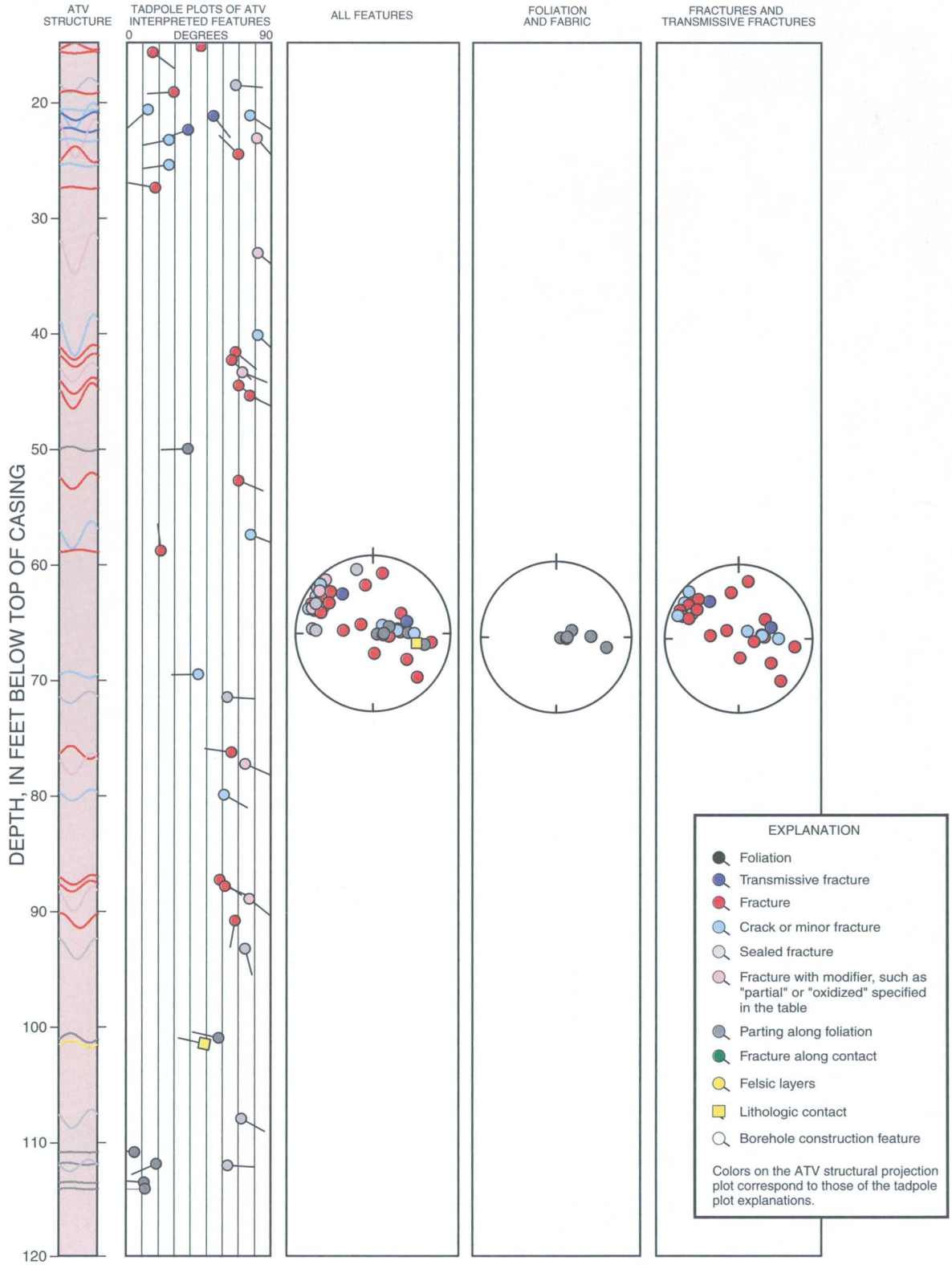

Appendix 5. Borehole-geophysical logs from borehole MW302R in the UConn landfill study area, Storrs, Connecticut

Appendix 5A. Deviation log of borehole MW302R in the UConn landfill study area, Storrs, Connecticut
[ft, feet]

MW302R

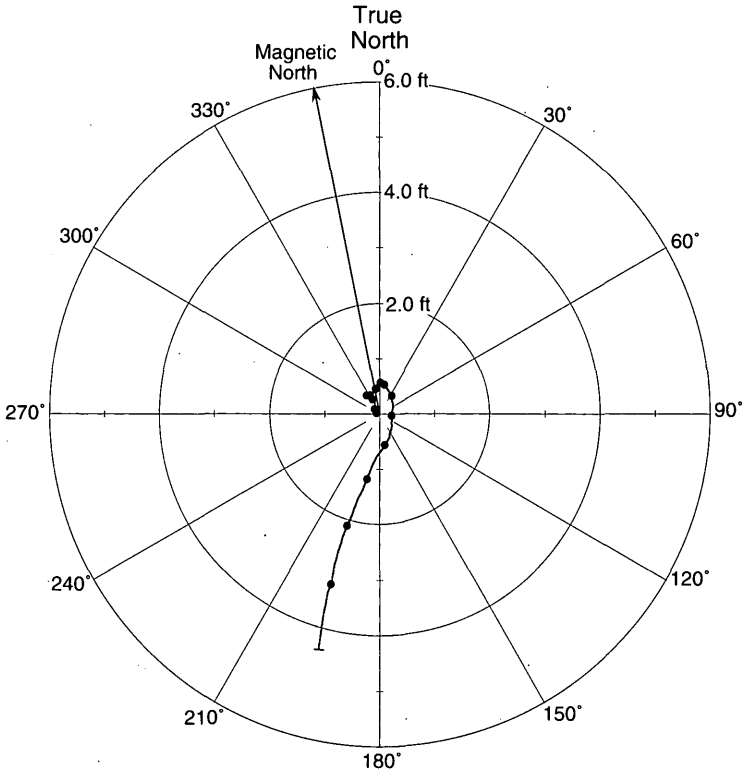

Depth along borehole in 20-foot increments between circles (•)

Projection along N180°E

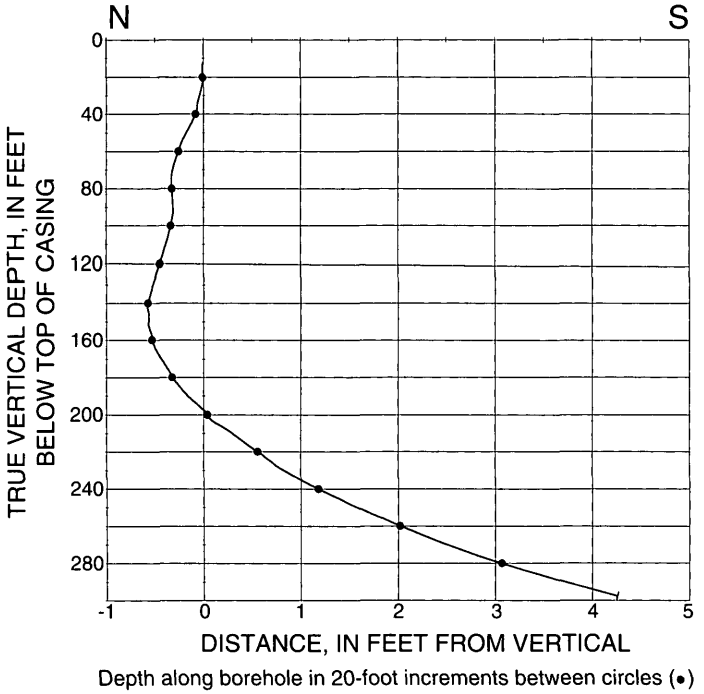

Depth along borehole in 20-foot increments between circles (•)

Projection along N90°E

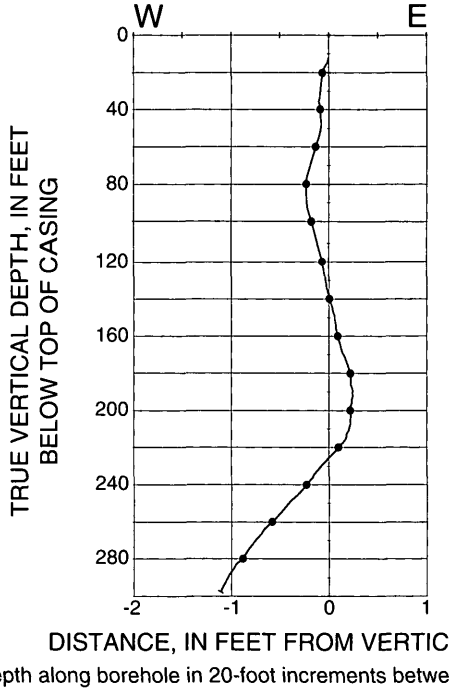

Depth along borehole in 20-foot increments between circles (•)

Appendix 5B. Composite log of natural-gamma, electromagnetic induction, fluid-temperature, specific-conductance, and heat-pulse flowmeter logs from borehole MW302R in the UConn landfill study area, Storrs, Connecticut

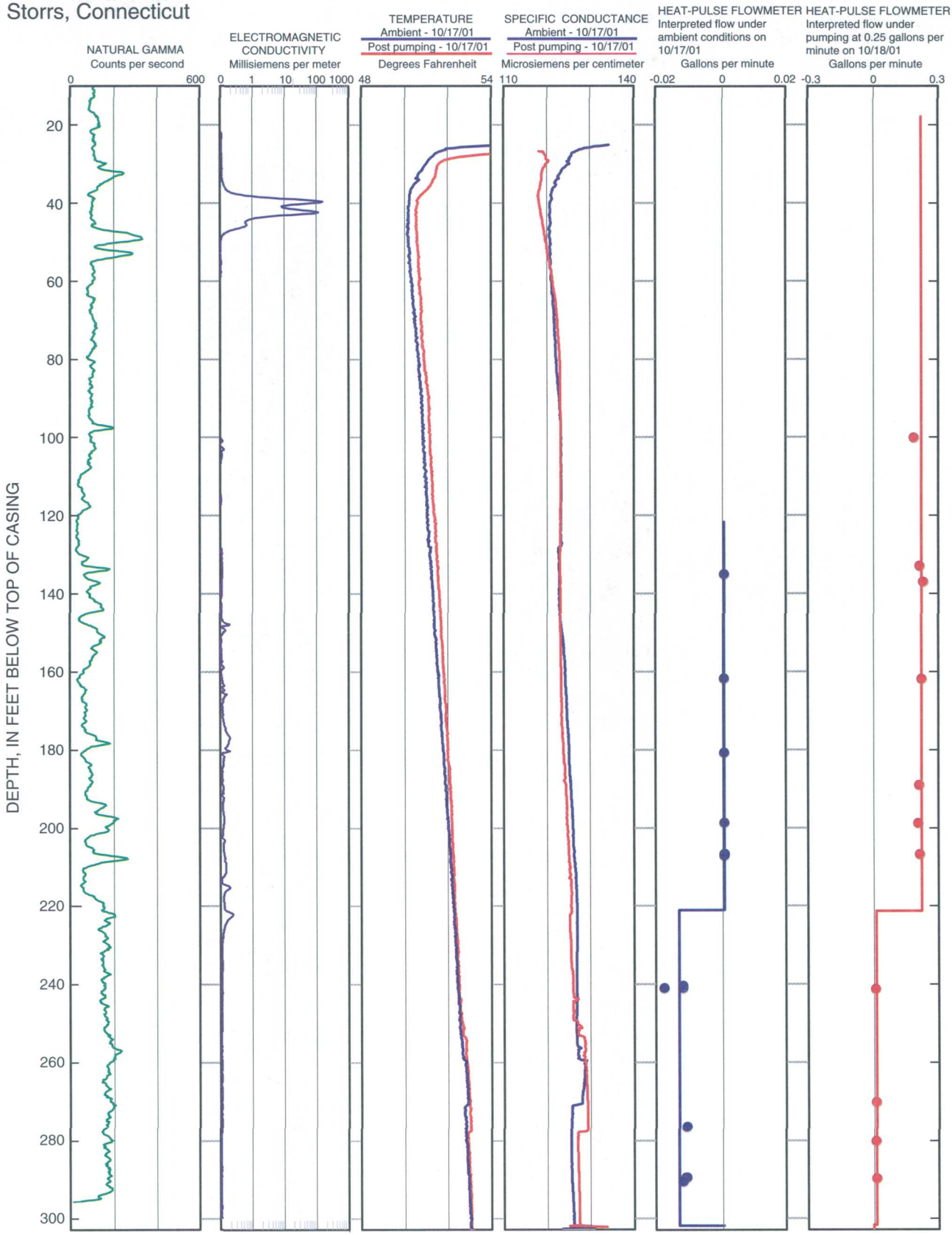

Appendix 5C. Caliper, acoustic-caliper, acoustic-televiewer, and optical-televiewer images and interpreted structures from borehole MW302R in the UConn landfill study area, Storrs, Connecticut

[Interpreted features indicated by color: black - foliation; dark blue - transmissive fracture; red - fracture; light blue - crack or minor fracture; gray - sealed fracture; pink - fracture with modifier, such as "partial" or "oxidized"; blue-gray - parting along foliation; green - fracture along contact; yellow - felsic layer]

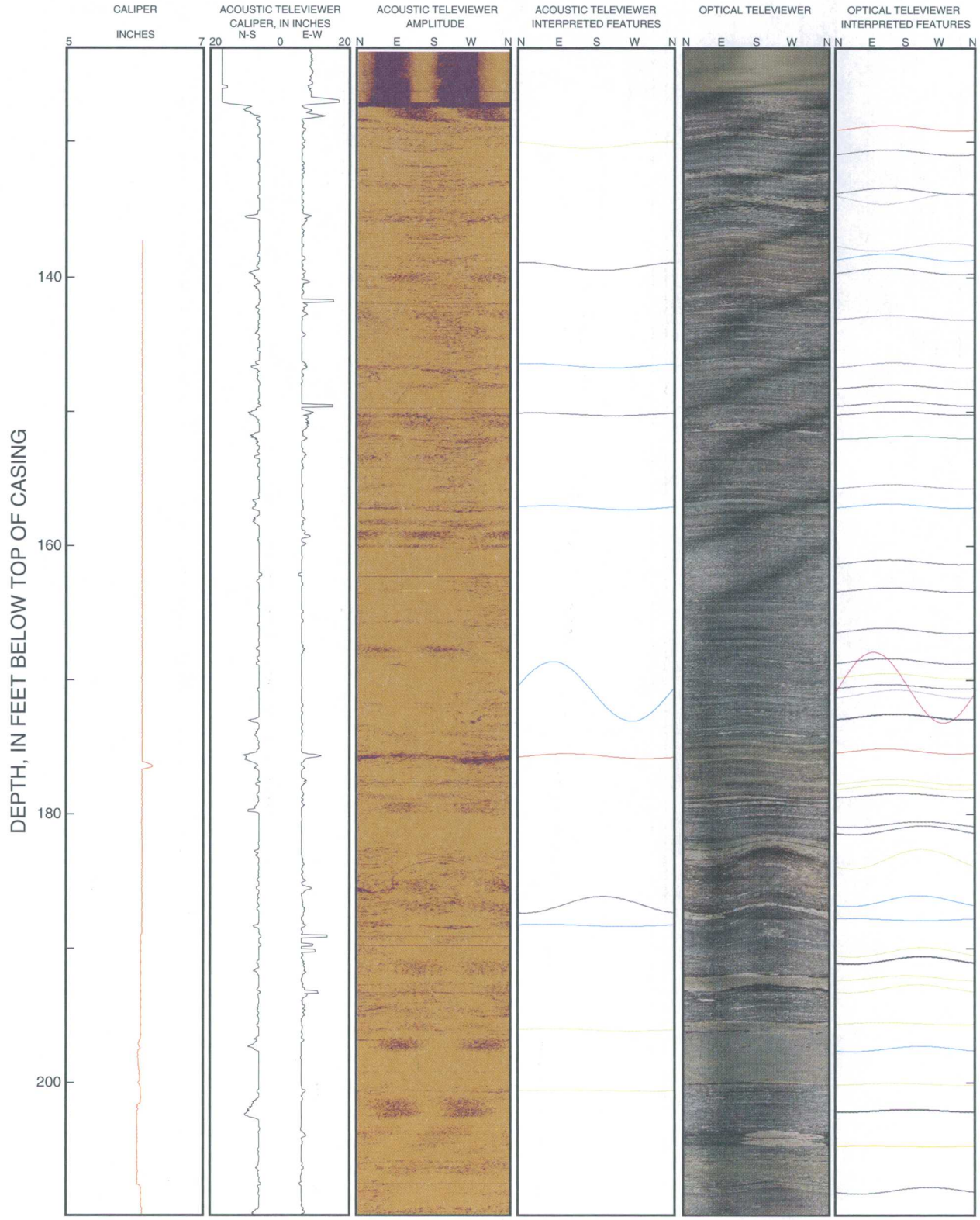

Appendix 5C. Caliper, acoustic-caliper, acoustic-televiewer, and optical-televiewer images and interpreted structures from borehole MW302R in the UConn landfill study area, Storrs, Connecticut--Continued

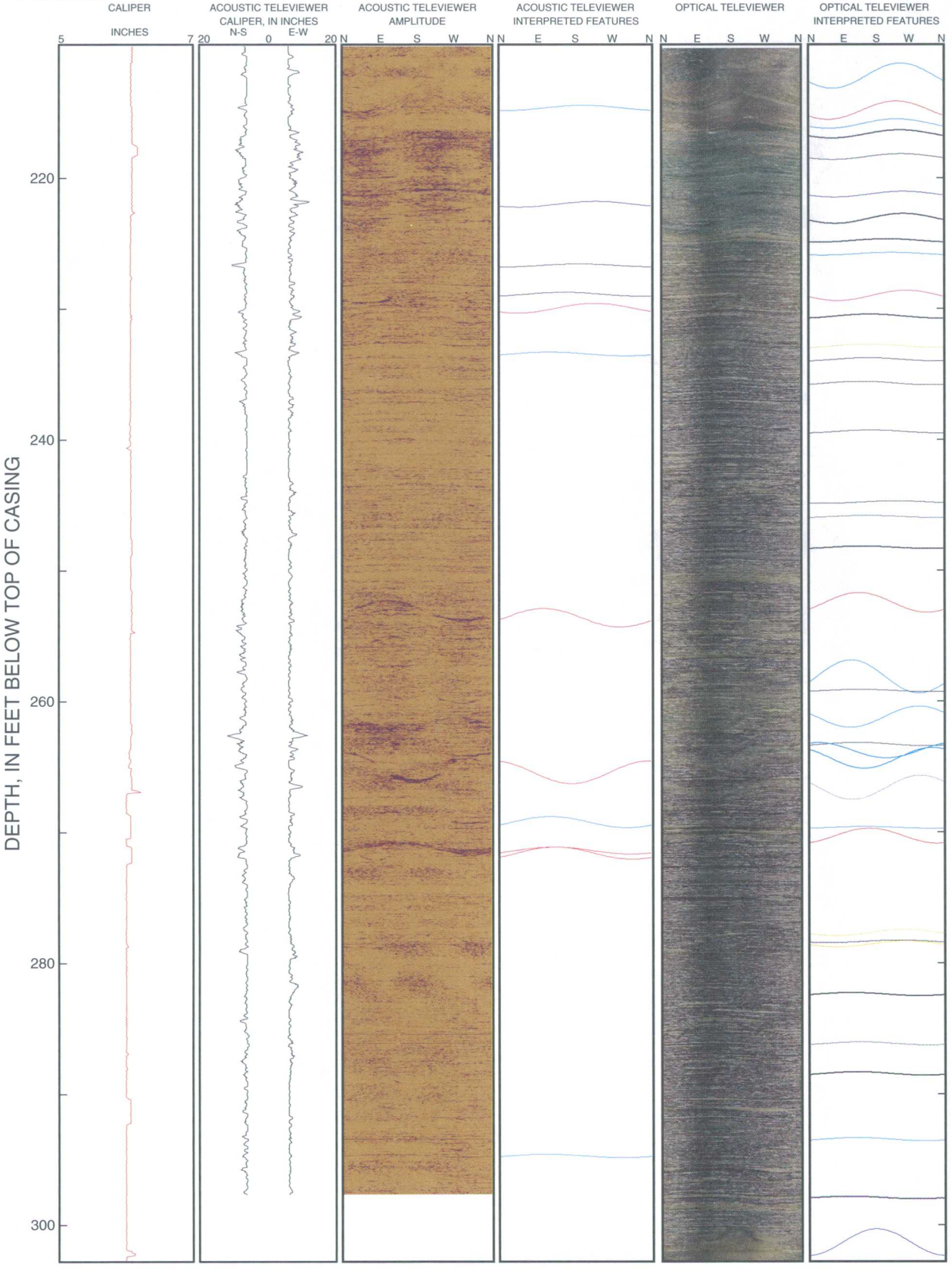

Appendix 5D. Processed borehole-radar reflection logs from borehole MW302R in the UConn landfill study area, Storrs, Connecticut

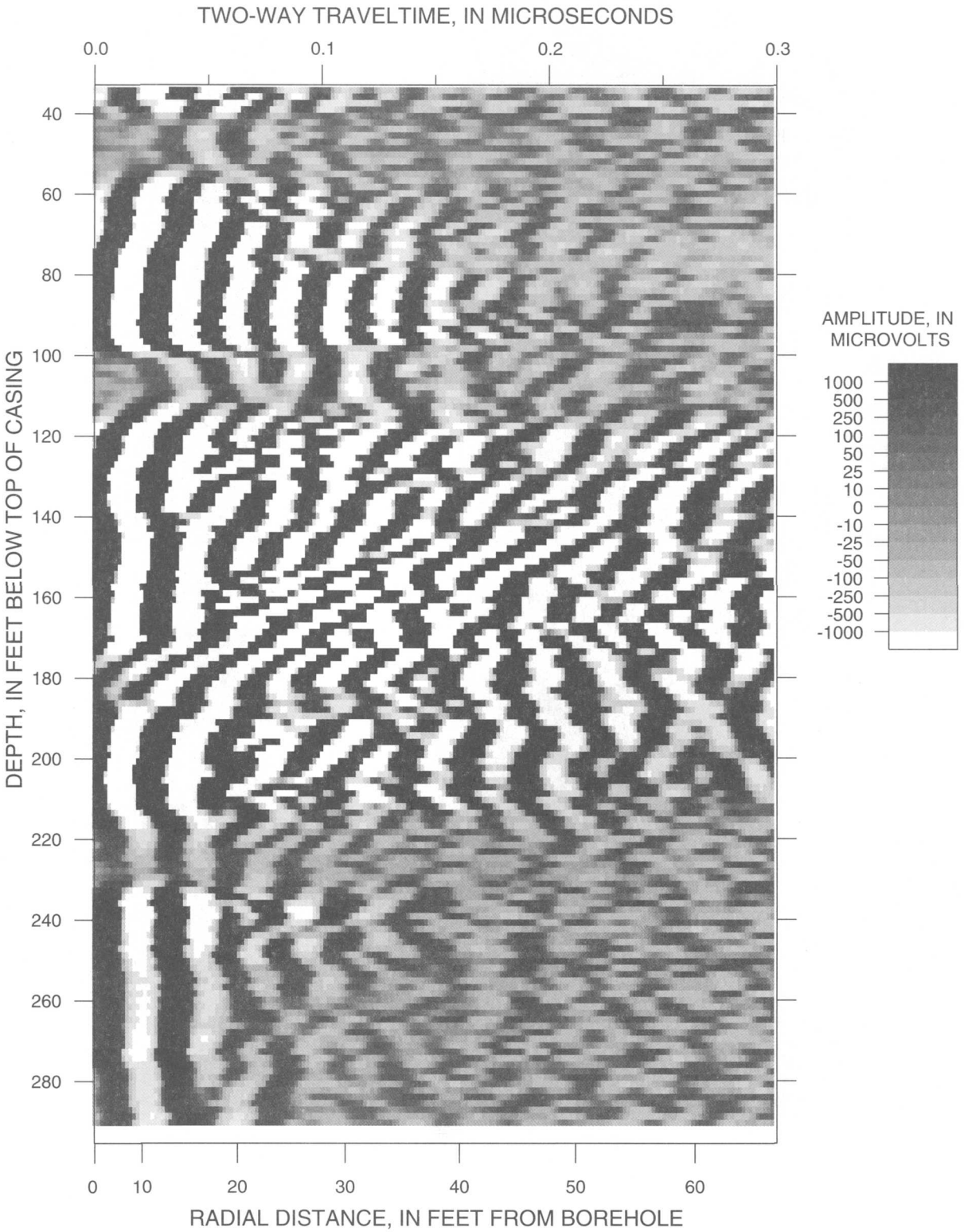

Appendix 5E. Midpoint depth, strike, and dip of features identified in optical-televiewer logs from borehole MW302R in the UConn landfill study area, Storrs, Connecticut

[Depth in feet below top of casing. Strike is reported in "right-hand rule" (RHR) where the direction of dip is to the right of the strike. -, no measurement]

Midpoint depth, in feet	Dip azimuth, in degrees	Strike, RHR in degrees	Dip, in degrees	Dip direction	Description
126.9	-	-	0	-	bottom of plastic casing
127.2	197	107	1	S	bottom of 8-inch diameter
129.0	314	224	38	NW	fracture
130.8	313	223	39	NW	foliation
133.7	315	225	43	NW	foliation
134.3	123	33	57	SE	sealed fracture
137.9	105	15	49	E	sealed fracture
138.6	310	220	47	NW	minor fracture
139.7	311	221	44	NW	foliation
143.1	324	234	33	NW	parting parallel to foliation
146.7	329	239	37	NW	parting parallel to foliation
148.3	329	239	31	NW	foliation
149.5	344	254	34	N	foliation
150.2	328	238	28	NW	foliation
152.0	5	275	21	N	possible fracture parallel to foliation
155.7	327	237	31	NW	parting parallel to foliation
157.2	317	227	32	NW	minor fracture
161.3	317	227	35	NW	foliation
163.4	319	229	33	NW	foliation
166.5	309	219	40	NW	foliation
168.7	314	224	40	NW	foliation
169.8	313	223	40	NW	lithologic feature
170.7	314	224	34	NW	foliation
170.7	277	187	85	W	partial trace of fracture
171.2	336	246	50	NW	sealed fracture
172.9	334	244	40	NW	foliation
175.5	307	217	38	NW	fracture
177.8	320	230	39	NW	lithologic feature
178.1	318	228	37	NW	lithologic feature
178.8	349	259	30	N	foliation
180.9	41	311	40	NE	foliation
181.4	45	315	52	NE	foliation
183.5	40	310	71	NE	lithologic feature
186.6	33	303	58	NE	minor fracture
188.0	219	129	18	SW	minor fracture
190.5	43	313	54	NE	lithologic feature
191.0	42	312	48	NE	foliation
192.4	358	268	36	N	lithologic feature
193.2	31	301	50	NE	lithologic feature
195.8	301	211	19	NW	lithologic feature
197.6	39	309	38	NE	minor fracture
200.3	324	234	15	NW	lithologic feature

Appendix 5E. Midpoint depth, strike, and dip of features identified in optical-televiewer logs from borehole MW302R in the UConn landfill study area, Storrs, Connecticut—Continued

[Depth in feet below top of casing. Strike is reported in "right-hand rule" (RHR) where the direction of dip is to the right of the strike. -, no measurement]

Midpoint depth, in feet	Dip azimuth, in degrees	Strike, RHR in degrees	Dip, in degrees	Dip direction	Description
202.2	9	279	20	N	foliation
204.9	258	168	7	W	lithologic feature
208.2	59	329	44	NE	foliation
212.3	64	334	75	NE	minor fracture
214.9	53	323	70	NE	fracture
216.0	54	324	55	NE	minor fracture
216.7	62	332	51	NE	foliation
218.5	64	334	41	NE	foliation
221.3	70	340	41	E	transmissive fracture
223.2	70	340	56	E	foliation
224.9	26	296	26	NE	foliation
225.9	38	308	22	NE	minor fracture
229.1	79	349	57	E	partial trace of fracture
230.7	341	251	31	N	foliation
232.9	340	250	28	N	lithologic feature
234.0	337	247	26	NW	foliation
235.8	318	228	28	NW	foliation
239.5	342	252	23	N	foliation
244.9	49	319	19	NE	foliation
246.0	333	243	17	NW	parting parallel to foliation
248.4	321	231	20	NW	foliation
252.6	313	223	72	NW	fracture
258.2	291	201	79	W	minor fracture
259.3	312	222	19	NW	foliation
261.3	110	20	72	E	minor fracture
263.4	308	218	27	NW	foliation
263.9	204	114	67	SW	minor fracture
264.4	146	56	72	SE	minor fracture
266.7	115	25	75	SE	sealed fracture
269.8	325	235	15	NW	minor fracture
270.4	340	250	66	N	fracture
277.8	72	342	45	E	lithologic feature
278.5	55	325	19	NE	foliation
278.7	75	345	42	E	lithologic feature
282.5	290	200	26	W	foliation
286.3	316	226	24	NW	parting parallel to foliation
288.6	305	215	26	NW	foliation
293.6	306	216	26	NW	minor fracture
298.0	285	195	20	W	foliation
301.5	358	268	76	N	transmissive fracture

Appendix 5F. Midpoint depth, strike, and dip of features identified in acoustic-televiewer logs from borehole MW302R in the UConn landfill study area, Storrs, Connecticut

[Depth in feet below top of casing. Strike is reported in "right-hand rule" (RHR) where the direction of dip is to the right of the strike.
-, no measurement]

Midpoint depth, in feet	Dip azimuth, in degrees	Strike, RHR in degrees	Dip, in degrees	Dip direction	Description
126.8	-	-	0	-	bottom of casing
127.1	-	-	0	-	bottom of 8-inch diameter
130.3	154	64	42	SE	lithologic feature
139.3	190	100	49	S	foliation
146.7	209	119	33	SW	minor fracture
150.3	218	128	23	SW	foliation
157.3	247	157	31	SW	minor fracture
171.0	260	170	83	W	minor fracture
175.8	290	200	37	W	fracture
186.9	14	284	68	N	foliation
188.4	237	147	19	SW	minor fracture
196.2	252	162	17	W	lithologic feature
200.7	280	190	8	W	lithologic feature
214.7	18	288	38	N	minor fracture
222.1	48	318	41	NE	transmissive fracture
226.8	8	278	25	N	foliation
229.0	332	242	31	NW	foliation
230.1	46	316	56	NE	partial trace of fracture
233.5	299	209	30	NW	minor fracture
253.7	285	195	70	W	fracture
265.5	171	81	74	S	fracture
269.3	301	211	59	NW	minor fracture
271.5	309	219	47	NW	fracture
271.7	313	223	62	NW	fracture
294.8	290	200	27	W	minor fracture

Appendix 5G. Location, orientation, and length of reflectors interpreted from borehole-radar data from borehole MW302R in the UConn landfill study area, Storrs, Connecticut

[Depth in feet below top of casing. Strike is reported in "right-hand rule" (RHR) where the direction of dip is to the right of the strike. Reflector continuity is on a scale of 1 (good) to 5 (poor)]

Midpoint depth, in feet	Dip azimuth, in degrees	Strike, RHR in degrees	Dip, in degrees	Dip direction	Estimated reflector length, in feet	Reflector continuity
18.0	335	245	60	NW	32.2	3
70.9	345	255	65	N	69.7	3
138.8	305	215	47	NW	18.1	4
140.8	305	215	61	NW	39.0	4
184.4	305	215	29	NW	115.1	2
186.7	33	303	58	NE	48.8	5
197.5	40	310	37	NE	30.0	3
203.1	325	235	66	NW	38.5	4
217.2	165	75	53	S	27.3	2
217.9	175	85	12	S	22.1	3
229.0	77	347	56	E	14.3	4
250.3	275	185	56	W	28.9	4
293.0	285	195	60	W	21.5	3
357.0	65	335	63	NE	52.1	4

Appendix 5H. Heat-pulse flowmeter measurements in MW302R at the UConn landfill study area, Storrs, Connecticut

[--indicates no flow; for interpretation, if nothing is listed, there is no change in inflow or outflow]

Date	Depth of measurement, in feet below top of casing	Flow direction	Average rate, in gallons per minute	Normalized average rate, in gallons per minute	Interpretation
February 26, 2001	Ambient conditions				
	135.2	--	0.000	--	
	162.0	--	0.000	--	
	181.0	--	0.000	--	
	199.0	--	0.000	--	
	206.9	--	0.000	--	
	207.0	down	-0.060	--	Inflow at 221 feet
	241.4	down	-0.014	--	
	276.9	down	-0.080	--	
	290.0	down	-0.012	--	
	291.0	down	-0.013	--	Outflow at 301 feet

Appendix 5H. Heat-pulse flowmeter measurements in MW302R at the UConn landfill study area, Storrs, Connecticut—Continued

[--indicates no flow; for interpretation, if nothing is listed, there is no change in inflow or outflow]

Date	Depth of measurement, in feet below top of casing	Flow direction	Average rate, in gallons per minute	Normalized average rate, in gallons per minute	Interpretation
February 26, 2001	Pumping at 0.25 gallon per minute				Poor seal in 6-inch casing
	130.01	up	0.090	0.250	Inflow at base of casing
	172.05	up	0.097	0.270	
	180.81	up	0.088	0.245	
	180.81	up	0.090	0.250	
	198.94	up	0.081	0.224	Inflow at 221 feet
	242.01	--	0.000	0.000	
	259.81	--	0.000	0.000	
	275.98	--	0.000	0.000	
October 17, 2001	Ambient conditions				
	135.19	--	0.000	--	
	162.00	--	0.000	--	
	181.02	--	0.000	--	
	199.03	--	0.000	--	
	206.92	--	0.000	--	
	206.99	--	0.000	--	
	207.00	--	0.000	--	
	241.39	down	-0.013	--	Inflow at 221 feet
	241.42	down	-0.018	--	
	241.42	down	-0.013	--	
	276.91	down	-0.012	--	
	289.95	down	-0.012	--	
	290.97	down	-0.013	--	Outflow at 301 feet
October 18, 2001	Pumping at 0.25 gallon per minute				Poor seal in 8-inch casing
	100.0	up	0.126	0.203	
	133.0	up	0.144	0.232	
	137.0	up	0.155	0.250	
	162.0	up	0.149	0.240	
	190.9	up	0.141	0.227	
	199.0	up	0.138	0.223	Inflow at 221 feet
	207.0	up	0.144	0.232	
	241.5	up	0.007	0.011	
	270.5	up	0.008	0.013	
	280.5	up	0.008	0.013	
	290.0	up	0.010	0.016	Inflow at 301 feet

Appendix 5I. Tadpole plots and stereoplots of fractures and foliations interpreted in optical-televiewer images from borehole MW302R in the UConn landfill study area, Storrs, Connecticut

[OTV, optical televiewer]

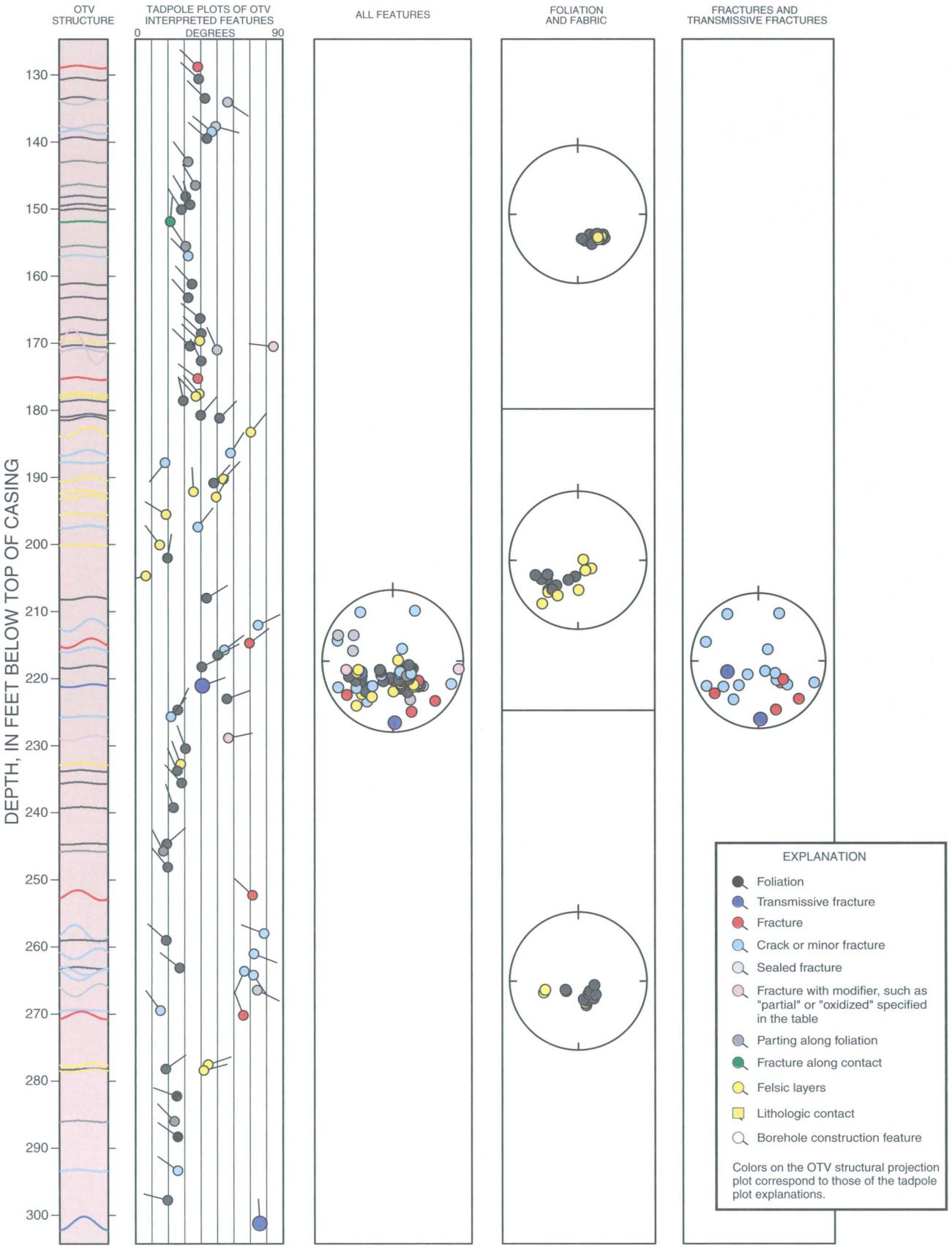

Appendix 5J. Tadpole plots and stereoplots of fractures and foliations interpreted in acoustic-televiewer images from borehole MW302R in the UConn landfill study area, Storrs, Connecticut

[ATV, acoustic televiewer]

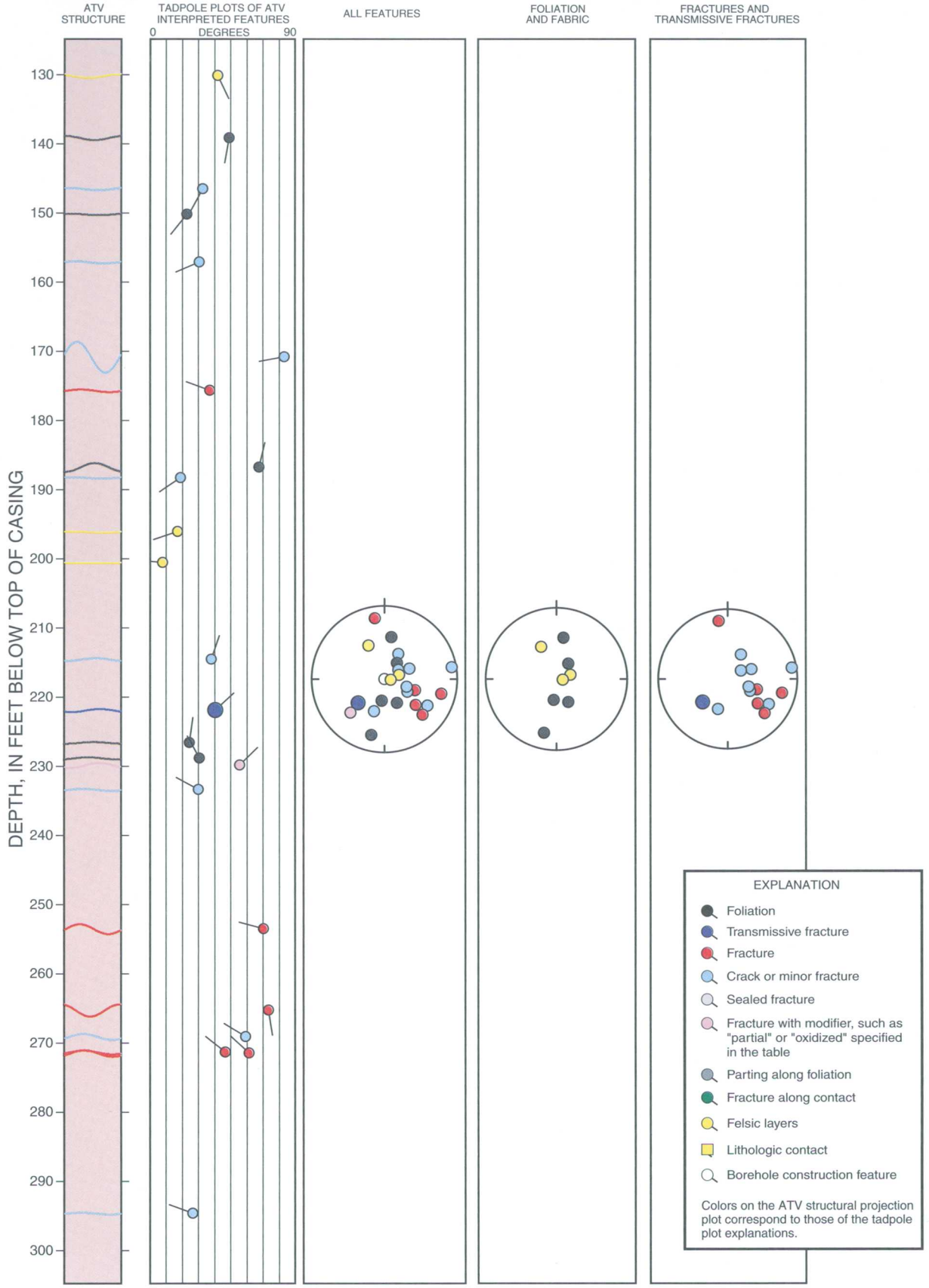

Appendix 6. Borehole-geophysical logs from domestic well W202-NE in the UConn landfill study area, Storrs, Connecticut

Appendix 6A. Deviation log of domestic well W202-NE in the UConn landfill study area, Storrs, Connecticut
[ft, feet]

W202-NE

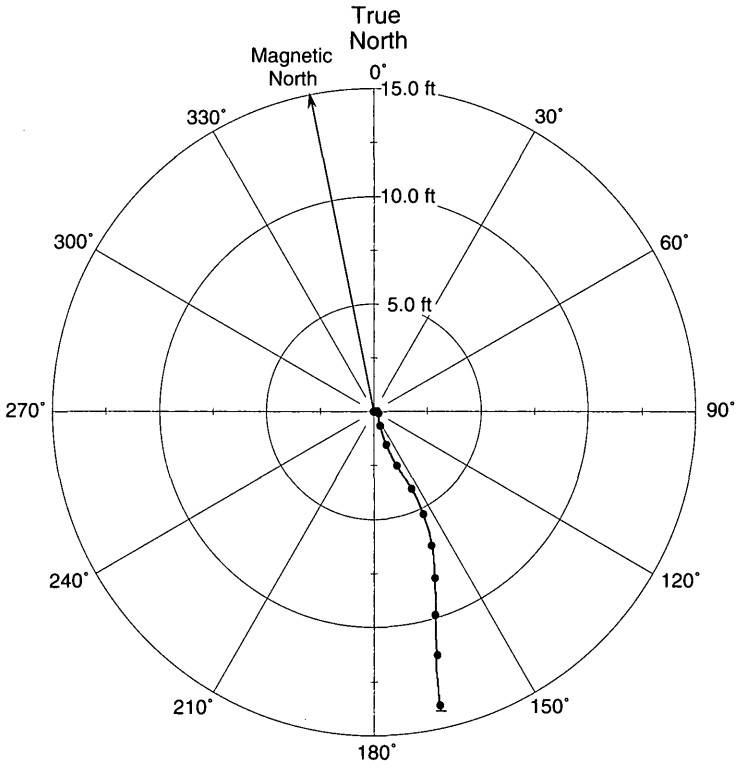

Depth along borehole in 20-foot increments between circles (•)

Projection along N170°E

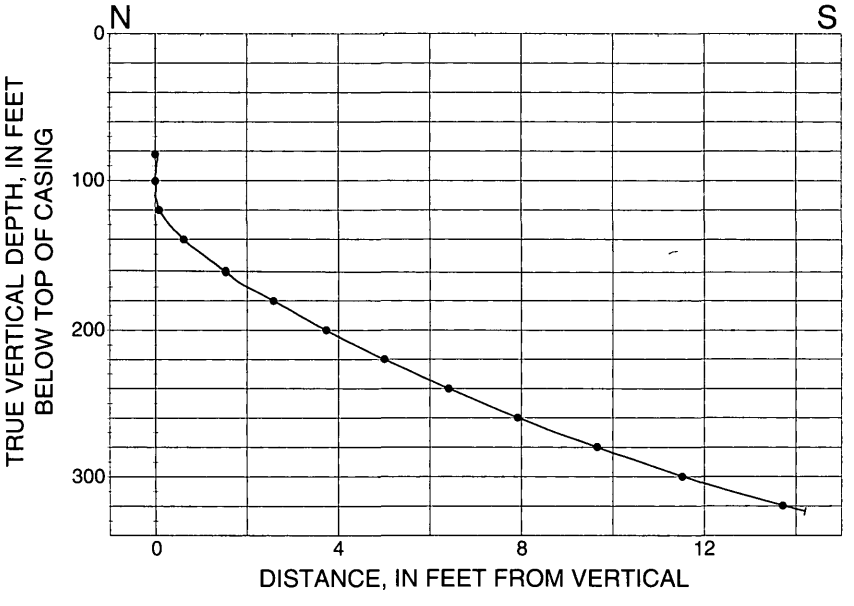

Depth along borehole in 20-foot increments between circles (•)

Projection along N90°E

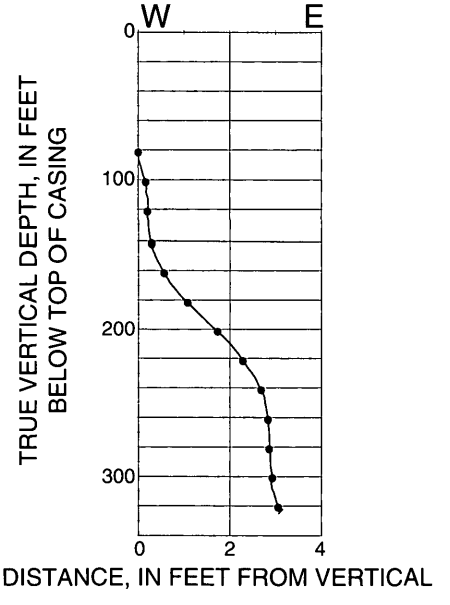

Depth along borehole in 20-foot increments between circles (•)

Appendix 6B. Composite log of natural-gamma, electromagnetic induction, fluid-temperature, specific-conductance, and heat-pulse flowmeter logs from domestic well W202-NE in the UConn landfill study area, Storrs, Connecticut

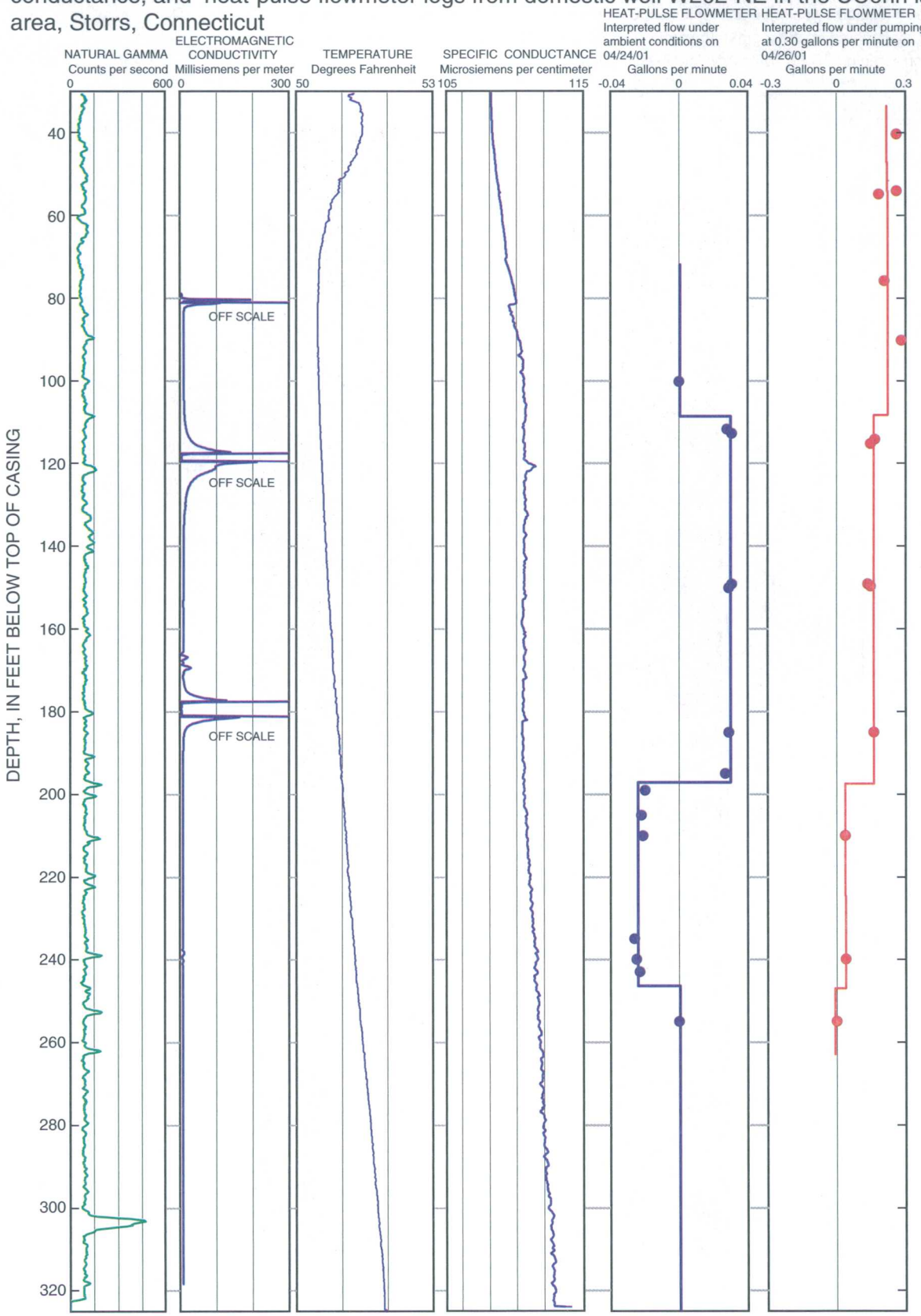

Appendix 6C. Caliper, acoustic-caliper, acoustic-televiewer, and optical-televiewer images and interpreted structures from domestic well W202-NE in the UConn landfill study area, Storrs, Connecticut

[Interpreted features indicated by color: black - foliation; dark blue - transmissive fracture; red - fracture; light blue - crack or minor fracture; gray - sealed fracture; pink - fracture with modifier, such as "partial" or "oxidized"; blue-gray - parting along foliation; green - fracture along contact; yellow - felsic layer]

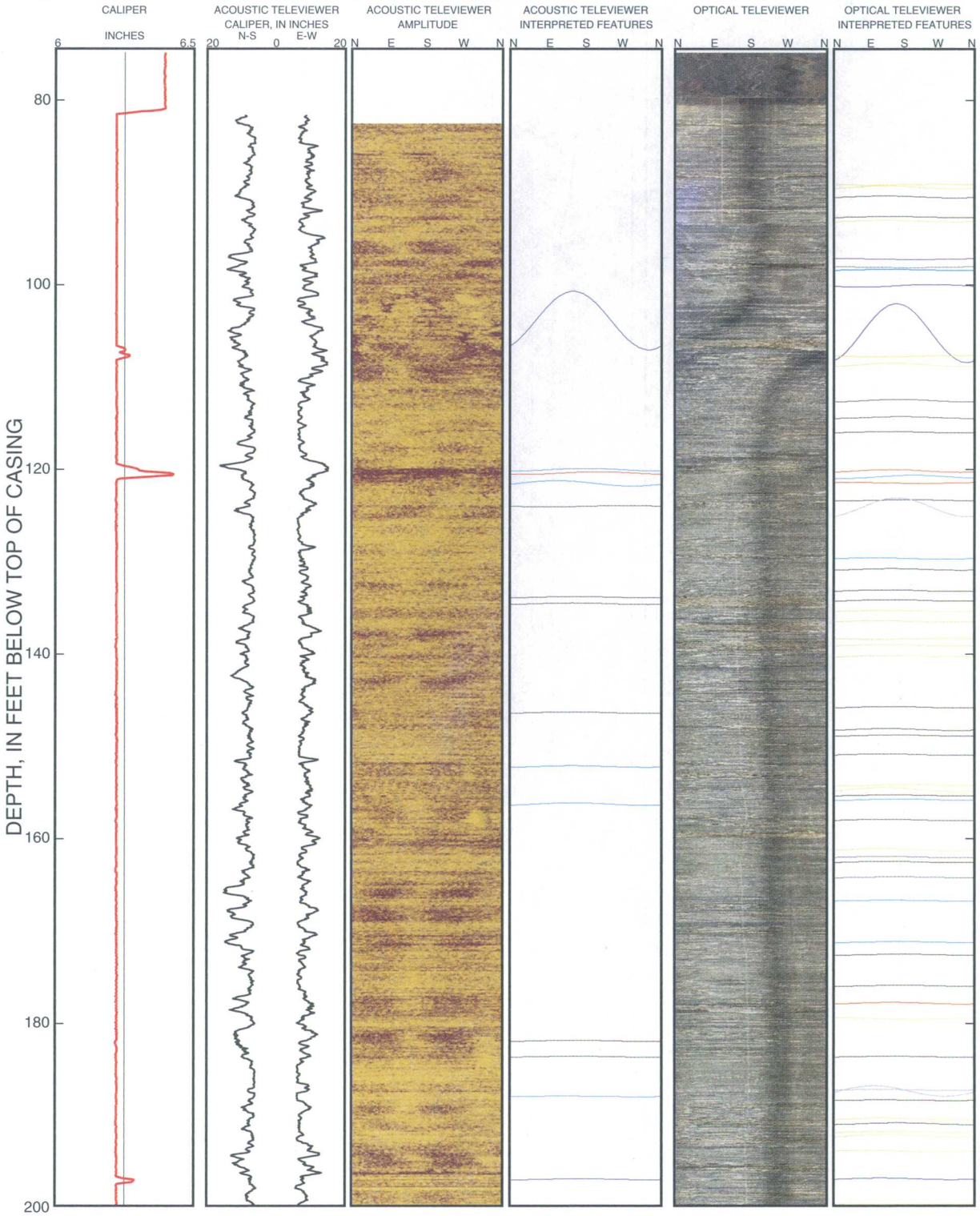

Appendix 6C. Caliper, acoustic-caliper, acoustic-televiewer, and optical-televiewer images and interpreted structures from domestic well W202-NE in the UConn landfill study area, Storrs, Connecticut--Continued

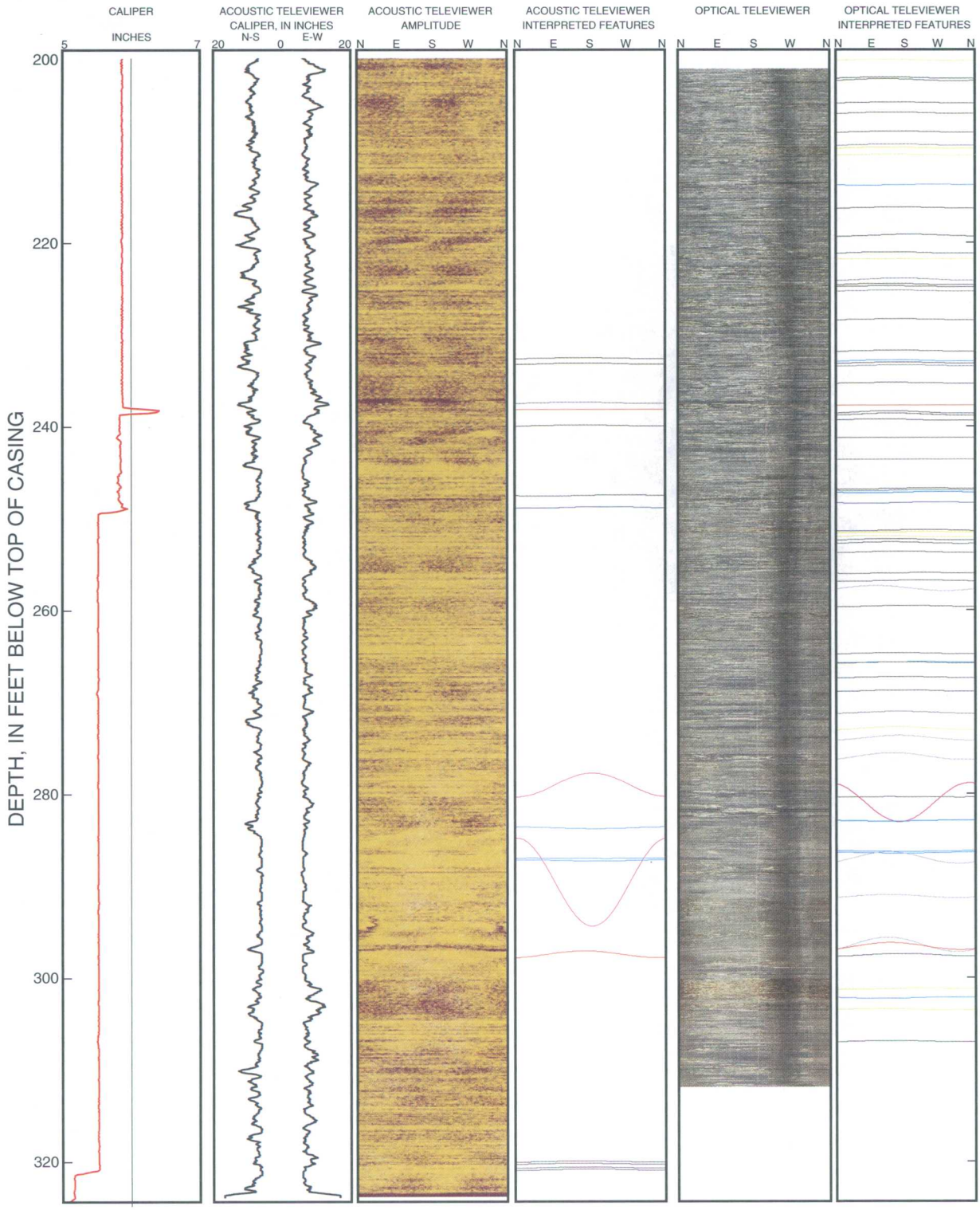

Appendix 6D. Processed borehole-radar reflection logs from domestic well W202-NE in the UConn landfill study area, Storrs, Connecticut

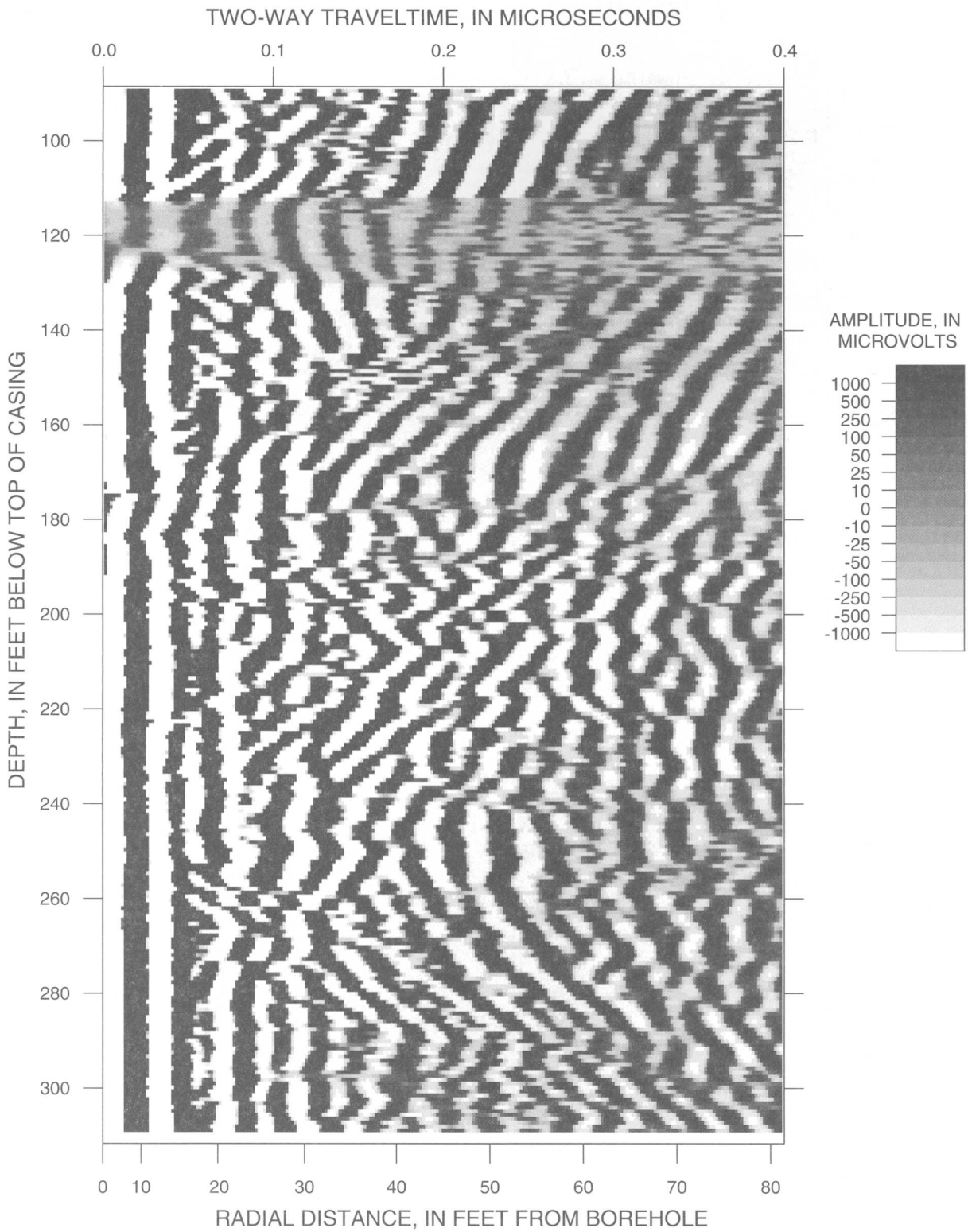

Appendix 6E. Midpoint depth, strike, and dip of features identified in optical-televiewer logs from domestic well W202-NE in the UConn landfill study area, Storrs, Connecticut

[Depth in feet below top of casing. Strike is reported in "right-hand rule" (RHR) where the direction of dip is to the right of the strike.
-, no measurement]

Midpoint depth, in feet	Dip azimuth, in degrees	Strike, RHR in degrees	Dip, in degrees	Dip direction	Description
81.8	-	-	0	-	bottom of casing
89.3	84	354	7	E	lithologic feature
89.7	311	221	34	NW	lithologic feature
90.6	308	218	22	NW	foliation
92.8	323	233	13	NW	foliation
93.3	307	217	21	NW	lithologic feature
97.4	208	118	10	SW	possible transmissive fracture
98.2	192	102	9	S	parting parallel to foliation
98.5	317	227	12	NW	lithologic feature
100.3	69	339	29	E	possible transmissive fracture
105.4	339	249	85	N	possible transmissive fracture
107.9	118	28	18	SE	lithologic feature
108.9	326	236	37	NW	lithologic feature
112.8	344	254	28	N	foliation
114.6	349	259	21	N	foliation
116.2	319	229	15	NW	foliation
120.4	322	232	30	NW	fracture
121.0	25	295	33	NE	minor fracture
121.7	222	132	11	SW	fracture
123.6	10	280	15	N	foliation
124.3	340	250	76	N	sealed fracture
129.8	278	188	14	W	minor fracture
131.0	326	236	20	NW	foliation
133.3	312	222	19	NW	foliation
134.4	322	232	19	NW	foliation
135.6	300	210	11	NW	lithologic feature
136.7	289	199	15	W	lithologic feature
138.6	114	24	10	SE	lithologic feature
139.3	302	212	16	NW	lithologic feature
140.5	313	223	19	NW	lithologic feature
146.0	321	231	18	NW	foliation
148.4	313	223	24	NW	foliation
149.1	334	244	16	NW	foliation
151.1	304	214	15	NW	foliation
154.5	7	277	19	N	lithologic feature
155.0	309	219	42	NW	lithologic feature
155.5	322	232	12	NW	foliation
156.0	342	252	19	N	minor fracture
158.2	309	219	17	NW	foliation
161.5	298	208	24	NW	lithologic feature
162.2	304	214	15	NW	parting parallel to foliation
162.8	310	220	16	NW	foliation

Appendix 6E. Midpoint depth, strike, and dip of features identified in optical-televiewer logs from domestic well W202-NE in the UConn landfill study area, Storrs, Connecticut—Continued

[Depth in feet below top of casing. Strike is reported in "right-hand rule" (RHR) where the direction of dip is to the right of the strike. -, no measurement]

Midpoint depth, in feet	Dip azimuth, in degrees	Strike, RHR in degrees	Dip, in degrees	Dip direction	Description
164.4	335	245	10	NW	parting parallel to foliation
166.9	317	227	10	NW	minor fracture
171.5	345	255	12	N	minor fracture
172.8	348	258	12	N	foliation
176.2	348	258	14	N	foliation
178.0	325	235	21	NW	fracture
179.8	206	116	20	SW	lithologic feature
183.9	319	229	11	NW	foliation
187.5	291	201	12	W	sealed fracture
187.6	282	192	66	W	sealed fracture
188.6	299	209	9	NW	foliation
190.6	298	208	21	NW	lithologic feature
191.1	342	252	21	N	foliation
192.0	315	225	15	NW	lithologic feature
192.5	310	220	31	NW	lithologic feature
194.1	258	168	18	W	lithologic feature
197.1	298	208	20	NW	transmissive fracture
199.9	151	61	7	SE	lithologic feature
200.3	300	210	17	NW	lithologic feature
202.2	306	216	15	NW	foliation
202.4	303	213	24	NW	foliation
204.9	326	236	13	NW	foliation
206.0	324	234	16	NW	foliation
208.1	330	240	14	NW	foliation
209.5	328	238	16	NW	parting parallel to foliation
209.8	316	226	16	NW	lithologic feature
210.6	317	227	10	NW	lithologic feature
213.9	71	341	10	E	minor fracture
216.4	339	249	13	N	foliation
219.4	8	278	23	N	foliation
221.2	317	227	19	NW	foliation
221.9	121	31	3	SE	lithologic feature
224.1	344	254	28	N	parting parallel to foliation
224.7	309	219	19	NW	foliation
224.9	308	218	10	NW	foliation
225.4	323	233	13	NW	parting parallel to foliation
228.5	334	244	11	NW	foliation
232.0	334	244	12	NW	foliation
233.0	326	236	18	NW	minor fracture
233.3	341	251	13	N	foliation
233.5	348	258	14	N	parting parallel to foliation
235.4	322	232	9	NW	foliation
237.9	227	137	3	SW	fracture

Appendix 6E. Midpoint depth, strike, and dip of features identified in optical-televiewer logs from domestic well W202-NE in the UConn landfill study area, Storrs, Connecticut—Continued

[Depth in feet below top of casing. Strike is reported in "right-hand rule" (RHR) where the direction of dip is to the right of the strike. -, no measurement]

Midpoint depth, in feet	Dip azimuth, in degrees	Strike, RHR in degrees	Dip, in degrees	Dip direction	Description
238.6	317	227	28	NW	foliation
238.9	322	232	24	NW	foliation
238.9	324	234	24	NW	foliation
239.4	292	202	17	W	foliation
241.4	144	54	5	SE	foliation
243.8	53	323	3	NE	parting parallel to foliation
247.0	57	327	11	NE	foliation
247.1	71	341	16	E	parting parallel to foliation
247.4	83	353	15	E	minor fracture
248.5	77	347	13	E	transmissive fracture
251.5	47	317	14	NE	foliation
251.7	51	321	10	NE	lithologic feature
252.2	292	202	18	W	lithologic feature
252.5	321	231	17	NW	foliation
252.9	321	231	21	NW	foliation
253.9	342	252	17	N	foliation
256.1	48	318	9	NE	foliation
257.0	37	307	12	NE	foliation
257.8	282	192	48	W	sealed fracture
259.8	1	271	14	N	foliation
264.9	335	245	14	NW	foliation
265.8	39	309	8	NE	minor fracture
265.9	349	259	14	N	foliation
267.5	346	256	13	N	foliation
269.0	349	259	19	N	foliation
271.3	341	251	23	N	parting parallel to foliation
273.0	338	248	34	N	lithologic feature
274.1	340	250	47	N	sealed fracture
276.1	324	234	56	NW	sealed fracture
280.6	317	227	7	NW	foliation
281.1	164	74	83	S	partial trace of a fracture
283.2	135	45	11	SE	minor fracture
286.4	183	93	9	S	minor fracture
286.7	170	80	11	S	minor fracture
287.2	314	224	68	NW	sealed fracture
291.3	312	222	35	NW	sealed fracture
296.6	311	221	72	NW	sealed fracture
296.8	319	229	57	NW	fracture
297.8	348	258	29	N	foliation
301.4	48	318	10	NE	lithologic feature
302.4	119	29	18	SE	minor fracture
303.6	291	201	18	W	lithologic feature
307.1	319	229	17	NW	foliation

Appendix 6F. Midpoint depth, strike, and dip of features identified in acoustic-televiewer logs from domestic well W202-NE in the UConn landfill study area, Storrs, Connecticut

[Depth in feet below top of casing. Strike is reported in "right-hand rule" (RHR) where the direction of dip is to the right of the strike. -, no measurement]

Midpoint depth, in feet	Dip azimuth, in degrees	Strike, RHR in degrees	Dip, in degrees	Dip direction	Description
104.0	330	240	85	NW	transmissive fracture
120.2	358	268	29	N	minor fracture
120.6	28	298	30	NE	fracture
121.7	290	200	49	W	minor fracture
124.2	91	1	15	E	foliation
134.1	334	244	17	NW	foliation
134.8	328	238	19	NW	foliation
146.6	324	234	18	NW	foliation
152.4	325	235	20	NW	minor fracture
156.5	327	237	28	NW	minor fracture
182.1	331	241	15	NW	foliation
183.8	332	242	12	NW	foliation
188.1	303	213	9	NW	minor fracture
197.2	342	252	13	N	transmissive fracture
232.7	334	244	12	NW	foliation
233.3	344	254	18	N	foliation
237.6	326	236	14	NW	parting parallel to foliation
238.3	249	159	1	W	fracture
240.1	337	247	14	NW	foliation
247.6	74	344	14	E	foliation
249.0	36	306	19	NE	transmissive fracture
279.2	6	276	79	N	partial fracture trace
283.8	191	101	21	S	minor fracture
287.2	219	129	7	SW	minor fracture
287.4	201	111	14	S	minor fracture
289.8	186	96	87	S	partial fracture trace
297.6	346	256	55	N	fracture
320.2	338	248	13	N	foliation
320.4	332	242	12	NW	foliation
320.8	347	257	15	N	foliation
321.1	355	265	15	N	foliation

Appendix 6G. Location, orientation, and length of reflectors interpreted from borehole-radar data from domestic well W202-NE in the UConn landfill study area, Storrs, Connecticut

[Depth in feet below top of casing. Strike is reported in "right-hand rule" (RHR) where the direction of dip is to the right of the strike. Reflector continuity is on a scale of 1 (good) to 5 (poor)]

Midpoint depth, in feet	Dip azimuth, in degrees	Strike, RHR in degrees	Dip, in degrees	Dip direction	Estimated reflector length, in feet	Reflector continuity
120.4	321	231	30	NW	25.6	3
121.7	219	129	12	SW	36.9	2
135.5	293	203	10	NW	15.6	3
147.3	255	165	53	W	20.9	2
156.2	342	252	16	N	4.3	5
178.2	325	235	17	NW	21.4	2
230.3	5	275	47	N	39.5	3
239.2	275	185	25	W	16.5	3
248.4	88	358	13	E	23.0	4
281.2	135	45	48	SE	28.7	3
302.5	133	43	21	SE	9.8	5
329.4	105	15	35	E	9.9	4

Appendix 6H. Heat-pulse flowmeter measurements in domestic well W202-NE at the UConn landfill study area, Storrs, Connecticut

[--indicates no flow; for interpretation, if nothing is listed, there is no change in inflow or outflow]

Date	Depth of measurement, in feet below top of casing	Flow direction	Average rate, in gallons per minute	Normalized average rate, in gallons per minute	Interpretation
April 24, 2001	Ambient conditions				
	100.0	--	0.000	--	
	111.5	up	0.028	--	Outflow at 108 feet
	112.6	up	0.031	--	
	149.0	up	0.031	--	
	150.0	up	0.029	--	
	185.0	up	0.027	--	
	195.0	up	0.027	--	
	199.0	down	-0.020	--	Inflow at 197 feet
	201.0	down	-0.023	--	
	205.0	down	-0.022	--	
	210.0	down	-0.021	--	
	235.0	down	-0.026	--	
	240.0	down	-0.025	--	
	243.0	down	-0.023	--	Outflow at 249 feet
	255.0	--	0.000	--	
April 26, 2001	Pumping at 0.30 gallon per minute				
	40.0	up	0.210	0.289	
	53.8	up	0.209	0.288	
	54.5	up	0.193	0.266	
	75.5	up	0.201	0.277	
	90.0	up	0.218	0.300	
	114.0	up	0.168	0.231	Inflow at 108 feet
	115.0	up	0.148	0.204	
	149.0	up	0.136	0.187	
	149.5	up	0.148	0.204	
	185.0	up	0.163	0.224	
	210.0	up	0.037	0.051	Inflow at 197 feet
	240.0	up	0.039	0.054	
	255.0	--	0.000	0.000	Inflow at 249 feet

Appendix 6I. Tadpole plots and stereoplots of fractures and foliations interpreted in optical-televiewer images from domestic well W202-NE in the UConn landfill study area, Storrs, Connecticut

[OTV, optical televiewer]

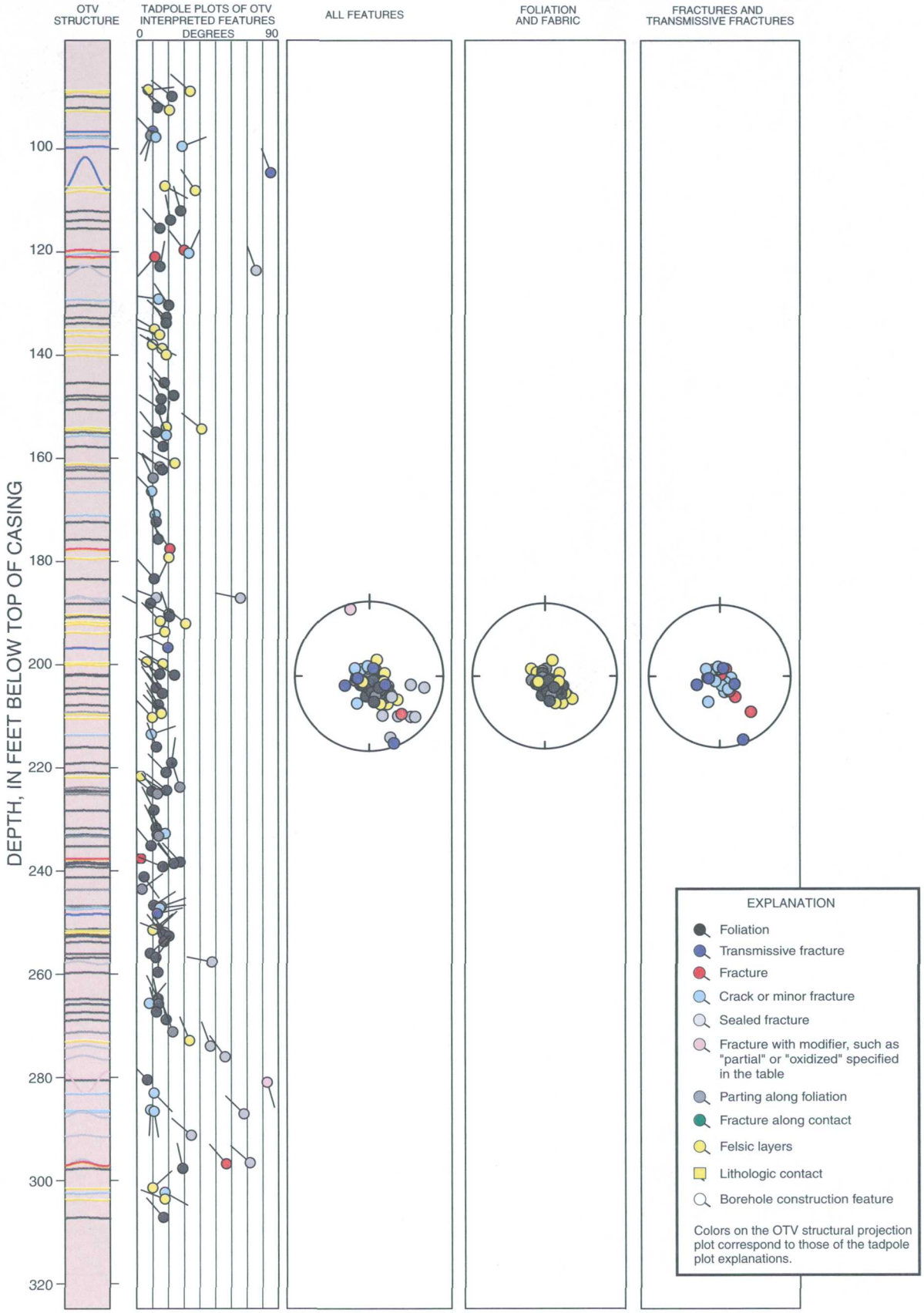

Appendix 6J. Tadpole plots and stereoplots of fractures and foliations interpreted in acoustic-televiewer images from domestic well W202-NE in the UConn landfill study area, Storrs, Connecticut

[ATV, acoustic televiewer]

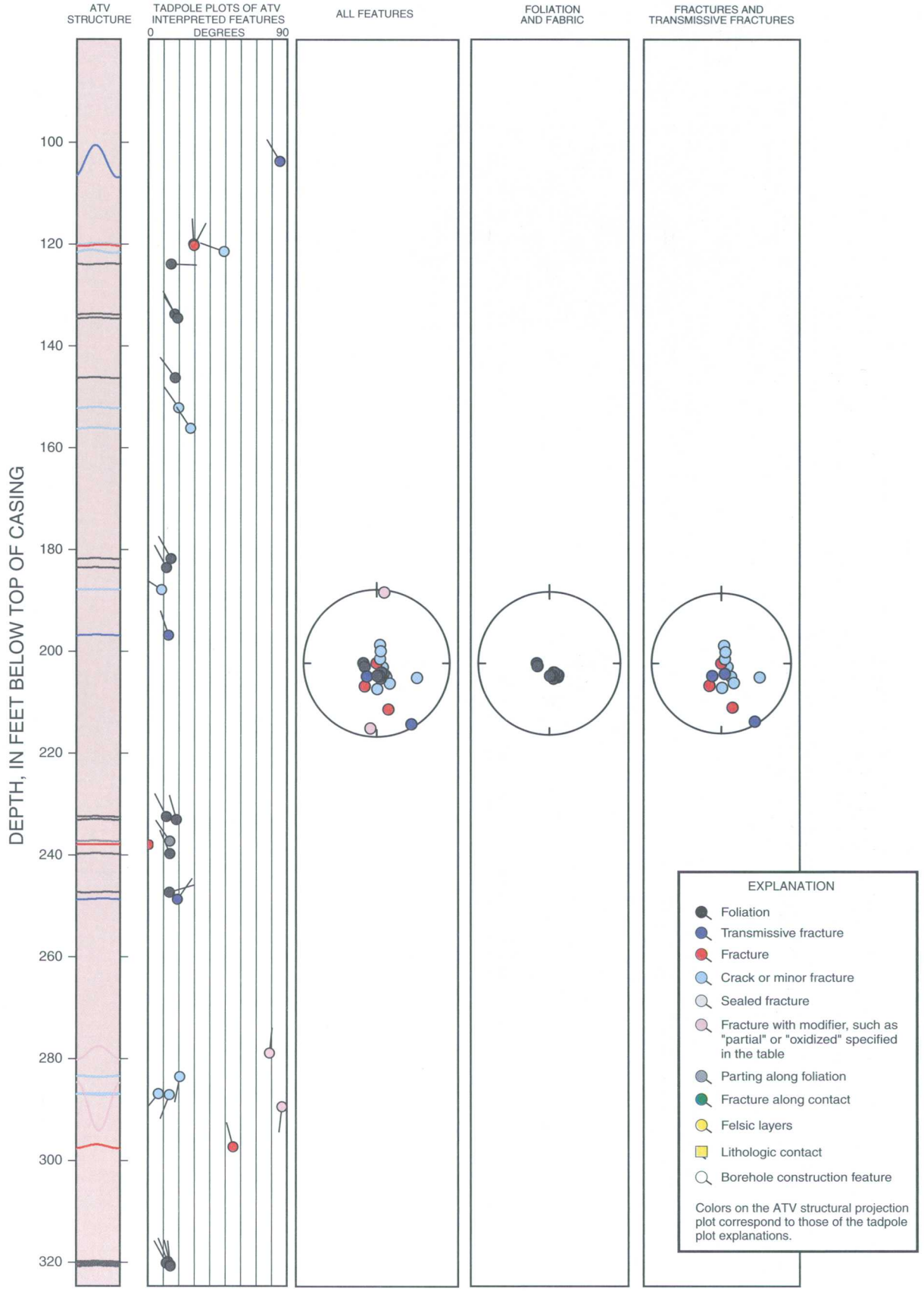

Appendix 7. Specific capacity, open-hole transmissivity, and discrete-interval transmissivity for boreholes in the UConn landfill study area, Storrs, Connecticut

Appendix 7. Specific capacity, open-hole transmissivity, and discrete-interval transmissivity for boreholes in the UConn landfill study area, Storrs, Connecticut

A. Open-hole specific-capacity tests conducted August to September 2000. Estimates of transmissivity based on an algorithm of Bradbury and Rothschild (1985)

Borehole	Date tested	Pumping rate, in gallons per minute	Elapsed time, in hours	Specific capacity, in gallons per minute per foot	Transmissivity	
					in feet squared per day	in feet squared per second
MW201R	08/29/00	0.25	1.42	0.060	9.7	1.1×10^{-4}
MW201R	08/29/00	0.25	2.67	0.056	9.8	1.1×10^{-4}
MW201R	08/29/00	0.25	3.52	0.051	9.0	1.0×10^{-4}
MW201R	08/31/00	0.25	1.98	0.092	16	1.9×10^{-4}
MW204R	08/22/00	0.33	2.42	0.038	6.3	7.3×10^{-5}
MW204R	08/30/00	0.25	3.02	0.059	10	1.2×10^{-4}
MW204R	09/11/00	0.25	3.35	0.030	4.9	5.7×10^{-5}
MW302R	10/18/01	0.30	1.5	0.090	15	1.7×10^{-4}
W202-NE	05/16/01	0.3	0.5	0.180	30	3.5×10^{-4}

B. Open-hole estimates of transmissivity from Cooper-Jacob straight-line solutions

Borehole	Date tested	Pumping rate, in gallons per minute	Elapsed time, in hours	Transmissivity	
				in feet squared per day	in feet squared per second
MW201R	09/07/00	0.5	2.25	3.2	3.7×10^{-5}
MW202R	08/16/00	0.25	2.43	1.8	2.0×10^{-5}
MW202R	09/06/00	0.25	4.08	0.98	1.1×10^{-5}
MW203R	09/12/00	0.25	2.00	1.0	1.2×10^{-5}

C. Estimates of transmissivity using data from BAT[3] tests

[TOC, top of casing]

Borehole	Date tested	Depth of fracture, in feet below TOC	Top of test interval, in feet below TOC	Bottom of test interval, in feet below TOC	Pumping rate, in gallons per minute	Transmissivity	
						in feet squared per day	in feet squared per second
MW201R	09/28/00	38	37.1	43.5	0.15	0.61	7.0×10^{-6}
MW201R	09/29/00	60	56.1	62.5	0.25	0.57	6.5×10^{-6}
MW202R	10/05/00	105-107	104	110.7	0.15	0.21	2.5×10^{-6}
MW203R	10/13/00	32	28.3	35.7	0.22	3.2	3.7×10^{-5}
MW204R	10/11/00	21-22	13.1	29.7	0.20	8.2	9.4×10^{-5}
MW204R	10/12/00	21-22	13.1	29.7	0.50	11	1.3×10^{-4}
W202-NE	05/18/01	197	195.4	206.2	0.20	4.7	5.5×10^{-5}